Report DTRC/SME-CR-04-89

EXPERIMENTAL STUDY OF VACUUM TRANSPORT IN A HORIZONTAL 50-MILLIMETER PIPE

by

Donald D. Gray, Ph.D.
Laura L. Miller
Edward H. Winant

Department of Civil Engineering
West Virginia University
Morgantown, West Virginia 26506-6101

Contract N00167-85-K0-100

April 1989

Approved for public release; distribution unlimited.

Prepared for

Frederick W. Burns
Anthony T. Rodriguez
David Taylor Research Center
Bethesda, Maryland 20084-5000

UNCLASSIFIED
SECURITY CLASSIFICATION OF THIS PAGE

REPORT DOCUMENTATION PAGE

1a. REPORT SECURITY CLASSIFICATION UNCLASSIFIED	1b RESTRICTIVE MARKINGS
2a. SECURITY CLASSIFICATION AUTHORITY	3. DISTRIBUTION / AVAILABILITY OF REPORT Approved for public release; distribution unlimited.
2b. DECLASSIFICATION / DOWNGRADING SCHEDULE	
4. PERFORMING ORGANIZATION REPORT NUMBER(S)	5 MONITORING ORGANIZATION REPORT NUMBER(S) DTRC/SME-CR-04-89
6a. NAME OF PERFORMING ORGANIZATION West Virginia University 6b. OFFICE SYMBOL (If applicable)	7a. NAME OF MONITORING ORGANIZATION David Taylor Research Center (Code 2834)
6c. ADDRESS (City, State, and ZIP Code) Department of Civil Engineering Morgantown, West Virginia 26506-6101	7b. ADDRESS (City, State, and ZIP Code) Bethesda, Maryland 20084-5000
8a. NAME OF FUNDING / SPONSORING ORGANIZATION Office of Naval Technology 8b. OFFICE SYMBOL (If applicable) Code 226	9. PROCUREMENT INSTRUMENT IDENTIFICATION NUMBER Contract N00167-85-K0-100
8c. ADDRESS (City, State, and ZIP Code) 800 N. Quincy Street Arlington, Virginia 22217-5000	10. SOURCE OF FUNDING NUMBERS PROGRAM ELEMENT NO. 62233N; PROJECT NO. 2830-102; TASK NO YM3E8004; WORK UNIT ACCESSION NO. DN 778155

11. TITLE (Include Security Classification)
EXPERIMENTAL STUDY OF VACUUM TRANSPORT IN A HORIZONTAL 50-MILLIMETER PIPE (U)

12. PERSONAL AUTHOR(S)
Donald D. Gray, Ph.D.; Laura L. Miller; Edward H. Winant

13a. TYPE OF REPORT	13b TIME COVERED	14. DATE OF REPORT (Year, Month, Day)	15. PAGE COUNT
RDT&E	FROM _____ TO _____	1989 April	101

16. SUPPLEMENTARY NOTATION

17. COSATI CODES			18. SUBJECT TERMS (Continue on reverse if necessary and identify by block number)
FIELD	GROUP	SUB-GROUP	Vacuum Sewers; Sewage Collection; Vacuum Collection; Wastewater Collection; Two-Phase Flow

19. ABSTRACT (Continue on reverse if necessary and identify by block number)

The David Taylor Research Center, in collaboration with West Virginia University, is conducting a research program to develop a physically sound design model for shipboard vacuum sewers. This report covers a series of experiments dealing with flow in a horizontal 50-mm pipe. The test facility and instrumentation are described, with emphasis on the accuracy of the various transducers. The performance characteristics of an ejector vacuum pump are quantified. The variation of vacuum with space and time is discussed and related to the pattern of flow as revealed by high speed video recording. Large vacuum drops are found to be related to the transitory formation of slugs which bridge the pipe bore. Vacuum sewer flow appears to be a chaotic dynamical system. Profiles of time average vacuum are related to controllable parameters such as flush volume and frequency and are compared with the homogeneous and Lockhart-Martinelli head loss models. A correlation for the volume of air admitted in a single flush is proposed. The report closes with conclusions and recommendations for further work.

20 DISTRIBUTION / AVAILABILITY OF ABSTRACT	21. ABSTRACT SECURITY CLASSIFICATION
☐ UNCLASSIFIED/UNLIMITED ☒ SAME AS RPT ☐ DTIC USERS	UNCLASSIFIED
22a. NAME OF RESPONSIBLE INDIVIDUAL Frederick W. Burns	22b TELEPHONE (Include Area Code) (301) 267-2595 22c OFFICE SYMBOL Code 2834

DD FORM 1473, 84 MAR 83 APR edition may be used until exhausted. All other editions are obsolete

SECURITY CLASSIFICATION OF THIS PAGE

☆ U.S. Government Printing Office: 1986—607-044

UNCLASSIFIED

TABLE OF CONTENTS

LIST OF FIGURES

LIST OF TABLES

LIST OF ABBREVIATIONS

^{o}C	degrees Celsius
Hz	Hertz
ID	internal diameter
kW	kilowatts
m	meters
ml	milliliters
mm	millimeters
ms	milliseconds
m/s	meters per second
Pa	Pascals
psi	pounds per square inch
PVC	polyvinyl chloride
s	seconds
TIC	Test Identification Code
rpm	revolutions per minute
v	volts
W	watts

SI UNITS

1 inch = 25.4 mm

1 foot = 0.3048 m

1 cfm = 4.719×10^{-4} m^3/s

1 gpm = 6.309×10^{-5} m^3/s

1 psi = 6.895 kPa

1 horsepower = 746 W

1 gallon = 3.785×10^{-3} m^3

1 liter = 10^{-3} m^3

ABSTRACT

The David Taylor Research Center, in collaboration with West Virginia University, is conducting a research program to develop a physically sound design model for shipboard vacuum sewers. This report covers a series of experiments dealing with flow in a horizontal 50-mm pipe. The test facility and instrumentation are described, with emphasis on the accuracy of the various transducers. The performance characteristics of an ejector vacuum pump are quantified. The variation of vacuum with space and time is discussed and related to the pattern of flow as revealed by high speed video recording. Large vacuum drops are found to be related to the transitory formation of slugs which bridge the pipe bore. Vacuum sewer flow appears to be a chaotic dynamical system. Profiles of time average vacuum are related to controllable parameters such as flush volume and frequency and are compared with the homogeneous and Lockhart-Martinelli head loss models. A correlation for the volume of air admitted in a single flush is proposed. The report closes with conclusions and recommendations for further work.

ADMINISTRATION INFORMATION

This report describes the work performed under Work Unit 2830-102 in the Environmental Protection Branch of the Chemical and Physical Processes Division, Ship Materials Engineering Department, David Taylor Research Center. The work is sponsored by the Shipboard Pollution Abatement Exploratory Development Program, Element 62233N, Block YE2A, Project RH33E80. Technology Area manager at the ONT is LCDR Baivier, Code 226.

INTRODUCTION

Vacuum sewers offer many advantages over conventional gravity sanitary sewers in naval shipboard applications. These advantages include reduced volumes of wastewater, smaller pipe diameters, and increased flexibility in the routing of pipes. The practicality of the vacuum sewer concept has been established by experience with SPRUANCE class destroyers as well as with civilian marine and residential applications. Nevertheless, present design practices are largely empirical and cannot be extrapolated with confidence to new situations. Future naval applications, such as aircraft carriers and troop ships, will test the limits of vacuum transport technology. Improved

design models, solidly grounded in physical principles, will be needed if the Navy is to exploit the full potential offered by the vacuum sewer.

In order to meet this challenge, the David Taylor Research Center has initiated a research program which will culminate in a revised Design Guidance for shipboard vacuum sewers. One of the main components of this program is the experimental study of vacuum transport in a laboratory test facility. The present report describes what has been learned from these experiments about flow in horizontal 50-mm pipes.

The next section reviews the test facility and its instrumentation, emphasizing recent modifications and the accuracy of the measurements. The report then presents the results of tests which define the performance of the ejector vacuum pump. These equations will be an essential component of the new design procedures.

The report describes the program of horizontal 50-mm tests and comments in detail about the nature of the flow in several typical experiments. This leads to an in-depth examination of the the instantaneous variation of vacuum in a horizontal pipe, including the use of high speed video to relate the flow pattern to the loss of vacuum.

The report continues with a presentation of new insights into the variation along the pipe of the time average vacuum and its relationship to controllable parameters such as flush volume and frequency. The measured variation of vacuum is compared with two well-known vacuum loss models from gas-liquid hydraulics. Finally the report draws conclusions from this work and presents recommendations for the future.

EXPERIMENTAL PROCEDURES

TEST FACILITY

The vacuum transport test facility and its associated instrumentation have been described in detail in Bowers and Gray (1988), hereafter called Report 1. This abbreviated description is provided for completeness and to point out modifications affecting the tests described in this report.

Figure 1 shows a plan drawing of the test facility, which is located in Building 182 of the David Taylor Research Center Annapolis Laboratory. The facility consists of an inlet section, test section, discharge section, and control center. The inlet section contains three simulated vacuum urinals and three vacuum water closets. Filtered potable water and air are the test fluids.

From the inlet section, the flow passes through a set of full-ported ball valves into a double-L shaped test section made of 50-mm transparent cast acrylic pipe and glass bends. The cast acrylic flanged pipe sections are 1.52 m long and have an internal diameter of 50.4 ± 0.4 mm (95 % confidence). In the tests described in this report, both L's were horizontal. The outer L was about 300 mm higher than the inner L, with the drop occurring at the 180^{o}-bend. The transport pocket mentioned in Report 1 was removed for most of the tests described in this report.

The ball valves are used to change the direction of flow through the test section. Flow which enters the test section through the outer (upper) pipe is termed "Normal" flow; flow which enters thought the inner (lower) pipe is termed "Reverse" flow.

Flow exits the test section through a 3.5 m long, 50-mm clear PVC riser

inclined 20.0° to the horizontal. This riser is connected to the manifold of a single Evac Model 1122 multiphase ejector which discharges to a near-atmospheric pressure collection tank. The water in the collection tank is recirculated by a centrifugal pump to provide the driving fluid for the ejector. The pump is powered by a 3-kW, 460-v, 3-phase motor.

The test facility is highly automated. Each simulated urinal uses a modified Airvac 2-inch vacuum interface valve. The operation of each urinal is controlled by three solenoid valves. The first allows the addition of water, the second initiates the opening of the interface valve, and the third holds the interface valve open. When the latter solenoid is de-energized, the interface valve closes at a rate dictated by an adjustable needle valve in the Airvac valve controller. Solenoids are also used to trigger the operation of the Evac vacuum water closets and to control the addition of water to the water closet bowls. The activation of all of these solenoids and the collection of data from the various transducers is performed by a Zenith Z-248 microcomputer with Metrabyte plug-in cards. The control and data acquisition programs are written using the Labtech Notebook software package.

The microcomputer is housed in the control center, an air conditioned, relocatable office adjacent to the inlet section. The environmental regulation made possible by the relocatable office has greatly reduced microcomputer maintenance and operator fatigue, leading to increased productivity.

INSTRUMENTATION

The transducers used in these tests are summarized in Table 1. Ten

differential pressure transducers were mounted at the locations shown in Figure 1 and specified in Tables 2 and 3. These Sensotec Model WD-Z/5107-01 transducers were mounted with their dry ports open to the atmosphere so that they would respond to the vacuum pressure at their wet ports. Contrary to Report 1, the 9 test section transducers were mounted directly above 3-mm pressure taps in the pipe crown. This assured that the wet cavities were filled with air, except perhaps when liquid slugs passed the taps. Transducer 2 was mounted on the underside of the ejector manifold.

The pressure transducers have a 15 ms response time, ± 103 kPa range, and ± 5 v output. The manufacturer claims an accuracy of ± 0.25 % of full scale, which corresponds to ± 0.0125 v (± 0.259 kPa). To this must be added the uncertainty inherent in the analog to digital conversion performed by the Metrabyte DASH-16 board, which divides the ± 5 v input range into 0.0024 v steps. The result is a combined uncertainty of ± 0.0137 v (± 0.284 kPa) based on the manufacturers' specifications.

The pressure transducers were calibrated in place on July 11, 1988, by DTRC Instrumentation personnel using an Inficon Model CM-3 Capacitance Manometer as the calibration standard. The Inficon has an accuracy of ± 0.01 % of reading. Readings were made for five vacuums ranging from 0 to 68.60 kPa. Each transducer was read at 30 Hz for 10 s and the average voltage V was recorded. The zero-vacuum voltage V_o for the various transducers ranged from 0 to 0.0024 v. For each transducer, Lotus 1-2-3 software was used to fit a regression equation of the form

$$P = K (V - V_o) \qquad (1)$$

where P = vacuum pressure (kPa)

K = calibration constant (kPa/v)

In every case the coefficient of determination exceeded 0.9999. The largest deviation between the regression equation and the Inficon vacuum measurements was 0.253 kPa, which is within the manufacturers' specifications for accuracy.

Following this calibration, the transducers were powered continuously (except during electrical outages) and their amplifiers were not readjusted. In order to counter the effects of drift and improve the precision of the measurements, the calibration constants were adjusted each test day using the following procedure. With the ejector off and the test section vented to the atmosphere, each transducer was sampled at 30 Hz for 10 s. These data were averaged to provide new values of V_o for each transducer. This procedure was repeated at the maximum vacuum which could be maintained with the ejector off. Using the new V_o and the calibration value of K, the maximum vacuum was calculated for each transducer from equation (1). Asuming that the transducers had drifted randomly, the average of the ten maximum vacuums $\bar{P}$ was taken as the true value. This allowed the calculation of a new value of K for each transducer according to

$$K = \bar{P} / (V - V_o)$$

In this way new values of K and V_o were found each test day. Until August 16, 1988, the largest zero-vacuum voltage V_o for any transducer was 0.0245 v. On that date V_o for transducers 9 and 10, which share the same amplifier card, shifted about 0.7 v for no apparent reason. This did not seem to affect the K values much. For the entire period, the maximum deviation between the daily K values and the calibration K values was 0.39 %.

Overnight monitoring revealed that the zero-vacuum voltage of the

transducers seldom varied by more than 0.0096 v (0.200 kPa) during an 8-hour period. In view of this experience, the experimenters conclude that that data of the vacuum transducers are accurate to within ± 0.3 kPa and have a precision of ± 0.1 kPa in any particular run.

Air flow into the test facility is measured by velocity transducers mounted in the inlet stacks of each simulated urinal and of water closet 1. These Kurz Model 435 DC Linear Air Velocity Transducers contain a constant-temperature thermal anemometer sensor and a temperature sensor. They are responsive to the product of air density and velocity and are calibrated assuming that the air is at standard conditions (25° C and 101.3 kPa). The actual air velocity is related to the indicated velocity by

$$v_a = (\rho_s / \rho_a)\, v_s$$

where v_a = actual air velocity

ρ_s = air density at standard conditions

ρ_a = actual air density

v_s = air velocity at standard conditions

This correction, which would not have exceeded ± 3 % in the tests reported here, was not performed.

The velocity transducers have a response time of 35 ms, an output of 0-5 v and a range of 0-30.5 m/s. They were calibrated by the manufacturer using NBS-traceable standards and were certified to be accurate to ± 3 % of reading and ± 0.5 % of full scale. This translates to a maximum transducer uncertainty of ± 1.1 m/s. The effect of digitizing this signal is negligible. The manufacturer specifies a repeatability of ± 0.25 % of reading.

The inlet air flowrate was calculated by multiplying the measured centerline velocity by the area of the inlet stack (ID = 77.3 mm). The inlet stacks are long enough to insure fully developed turbulent velocity profiles, but the appropriate peaking factors have not yet been accounted for. This means that the air flowrates reported here may be too high by 10 to 30 %.

The discharge air mass flowmeter described in Report 1 failed. It was replaced by an Omega Model FMA-605-V velocity transducer centered in a 48.6 mm ID discharge pipe at a station where the velocity profile should be fully developed. This device is nearly identical to the inlet air velocity transducers described above. As in the previous instance, the corrections for air density and peak factor have not yet been made. The Omega velocity transducer has a response time of 50 ms, and output of 0-5 v, and a range of 0-25.4 m/s. The manufacturer specifies an accuracy of ± 2 % of full scale, equivalent to ± 0.1 v or ± 0.5 m/s. The repeatability is given as ± 0.5 % of full scale (± 0.13 m/s).

Frequently, depending on the weather, there was considerable moisture present in the discharge air pipe. This moisture is probably the greatest source of uncertainty in the discharge air velocity data.

Several tests were performed to check the consistency of the inlet and discharge air velocity measurements. A statistically steady air flow was established by holding open one of the urinal valves, but not admitting any water. The inlet and discharge velocity transducers were sampled at 30 Hz for 60 s. Based on the average velocities, the discharge air flowrate was consistently 11 - 14 % less than the inlet air flowrate. The experimenters believe that the major portion of this discrepancy is attributable to inaccuracies in the discharge measurement.

Badger Model SC-ER nutating disk water meters are used to measure the flow of water into the plumbing fixtures. The urinal feeds are monitored by 3/4-inch (19-mm) meters and the water closet bowl feeds by 5/8-inch (16-mm) meters. The water closet flush mechanisms discharge 1.2 liters per flush and are not metered. Each water meter is fitted with an EPT-1 pulse transmitter connected to one of the counter channels in the data acquisition system. Severe problems involving spurious counts described in Report 1 were attributed to electromagnetic noise and pulse generator backlash. These have been largely eliminated by using solid state relays to control the solenoid valves, and custom software to gate each counter so that it is recorded only when the appropriate solenoid valve is open.

The water meters were calibrated by measuring the volume of water V and the number of pulses N for various periods of flow. Least squares regression was used to fit equations for each meter of the form

$$V = K N$$

where K = calibration constant (ml/pulse)

The smallest coefficient of determination was 0.9995. The greatest deviation between the measured volume and the regression volume was 6.4 % for a 1 s flow period. This uncertainty resulted largely from starting and stopping the flow and dropped rapidly as the flow period increased. It was 2.6 % for 2 s of flow and 1.1 % for 4 s.

Three independent regulators control the pressure in the urinal feed lines, the water closet bowl feeds, and the water closet flush mechanisms. Increasing the line pressure increases the flow rates as well as the speed of operation of the water closet flush mechanisms. During the course of testing, urinal feed flowrates were varied from about 120 to 230 ml/s. The

water closet bowl feed flowrates were varied from about 180 to 250 ml/s.

The collection tank water level is monitored by a wet-dry differential pressure transducer mounted near the bottom of the collection tank. The wet port is connected to the collection tank with a short, flexible hose and the dry port is connected to the roof of the tank through a moisture trap so that the transducer responds to the depth of water in the tank. This transducer is a Sensotec Model WD-Z/5965-01 having a response time of 15 ms, a range of 0-13.8 kPa, and a 0-5 v output. The manufacturer specifies an accuracy of ± 0.25 % of full scale; but, as calibrated by DTRC Instrumentation personnel on July 1, 1988, the range of deviation from the least squares regression line was from -0.56 % to +0.12 % of full scale (-0.028 v to +0.0060 v or -0.077 kPa to +0.017 kPa). When the digitization process is considered, the combined uncertainty is estimated to be ± 0.030 v (± 0.084 kPa)

The volume of water in the tank V above the level of the pressure tap is related to the pressure P by

$$V = (P / w) A$$

where w = specific weight of water (N / m^3)

A = cross section of tank ($1.252\ m^2$)

The variation of specific weight with water temperature is less than 0.4 % from 15 to 30 ^{o}C. Thus the total uncertainty under static conditions is ± 8.6 mm (± 110. ml).

With the ejector in operation, the transducer output was contaminated both by 30 Hz noise and by the seiching of the water level with a dominant period of 1.8 Hz. This problem was reduced by the installation of a low pass active filter with a 1.5 Hz cutoff on August 1, 1988. Nevertheless,

instantaneous water level readings cannot be relied upon if the ejector is in operation.

The working volume of the collection tank is about 1.2 m^3. The tank can be drained through a 1.5-inch (38-mm) Badger Model SC-ER-C nutating disk water meter. The manufacturer specifies that this meter has an uncertainty of ± 1.5 % of flow over the range from 320-6300 ml/s. The typical rate of collection tank discharge is about 2450 ml/s.

The drain line water meter is fitted with an EPT-1 pulse generator which was calibrated on August 12, 1988, by recording the number of pulses generated and the collection tank water level as the tank was drained. A least squares linear regression gave a calibration constant of 26.3 ml/pulse with a 0.9996 coefficient of determination.

The temperatures of the inlet air, inlet water, and exhaust air are monitored using Yellow Springs Instrument 44018 Thermilinear composite probes with 44303 resistor sets. These probes use two matched precision thermistors to produce a voltage output which is a linear function of temperature over the range from -30 to +50 ^{o}C. For the particular devices used in this experiment, the equation is

$$T = 48.719\ (V - 1.054)$$

where T = temperature in ^{o}C

V = voltage output in volts

The manufacturer specifies a time constant of 10 s in air and an accuracy of ± 0.15 ^{o}C. The ± 0.0024 v uncertainty due to digitization increases the overall uncertainty to ± 0.27 ^{o}C. The temperature probes had been plagued by electrical noise in the 40 Hz range with an amplitude of ± 0.5 ^{o}C, but the addition of capacitors reduced the amplitude of the noise to 1 digitization

step, well below the uncertainty of the measurements.

The power required to drive the centrifugal pump was measured by an Ohio Semitronics EW5-15B Electronic Precision Watt Transducer. This device has a range of 0-8 kW with an output of 0-8 v, but the actual output never exceeded about 3.5 v. The manufacturer specifies an accuracy of ± 0.2 % of reading, and this was confirmed by DTRC Instrumentation personnel in a January, 1987, calibration. Accounting for digitization, the maximum uncertainty is ± 0.009 kW.

High speed video recording of the flow patterns was performed using a Spin Physics SP-2000 dual camera system. Speeds from 60 to 2000 frames per second were used in different runs. In each case a split screen was used to record scenes centered on transducers 6 and 10. The field of view was about 25 cm long and the pipes were backlit through a translucent screen on which 2 cm squares were inscribed. The black-and-white images were recorded on 1/2-inch (13-mm) video tape using NTSC-compatible format.

A signal from a DASH-16 digital output channel was used to start and stop the video recording. Because the tape reels must come up to speed before taping can begin, there is a time lag of from 0.3 to 2.3 s between the triggering pulse and the start of taping. In order to synchronize the video images with other data, a circuit was devised which generated a 4.5 v signal when video recording was underway. This signal was fed to one of the DASH-16 analog input channels for recording.

The video recording system was subject to seemingly random bouts of interference, poor picture quality, and other intermittent electrical problems. Careful erasing of the tape cassettes prior to use and frequent cleaning of the recording heads helped reduce these problems.

In addition to the electronic instruments, several bimetal thermometers and compound vacuum gauges were used to monitor conditions in the test facility. Barometric pressures were obtained one or more times per test day from the DTRC Instrumentation laboratory or the Baltimore-Washington International Airport weather information office.

RESULTS

EJECTOR PERFORMANCE TESTS

The Evac multiphase ejector is the figurative heart of the test facility and of future naval shipboard installations. The understanding of its performance characteristics is paramount to the optimum design of vacuum collection systems. Tests were performed on July 7-8, 1988, in order to define the steady state vacuum-discharge curve for the ejector.

The ball valves were set to allow a straight run from the inlet section to the ejector and the pipe was drained of water. The ejector was set to constant run and urinal 3 was held in the open position. After waiting 62.5 s for the flow to reach steady state, inlet air velocity, ejector manifold vacuum, and electrical power were recorded at 20 Hz for 62.5 s. Figure 2 illustrates that although the boundary conditions were steady, the details of the flow varied randomly. The tests were repeated for eight air flowrates with no water flow, and for four cases with a water flowrate of 200 ml/s. The air flowrate was throttled using one of the ball valves. The air temperature was about 30 ^{o}C, the inlet water temperature about 20 ^{o}C, and the water temperature in the collection tank about 44 ^{o}C. The tank water level rose from 500 mm to 580 mm as water was collected.

When the average manifold vacuum was plotted against the average air flowrate for each test, a definite gaussian pattern emerged. Figure 3 shows that regardless of water flowrate, the data are well represented by

$$V = V_o \exp (-0.03 Q_a^2) \quad (2)$$

Where V = manifold vacuum (kPa)

V_o = manifold vacuum at zero air flow (kPa)

Q_a = air flowrate (standard liters/s)

The constants in this equation should vary with the head-discharge curve of the centrifugal pump which drives the primary flow, and with the level and temperature of the water in the collection tank. The small effect produced by the water flowrate should come as no surprise since the air to water volume flowrate ratio exceeds 11.5 in each case. The primary-fluid pump was an ABS Model AFP-004 with a 170-mm, single vane, open impeller driven by a 1750-rpm, 3-kW electrical motor.

An indication of the universality of equation (2) was found by replotting some ejector test data received from the ejector manufacturer. The results of these tests had been furnished as graphs of vacuum and air flowrate against time. Tests had been performed for two centrifugal pump impeller diameters with four levels of water in the collection tank. The data for the 184-mm impeller have been replotted as vacuum vs. discharge curves in Figure 4. The effect of the varying water level on the shut-off vacuum, and the gaussian shape of the curves are evident. Dividing these data by the respective shut-off vacuums allows the comparison with equation (2) shown in Figure 5. The equation provides a fairly conservative representation of the data which is faithful to the overall trend. Equation (2) will be useful in

formulating design programs for systems using Evac multiphase ejectors.

The power required to drive the ejector is also of interest. Figure 6 shows that the power vs. air flow data can be represented by

$$P = P_o + (P_m - P_o) \exp(-0.2\, Q_a) \qquad (3)$$

where P = electrical power (kW)
P_o = electrical power at zero air flow (kW)
P_m = electrical power at maximum air flow (kW)
Q_a = air flowrate (standard liters/s)

The constants in this equation should depend on the motor characteristics as well as the factors which govern the vacuum-discharge relation, but it is interesting that the power drops as the air flowrate increases. This can be understood by noting that as the air flowrate increases, the pressure difference across the ejector drops. It is also clear that the power goes up as the water flowrate increases, although this effect is relatively small for the range of flows considered.

TEST PROGRAM

Table 4 summarizes the manner in which the solenoids and transducers were connected to the control and data acquisition boards for the tests described in this report. Since the period covered by Report 1, it was found that all of the transducers could be connected in the single-ended mode without loss of accuracy. This allowed all of the vacuum transducers to be wired to the number 1 DASH-16 board. It should be noted that the scale factors and offset constants for the vacuum transducers were recalculated on a daily basis, as described in a previous section.

Each test is identified by a Test Identification Code (TIC) and a Run number.

The general form of the TIC is

Dd-Ss-Ll-Uu-Ww-(N or R)-(I or C)

where d = nominal diameter of test section pipe in inches.

s = inclination of main test section to horizontal in degrees.

l = approximate vertical lift of main test section in feet.

u = number of urinal valves in operation.

w = number of water closets in operation.

N or R = Normal or Reverse flow through the test section.

I or C = Intermittent or Continuous flow. In Continuous flow the urinal valves are always open. In Intermittent flow the valves cycle normally.

Each time the test parameters are changed, a unique Run number is assigned. Replications are usually identified by appending a dash and the number of the replication, e.g. Run 6-2 is the second replication of Run 6.

Tables 5, 6, and 7 are an inventory of the tests performed in July-August, 1988, and described in this report. All of the tests were for 50-mm (D2) pipe in a horizontal configuration (S0-L0) with either one urinal (U1-W0) or one water closet (U0-W1) operating. All of the tests were for intermittent valve operation (I) and were repeated in both normal (N) and reverse (R) flow directions. In each test the ejector was set to constant run so as to produce the maximum attainable vacuum. Either urinal 3 or water closet 1 was used in every Run.

In the urinal tests, the controllable parameters were the time the interface valve was open in one flush t, the period between flushes T, and the volume of water discharged per flush V. Tables 5 and 6 give the values assigned to these parameters in each Run. Figure 7 illustrates the pattern

of parametric variation according to nominal values and suggests which additional tests are needed.

In the water closet runs, the variables were the time between flushes T and the flush mechanism water line pressure P, which controls the flush time. Table 7 lists the values assigned to these parameters, and Figure 8 displays the pattern of variation. Several Runs share the same parameter set but differ in the length of the data collection period, camera speed, or other details. Run 11 was performed, but the data were garbled. In every case, 225 ml of water was added to the bowl, making a total nominal discharge of 1425 ml per flush.

The tests were performed in the order of Run number, as listed in Tables 5, 6, and 7, except that the Normal and Reverse cases were interleaved. It should be noted that in both urinal and water closet tests the nominal parameters for Normal and Reverse tests having the same Run number are the same.

It is convenient to divide the urinal tests into single-flush tests and periodic-flush tests. The single-flush tests focus attention on the basic atom of vacuum sewer flow - the isolated flush. The periodic-flush tests allow the performance to be studied at much higher flowrates. The protocols followed in these two sets of tests were slightly different.

Before each single-flush test, the test facility was "primed" by several flushes of equal volume in the same direction. The test proper was divided into three stages. During the preliminary stage, all active transducers were sampled at 1 Hz while water was added to the urinal. This stage lasted from 5 to 20 s depending on the volume added. In most cases, the video system was triggered during this stage so that the cameras would be recording before the

flush. After the fill was complete and just before the flush, the sampling rate was increased to 15 Hz. This stage lasted for 61 s and included the major portion of the transient. During the final approach to equilibrium, the transducers were sampled at 1 Hz for 45 s.

The periodic-flush tests were conducted in two stages. During the first stage, a periodic flow was established by flushing either 10 or 20 times, depending on the flush period. Data were then sampled at 15 Hz for either 32 or 42 s so that anywhere from 2 to 6 complete cycles were recorded.

All data have been recorded in ASCII files and stored on 5.25-inch floppy disks. The data files are imported into Lotus 1-2-3 spreadsheets for statistical and graphical analysis.

RESULTS OF TYPICAL TESTS

Table 5 shows that in Run 9, urinal 3 was filled with 1 liter of water, flushed once, and held open for 2 s before being allowed to close. Figure 9 illustrates the inlet and discharge air velocities for the Normal direction. The inlet velocity rises very rapidly when the valve opens, reaching a peak of 19.5 m/s. The fall of the inlet velocity is also very rapid. The response of the discharge air velocity is more gradual, reaching a peak of 5.9 m/s after the valve has already closed and trailing off to zero at about 50 s. Figure 10 illustrates the behavior of pressure transducers 2, 6, and 10. Transducers 6 and 10, although separated by 6 m, behave almost identically. Their vacuums drop precipitously when the valve opens, nearly reaching atmospheric pressure when the inlet velocity is at a maximum, and remaining close to atmospheric pressure until the valve is almost closed. Their vacuum recovery is essentially complete by 50 s. Transducer 2, mounted on the ejector manifold, loses its vacuum a bit more slowly, and drops to

only 2.3 kPa. Its recovery is similar to the others except that there is a pronounced oscillation superimposed on the general trend. This is probably caused by slugging in the riser pipe.

The inlet and outlet velocities for Run 9 in the Reverse direction are plotted in Figure 11. As expected, the qualitative features are the same as in the Normal case, but the peak inlet velocity only reaches 15.6 m/s and the secondary peak is somewhat more pronounced. Variations of this magnitude seem to occur randomly and are thought to be of no particular significance. The discharge velocity is almost identical in shape to the Normal case, but peaks a bit higher at 6.3 m/s. The response of transducers 2, 6, and 10 is shown in Figure 12. With the transducers farther from the valve, the loss of vacuum is not so rapid as in the Normal case. Transducer 10, which is closer to the valve, drops slightly before Transducer 6. The minimum vacuum now coincides with the secondary inlet velocity peak and is not sustained for any time. Although the minimum vacuum at transducers 6 and 10 is larger than in the Normal case, this is not caused by being closer to the ejector, but by the fact that the ejector vacuum is also about 2 kPa higher than before. Again, this variation appears to be a random event of no fundamental importance. In all other respects, the response of the vacuum transducers is similar in both Normal and Reverse flows.

Run 15 is a periodic-flush test in which the flush of Run 9 is repeated every 5 s. Table 5 shows that during each flush the valve remains open for 2.6 s and discharges 900 ml of water. (These are measured averages rather than nominal values.) The inlet and discharge velocities are displayed in Figure 13. Perhaps the most striking feature of this graph is the degree of variability from one flush to the next, even though a series of 20 identical

flushes preceded the data shown. It appears that vacuum sewer flow exhibits sensitive dependence on initial conditions, a hallmark of chaotic systems. In all likelihood, it is impossible to devise a theory capable of predicting exactly the behavior of a vacuum sewer, although a workable design model can be developed.

The maximum inlet velocity in Figure 13 is only 6.8 m/s, about one third of the maximum in Run 9. The discharge velocity generally peaks after the valve is closed, with a maximum of about 4.1 m/s. In most cycles, the minimum discharge velocity occurs while the valve is open.

Figure 14 portrays the variation of vacuum at transducers 2, 6, and 10. As in Figure 13, the deviation from strict periodicity is manifest. The traces of transducers 6 and 10 are very similar, but they do show some differences, particularly during the sharp drop in vacuum which coincides with the valve opening. The vacuum recovery seems to involve a steep rise as the valve closes, followed by a more gradual rise in vacuum while the valve is closed. Transducers 6 and 10 are indistinguishable during the recovery phase. It is notable that the vacuum does not drop as low as in the single-flush case nor does it ever recover fully. The latter fact explains the lower inlet velocities mentioned previously.

The vacuum at the ejector manifold (transducer 2) averages about 10 kPa higher than at transducers 6 and 10. In addition, the range of variation is much less because the vacuum drop in response to the valve opening is much smaller. The maxima and minima at the ejector tend to lag behind those in the test section.

The manifold vacuum and electrical power have been plotted together in Figure 15 using scale factors chosen to emphasize the remarkable shape

similarity of the two curves. As expected from the ejector characteristics presented in Figures 3 and 6, instants of high vacuum and low air discharge coincide with high power consumption.

The Reverse flow version of Run 15 used the same Notebook program as the Normal case, but as Table 6 shows, the average valve open time was only 2.2 s. The inlet and discharge air velocities are presented in Figure 16. Compared with the Normal case (Figure 13), there is an increased tendency toward a secondary velocity peak during the valve opening phase. The reason for this phenomenon is unknown. There are no other qualitative differences compared with Figure 13.

The vacuums at transducers 2, 6, and 10 are shown in Figure 17. The traces of transducers 6 and 10 are virtually indistinguishable except during the pressure drop at 121 s. The maximum vacuum coincides with the opening of the valve and the minimum vacuum with the valve being almost closed. The recovery phase seems more uniform than in the Normal case. The vacuum at transducer 2 is only about 5 kPa higher than the vacuum at transducers 6 and 10 because they are some 27 m closer together in the Reverse configuration compared to the Normal.

INSTANTANEOUS VACUUM LOSS

A vacuum sewer design model must account for the vacuum loss in a straight horizontal pipe during flow. Understanding this phenomenon is thus an important objective of the current research. Figure 1 shows that of the nine transducers located in the upper pipe of the test section, seven were in the long leg. They were placed at intervals of about 30 diameters so as to cover a 178-diameter reach near the middle of the 319-diameter leg. Two

transducers were in the short leg of the test section.

The results discussed previously indicated that the differences among the transducers in the long leg were surprising small in magnitude and brief in duration. Further insight into this behavior is offered by Figure 18, which shows the variation of gauge pressure with position at six instants during Run 15. (Gauge pressure is the negative of vacuum pressure.) The flow is in the Normal direction, from right to left in the figure. These profiles all occurred during the first flush shown in Figures 13 and 15. The vertical displacement of the successive profiles reflects the rise in gauge pressure due to the valve opening. It is clear that the temporal variation is far more dramatic than the spatial variation.

The lowest profile occurs less than 0.06 s after the valve opens, when the inlet air velocity is only 0.6 m/s. It shows a slight rise in pressure toward the collection tank. The second profile, when the inlet velocity is 2.5 m/s, exhibits a small linear drop in pressure in the flow direction. The third and fourth profiles, corresponding to inlet velocities of 4.4 m/s and 6.1 m/s, are dominated by a sharp drop in pressure between transducers 3 and 4. This drop has disappeared from the fifth profile (inlet velocity 5.3 m/s), which has a linear pressure decrease through the straight pipe. At the latest time shown, the inlet velocity has dropped to 4.7 m/s and the profile of pressure is fairly flat, except for a slight bump at transducer 5.

The details of the formation and disappearance of the sharp pressure drop between transducers 3 and 4 are provided by Figures 19 and 20. These figures show all thirteen profiles measured during the time between the second and fifth profiles of Figures 18. The sharp drop in pressure between transducers
3 and 4 first appears at 100.46 s, reaches its largest valve (4.8 kPa) at

100.53 s, and remains prominent until 100.86 s. By 100.93 s, the pressure difference between transducers 3 and 4 has declined to a more typical value. The large drop propagates only as far as transducers 4 and 5, where it appears at 100.60 s and persists until about 100.73 s. No other pair of adjacent transducers in the straight pipe exhibits this large pressure difference.

Another view of this behavior is given by plotting the pressure differences between adjacent transducers against time in Figure 21. Although the pressure drops always increase when the valve opens, only the 3-4 and 4-5 differences ever exceed 2 kPa. A "perspective" view of this data is offered by Figure 22. While the large drops are clearly the most important phenomenon in these figures, it is also interesting that small pressure rises which exceed the noise level occur fairly frequently.

Observation of the high speed video tapes show that the flow is in a stratified-smooth or stratified-wavy pattern the overwhelming majority of the time. Before a valve opens the flow is usually stratified-smooth with little motion taking place. As the valve opens, the rushing air creates waves which rapidly grow in amplitude. Often spray will be torn from the wave crests. In some cases, a slug forms and occludes the pipe. The formation of such a competent bridge seems to be associated with large pressure drops. Slugs tend to break down after moving some distance, which may explain why the large pressure drops are confined to a limited reach of pipe in Figures 18-22.

Figure 23 illustrates the correlation between video image and pressure drop in Run 19, when 1700 ml of water was discharged every 10 s. The valve was open for 3.1 s and the flow was in the Normal direction. The upper part

of the video frame shows flow from right to left at transducer 6, and the lower part shows flow from left to right at transducer 10. The graph depicts the pressure difference between the transducers in the video and their nearest upstream neighbors.

In the first frame, the flow at both transducers is stratified-wavy and the pressure difference is small. The second frame shows a foamy plug which appears to block the pipe for about two diameters at transducer 6. This is simultaneous with a pressure difference of 7 kPa between transducers 1 and 6. At the same instant, the flow at transducer 10 is stratified-wavy and the pressure difference there is small. The third image of transducer 6 contains a wisp of foam which appears to bridge the pipe and corresponds with a small secondary peak in the pressure difference. At this time the flow at transducer 10 is stratified-wavy and the pressure difference is small. In the final frame, both transducers experience stratified-wavy flow and small pressure differences.

TIME AVERAGE VACUUM LOSS

In order to construct a usable design model, it is necessary to understand how the time average vacuum varies with position during flow. To study this phenomenon, the vacuum at each transducer was averaged over the largest number of complete cycles available for each periodic-flush Run. The average vacuum of each transducer in the long test section pipe was subtracted from the average vacuum of the most upstream transducer: 1 for Normal Runs and 7 for Reverse Runs. These differences have been plotted

against station in Figures 24-35. Ideally, each plot contains Runs grouped to show the effect of varying one parameter at a time. Taken together, these figures show that the vacuum differences are always small, although usually exceeding the ± 0.1 kPa precision of the transducers. Only in Normal Run 22 does the total vacuum drop exceed 1 kPa. In every case except Run 18, the drop in the Normal direction exceeds the drop in the Reverse. This can be attributed to the decline in the vigor of the flow as it moves away from the inlet valve. Another pattern that emerges from these plots is the anomalous behavior of transducers 4 and 5, which are separated by 1.31 m. In seven out of ten Normal Runs, the vacuum loss between 4 and 5 is negative. In each of the Reverse cases, the loss between 5 and 4 is unusually large compared to other pairs of adjacent transducers. This suggests the possibility of a systematic error which was not corrected by the daily calibration routine described earlier. Yet a careful review of the daily data does not support the hypothesis of a systematic error. Finally it is clear that the vacuum variation is seldom linear, implying that the flows studied were not fully developed.

The parameters in Runs 13 and 15 were identical, so Figures 24 and 25 indicate the degree of random variability which characterizes vacuum sewer flows. The only important discrepancy between these cases occurs at transducer 10 in the Reverse flow.

Figures 26 and 27 compare Runs whose only significantly varying parameter is valve open time. In the Normal direction, the vacuum loss decreases as the open time increases. The opposite trend holds for the Reverse direction, although Runs 14 and 16 are virtually identical.

Figures 28 and 29 primarily show the effect of varying water volume, but there is also some variation in open time. In the Normal direction, there is

a clear tendency for vacuum loss to increase with water volume, although the effect is slight. A similar trend occurs in the Reverse cases, but is less consistent.

Figures 30 and 31 compare Runs which differ in both open time and cycle time. In the Normal case, the vacuum loss is larger for the Run with larger open and cycle times; but in the Reverse flows the opposite is true. Assuming from Figures 26 and 27 that the longer open times would produce smaller losses in the Normal flow and larger losses in the Reverse implies that a longer cycle time significantly increases the losses in the Normal direction and reduces them in the Reverse direction.

Figures 32 and 33 also compare Runs which differ in both open and cycle times. Once again, the Run with longer times has a higher loss in the Normal direction and a lower loss in the Reverse. This supports the hypothesized effect of cycle time. Run 18 is the only Run for which the Reverse loss exceeds the Normal loss.

Figures 34 and 35 compare Runs 20, 21, and 22. The three Runs differ in water volume, and Run 22 has a longer open time than the others. In both directions, Runs 20 and 21 are nearly identical. This leads to the conclusion that increasing the water volume from 0.5 to 0.9 liters has a negligible effect for these times. Run 22, with more than 3 liters of water as well as a longer open time, has a much greater loss.

In summary, varying the water volume from 0.5 to 1.7 liters per flush seems to produce only small increases in vacuum loss, but larger volumes may produce significantly larger losses. Increasing the open time of the valve appears to decrease losses near the inlet valve and increase them farther from the valve. The reason for this difference in trend is unknown. Doubling the cycle time from 10 to 20 s produces larger losses near the inlet

valve and smaller losses further away. These conclusions must be regarded as tentative; additional Runs are needed to fully define the effect of each parameter.

COMPARISON OF VACUUM LOSS WITH MODELS

Report 1 describes the computer program 2PHI which was written by Bowers and Gray to implement the homogeneous and Lockhart-Martinelli head loss models. These flow pattern independent, steady state models for gas-liquid pipe flow are well known in the two phase flow literature (Wallis, 1969). The key data required for 2PHI are the time average values of air flowrate and water flowrate. These were obtained for the periodic-flush runs by averaging over the largest number of complete cycles contained in the data records. In calculating the air flowrates, the velocity was set to zero when the valve was closed. Table 8 lists these flowrates together with their population equivalents calculated using Navy design flows. The populations simulated in these Runs ranged from 45-412 persons, well above the 296 man complement of a SPRUANCE-class destroyer. The air to water ratios range from 32-236. These values are extremely high compared to the 2-8 range considered typical of residential vacuum sewers.

In order to calculate the absolute pressure at the upstream station required by 2PHI, the time average vacuum at the most upstream transducer (1 for Normal Runs, 7 for Reverse Runs) was subtracted from 101.3 kPa, neglecting the actual day-to-day variations in atmospheric pressure. Air and water temperatures were taken from the data file for each Run, and the equivalent sand grain roughness of the cast acrylic pipe was assumed to be zero. The McAdams viscosity correlation was used in all homogeneous model calculations. The Cichitti viscosity correlation would have predicted greater losses; the Dukler correlation, lower losses. The absolute pressures

computed by 2PHI for each Run were subtracted from the upstream value and plotted against distance in Figures 36-55 together with the measured time average vacuum losses.

Program 2PHI allows the air density and other properties to vary with the pressure. Thus the predicted vacuum loss curves consist of straight line segments whose slope varies slightly from transducer to transducer. Overall, the near linearity of the predicted vacuum losses contrasts sharply with the complex shape of the measured loss profiles. It can be seen that the homogeneous model always predicted greater losses than the Lockhart-Martinelli model. As a means of evaluating global performance, the models were judged "consonant" with the data if a straight line, fit to the data by eye, was bracketed by the model predictions. Of the Normal Runs, the models are consonant in five, too high in one (Run 19), and too low in four (Runs 17, 20, 21, and 22). The models are consonant in only two of the Reverse Runs (18 and 22) and are too high in the other eight. Since the predicted losses are nearly identical in corresponding Normal and Reverse Runs, the tendency of the models to underpredict the Normal losses and overperdict the Reverse losses is probably due to the fact that the observed losses decline as the flow moves away from the inlet valve. The most positive conclusion that can be drawn from these comparisons is that the homogeneous model gives conservative results except for Normal Runs 17, 20, 21, and 22.

Examining the individual figures, the best agreement is with Normal Runs 13 and 15. This is reasonable since these Runs have the shortest cycle times (5 s) and so should produce flows which are closest to steady state. Yet in Reverse Runs 13 and 15 the agreement is especially poor. Conversely, the poor agreement with Normal Runs 20, 21, and 22 could be attributed to their

long cycle times; but the agreement with Reverse Runs 20, 21, and 22 is much better. These observations make it painfully obvious that the homogeneous and Lockhart-Martinelli models are too idealized to accurately describe vacuum sewer flow.

AIR FLOW CORRELATION

The losses in a vacuum sewer line surely depend on the flowrates of both sewage and air. In order to calculate the sewage flowrate, the engineer will multiply the design population and an assumed rate of sewage generation. Dividing the sewage flowrate by the sewage volume per flush gives the rate of flushing. At present, the air flowrate is estimated by assuming an air to water ratio. Since this ratio varies over nearly an order of magnitude, this procedure is unsatisfactory.

What is needed is a correlation between the volume of air admitted per flush and the governing physical parameters. These may include the valve open time, main vacuum, sewage volume being discharged, and perhaps other factors. The data gathered in Normal Runs 13-22 were used to investigate this relationship. By integrating the inlet air velocity during the time the valve was open, the average volume of air admitted per flush was calculated. It was hypothesized that the volume of air would be proportional to the open time of the valve and to the square root of the vacuum at the nearest transducer just prior to opening. Such a relationship is oversimplified, but the necessary data were available from these tests and could be reasonably estimated by the design engineer in future applications. The resulting

least squares regression equation is

$$V = 3.55\ t\ P^{0.5} \qquad (4)$$

where V = volume of air admitted per flush (standard liters)

t = open time of valve (s)

P = vacuum at nearest transducer just before valve opens (kPa)

The coefficient of determination is 0.85. Figure 56 compares equation (4) with the data. Although the basic trend is correct, the scatter is large. At least part of the scatter is attributable to variations in the water volume, but more data are needed to define this effect.

CONCLUSIONS

1. The experimental facility is operating well. Electrical noise problems which had affected the water meters, thermistors, and water level transducer have been overcome. Most of the instruments are performing within specifications. The accuracy and reliability of the pressure transducers have been quite satisfactory. The provision of an air conditioned control center greatly reduced microcomputer failures and operator fatigue, and led to major increases in productivity.
2. Excessive moisture in the air discharge line has caused two flowmeters to fail and has significantly degraded the accuracy of the air discharge measurements. The measured air discharge is 11-14% less than the inlet flow.
3. The high speed video system has been plagued by numerous electrical and mechanical problems. In many cases the picture quality has been poor. A scheme for synchronizing the video with other measurements has been perfected.
4. Successful test protocols have been devised. The control and data acquisition system has been mastered.

5. The measured air flowrates may be 10-30% high because they have not been corrected for actual air density and nonuniform velocity profiles.
6. Additional tests are needed to more nearly complete the systematic variation of controllable parameters illustrated in Figure 7.
7. The vacuum-discharge characteristics of the ejector vacuum pump have been defined by equation (2). High vacuum is associated with low air flowrates and high power requirements. These results are a basic element in the new design procedure.
8. Vacuum transport exhibits sensitive dependence on initial conditions, a hallmark of chaotic dynamical systems. Even after 25 periodic flushes, the details of the flow are not periodic.
9. When valves cycle frequently, the vacuum does not recover fully between flushes, leading to lower peak inlet velocities.
10. Instantaneous vacuum profiles indicate that regions of larger than normal loss are localized in space and exist only for brief instants. These regions are associated with the transitory existence of fluid or foam slugs which bridge the pipe bore. Normally the flow regime is stratified-smooth or stratified-wavy. Small increases in vacuum in the direction of flow are sometimes observed.
11. Profiles of time average vacuum show that the loss of vacuum in a straight pipe is small. The behavior of the time average vacuum at transducers 4 and 5 appears anomalous, but cannot be attributed to instrumentation problems. The vacuum loss decreases as the flow moves away from the inlet valve, probably because the flow becomes less vigorous. The vacuum loss profiles are highly nonlinear, suggesting that the flow is not fully developed.
12. Increasing the water volume from 0.5 to 1.7 liters per flush produces

only small increases in time average vacuum loss. Larger volumes may increases the loss considerably.

13. Increasing the valve open time decreases the loss of time average vacuum near the inlet valve, but increases the loss farther downstream. The reason for this inversion is not understood.

14. Increasing the period between flushes from 10 to 20 s produces a larger loss of time average vacuum near the inlet valve, but reduces the loss farther downstream. The reason is unknown.

15. Periodic-flush urinal tests were run with flows simulating populations of 45-412 persons. The air to water volumetric ratios ranged from 32-236, far larger than in residential vacuum sewer practice.

16. The homogeneous and Lockhart-Martinelli models tend to underpredict time average vacuum losses near the inlet valve and overpredict farther downstream. The homogeneous model is conservative in most cases. Both models are too simple to simulate the real physics of vacuum sewer flow.

17. Equation (4) is a first attempt at a correlation for the volume of air admitted in a single urinal flush as a function of controllable parameters. Additional data are needed to define all effects. This type of correlation will be a keystone of the new design procedure.

18. The research program to understand shipboard vacuum transport is well underway, but many more tests are needed to resolve the outstanding questions.

ACKNOWLEDGMENTS

The authors offer sincere thanks to the many persons whose efforts have contributed to this research:

Fred W. Burns, DTRC
Anthony T. Rodriguez, DTRC
Hank Lobe, DTRC
Walter Hunt, DTRC
Craig Alig, DTRC
Professor Frank Gomba, USNA
R. Bruce Bowers, West Virginia University
Benjamin D. Gray

TABLE 1. SUMMARY OF MEASUREMENTS AND INSTRUMENTS

MEASUREMENT	INSTRUMENT(S)
VACUUM PRESSURE	10 pressure transducers
AIR FLOWRATE	4 inlet stack velocity transducers 1 discharge velocity transducer
WATER FLOWRATE	3 urinal feed water meters 3 water closet bowl feed water meters 1 collection tank water level transducer 1 collection tank discharge water meter
TEMPERATURE	1 inlet water thermistor 1 inlet air thermistor 1 discharge air thermistor
POWER	1 digital wattmeter
HIGH SPEED VIDEO RECORDING	2 cameras

TABLE 2. LISTING OF STATIONS OF VARIOUS OBJECTS FOR NORMAL FLOW DIRECTION

OBJECT	STATION (meters)	COMMENTS
WATER CLOSET 3	0 + 56.89	inlet section
WATER CLOSET 2	55.98	inlet section
WATER CLOSET 1	55.24	inlet section
URINAL 1	54.44	inlet section
URINAL 2	53.55	inlet section
URINAL 3	52.79	inlet section
INLET TEE	51.49	inlet section
START OF ACRYLIC PIPE	50.79	upper L (long leg)
TRANSDUCER 1	46.04	upper L (long leg)
TRANSDUCER 6	44.56	upper L (long leg)
TRANSDUCER 3	43.04	upper L (long leg)
TRANSDUCER 4	41.57	upper L (long leg)
TRANSDUCER 5	40.27	upper L (long leg)
TRANSDUCER 10	38.61	upper L (long leg)
TRANSDUCER 7	37.05	upper L (long leg)
HIGH ELBOW	34.73	upper L (short leg)
TRANSDUCER 8	33.85	upper L (short leg)
TRANSDUCER 9	32.25	upper L (short leg)
HIGH 1/2-U	28.61	upper L (short leg)
LOW 1/2-U	28.28	lower L
LOW SWEEP	22.34	lower L
END OF ACRYLIC PIPE	6.95	discharge section
BOTTOM OF RISER PIPE	4.43	discharge section
TOP OF RISER PIPE	0.89	discharge section
TRANSDUCER 2	0 + 0.00	ejector manifold

TABLE 3. LISTING OF STATIONS OF VARIOUS OBJECTS FOR REVERSE FLOW DIRECTION

OBJECT	STATION (meters)	COMMENTS
WATER CLOSET 3	0 + 56.28	inlet section
WATER CLOSET 2	55.37	inlet section
WATER CLOSET 1	54.63	inlet section
URINAL 1	53.83	inlet section
URINAL 2	52.94	inlet section
URINAL 3	52.18	inlet section
INLET TEE	50.88	inlet section
START OF ACRYLIC PIPE	49.25	lower L
LOW SWEEP	33.87	lower L
LOW 1/2-U	27.93	lower L
HIGH 1/2-U	27.60	upper L (short leg)
TRANSDUCER 9	23.97	upper L (short leg)
TRANSDUCER 8	22.34	upper L (short leg)
HIGH ELBOW	21.48	upper L (long leg)
TRANSDUCER 7	19.16	upper L (long leg)
TRANSDUCER 10	17.60	upper L (long leg)
TRANSDUCER 5	15.95	upper L (long leg)
TRANSDUCER 4	14.64	upper L (long leg)
TRANSDUCER 3	13.17	upper L (long leg)
TRANSDUCER 6	11.65	upper L (long leg)
TRANSDUCER 1	10.17	upper L (long leg)
END OF ACRYLIC PIPE	6.02	discharge section
BOTTOM OF RISER PIPE	4.43	discharge section
TOP OF RISER PIPE	0.89	discharge section
TRANSDUCER 2	0 + 0.00	ejector manifold

TABLE 4. SCALE FACTORS AND SETUP DATA July - August, 1988

UNIT NAME	FUNCTION	BOARD	INTERFACE CHANNEL TYPE	#	ASCII CHAR.	SCALE FACTOR	OFFSET CONST.	UNITS
U-1	FILL	PIO-12	DO	1	1			
	FLUSH	PIO-12	DO	1	2			
	HOLD	PIO-12	DO	1	4			
	HOH COUNT	CTM-05	CTR	1		5.426	0	ml
	AIR VEL	DASH 16#2	AI	3		6.096	0	m/sec
U-2	FILL	PIO-12	DO	1	8			
	FLUSH	PIO-12	DO	1	16			
	HOLD	PIO-12	DO	1	32			
	HOH COUNT	CTM-05	CTR	2		5.398	0	ml
	AIR VEL	DASH 16#2	AI	4		6.096	0	m/sec
U-3	FILL	PIO-12	DO	2	1			
	FLUSH	PIO-12	DO	2	2			
	HOLD	PIO-12	DO	2	4			
	HOH COUNT	CTM-05	CTR	3		5.424	0	ml
	AIR VEL	DASH 16#2	AI	5		6.096	0	m/sec
WC-1	FILL	PIO-12	DO	0	2			
	FLUSH	PIO-12	DO	0	1			
	HOH COUNT	CTM-05	CTR	4		4.584	0	ml
	AIR VEL	DASH 16#2	AI	6		6.096	0	m/sec
WC-2	FILL	PIO-12	DO	0	8			
	FLUSH	PIO-12	DO	0	4			
	HOH COUNT	CTM-05	CTR	5		4.541	0	ml
WC-3	FILL	PIO-12	DO	0	32			
	FLUSH	PIO-12	DO	0	16			
	HOH COUNT	DASH 16#2	CTR	0		4.535	0	ml
INLET	HOH TEMP	DASH 16#2	AI	1		48.719	-1.054	C
	AIR TEMP	DASH 16#2	AI	0		48.719	-1.054	C
DISCH.	AIR VEL	DASH 16#2	AI	12		5.080	0	m/sec
	HOH COUNT	DASH 16#1	CTR	0		26.300	0	ml
	HOH LEVEL	DASH 16#2	AI	11		2.761	0	kPa
	AIR TEMP	DASH 16#2	AI	8		48.719	-1.054	C
	WATT METER	DASH 16#2	AI	15		1.000	0	kW
TEST SECTION	PRESS. 1	DASH 16#1	AI	1		20.620*	-V0**	kPa
	PRESS. 2	DASH 16#1	AI	2		20.580	-V0	kPa
	PRESS. 3	DASH 16#1	AI	3		20.580	-V0	kPa
	PRESS. 4	DASH 16#1	AI	4		20.577	-V0	kPa
	PRESS. 5	DASH 16#1	AI	5		20.612	-V0	kPa
	PRESS. 6	DASH 16#1	AI	6		20.557	-V0	kPa
	PRESS. 7	DASH 16#1	AI	7		20.584	-V0	kPa
	PRESS. 8	DASH 16#1	AI	8		20.585	-V0	kPa
	PRESS. 9	DASH 16#1	AI	9		20.589	-V0	kPa
	PRESS. 10	DASH 16#1	AI	10		20.583	-V0	kPa
VIDEO	PRE-TRIGGER	DASH 16#1	DO	0				
	POST-TRIGG.	DASH 16#1	DO	1				
	STROBE PULSE	DASH 16#1	AI	0				

* changed daily

** V0 = voltage at atmospheric pressure

DO = digital output AI = analog input CTR = counter

TABLE 5. SUMMARY OF INTERMITTENT URINAL RUNS PERFORMED DURING JULY-AUGUST, 1988 - NORMAL DIRECTION

TEST IDENTIFICATION CODE	RUN	t	T	V
D2-S0-L0-U1-W0-N-I	1	1	**	1
	2	1	**	2
	3	2	**	3
	4	2	**	4
	5	1	**	1
	6	1	**	2
	7	1	**	3
	8	1	**	4
	9	2	**	1
	10	2	**	2
	11	2	**	3
	12	2	**	4
	13*	2.6	5	0.9
	14*	2.6	10	1.8
	15*	2.6	5	0.9
	16*	2.8	10	1.8
	17*	2.7	10	0.5
	18*	2.8	10	0.9
	19*	3.1	10	1.7
	20*	3.6	20	0.5
	21*	3.7	20	0.9
	22*	4.6	20	3.3
	23	3	**	0.5
	24	2	**	0.5
	25	1	**	0.5
	26	0.5	**	0.5

* = actual rather than nominal values
** = "infinite" (single flush)
t = average valve open time per cycle (sec)
T = cycle period (sec)
V = average fill volume (liters) per cycle

TABLE 6. SUMMARY OF INTERMITTENT URINAL RUNS PERFORMED DURING JULY-AUGUST, 1988 - REVERSE DIRECTION

TEST IDENTIFICATION CODE	RUN	t	T	V
D2-S0-L0-U1-W0-R-I	1	1	**	1
	2	1	**	2
	3	2	**	3
	4	2	**	4
	5	1	**	1
	6	1	**	2
	7	1	**	3
	8	1	**	4
	9	2	**	1
	10	2	**	2
	11	2	**	3
	12	2	**	4
	13*	2.2	5	0.9
	14*	2.5	10	1.8
	15*	2.2	5	0.9
	16*	2.8	10	1.8
	17*	2.8	10	0.5
	18*	2.8	10	0.9
	19*	3.0	10	1.7
	20*	3.8	20	0.5
	21*	3.8	20	0.9
	22*	5.0	20	3.4
	23	3	**	0.5
	24	2	**	0.5
	25	1	**	0.5
	26	0.5	**	0.5

* = actual rather than nominal values
** = "infinite" (single flush)
t = average valve open time per cycle (sec)
T = cycle period (sec)
V = average fill volume (liters) per cycle

TABLE 7. SUMMARY OF INTERMITTENT WATER CLOSET RUNS PERFORMED DURING JULY-AUGUST,1988

TEST IDENTIFICATION CODE	RUN	p	T	V
D2-S0-L0-U0-W1-N-I	1	22	**	0.2
	2	50	**	0.2
	3	74	**	0.2
	4	74	10	0.2
	5	50	10	0.2
	6	22	10	0.2
	7	22	10	0.2
	8	50	10	0.2
	9	74	10	0.2
	10	50	10	0.2
	12	26	10	0.2
	13	50	10	0.2
D2-S0-L0-U0-W1-R-I	1	22	**	0.2
	2	50	**	0.2
	3	74	**	0.2
	4	74	10	0.2
	5	50	10	0.2
	6	22	10	0.2
	7	22	10	0.2
	8	50	10	0.2
	9	74	10	0.2
	10	50	10	0.2
	12	26	10	0.2
	13	50	10	0.2

** = "infinite" (single flush)
p = flush water pressure (psig)
T = cycle period (sec)
V = average fill volume (liters) per cycle added to the bowl

TABLE 8. AVERAGE FLOWRATES AND POPULATION EQUIVALENTS.

NORMAL DIRECTION:

RUN#	delta T sec	AVERAGE WATER FLOW l/sec	EQUIV. DESIGN POPUI'N persons	AIR/WAT RATIO scm/m**3
N13	2.6	0.211	403	37.97
N14	2.6	0.216	412	29.11
N15	2.6	0.214	409	37.18
N16	2.8	0.212	404	32.93
N17	2.7	0.046	88	146.02
N18	2.8	0.086	165	74.22
N19	3.1	0.169	323	37.98
N20	3.6	0.024	45	234.89
N21	3.7	0.044	85	123.67
N22	4.6	0.164	313	31.87

REVERSE DIRECTION:

RUN#	delta T sec	AVERAGE WATER FLOW l/sec	EQUIV. DESIGN POPUL'N persons	AIR/WAT RATIO scm/m**3
R13	2.2	0.210	400	37.81
R14	2.5	0.210	400	29.60
R15	2.2	0.206	394	37.76
R16	2.8	0.204	389	32.09
R17	2.8	0.046	88	146.87
R18	2.8	0.087	166	75.17
R19	3.0	0.168	321	38.65
R20	3.8	0.024	45	236.17
R21	3.8	0.044	84	121.90
R22	5.0	0.165	315	33.27

EQUIVALENT DESIGN POPULATION:

avg flow = (4.0 gal/cap-day)*(3.78542 liters/gal)
= 15.1 liters/cap-day

peaking factor, PF = 3

peak flow = 3*(15.1 liters/cap-day)*(1 day/86400 sec)
= 0.000524 liters/sec-cap

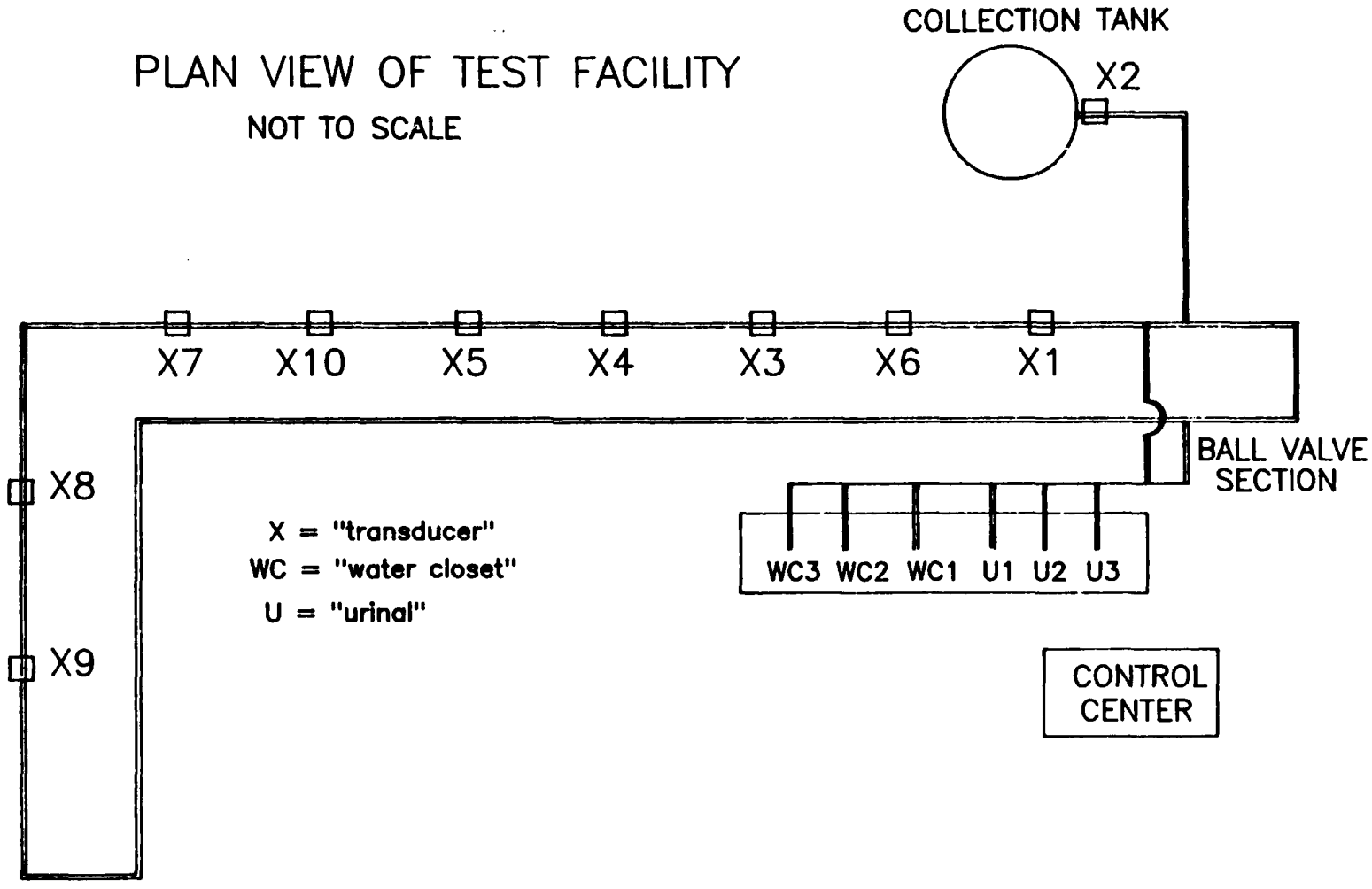

Figure 1. Plan view of test facility.

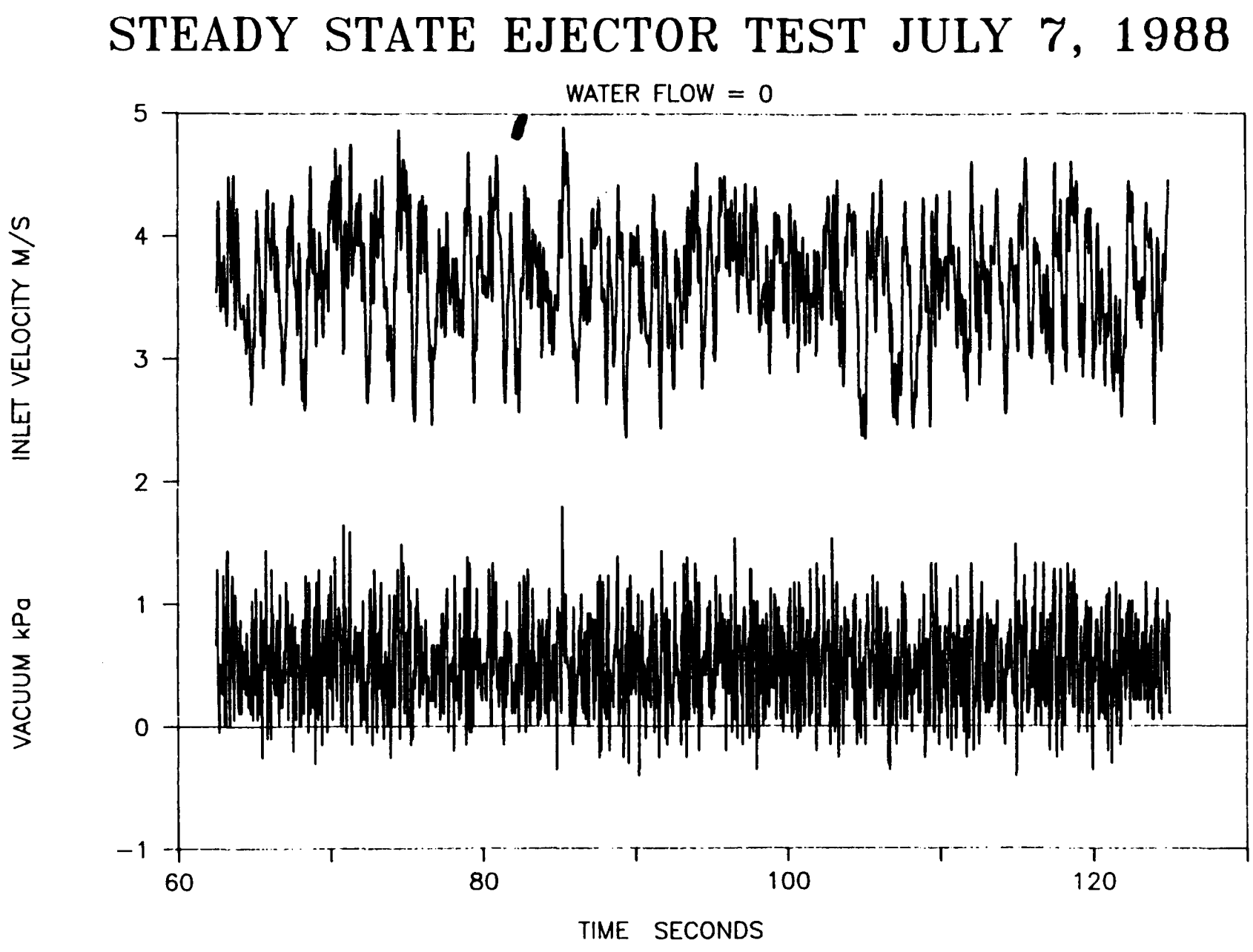

FIGURE 2. Random variablility at steady state.

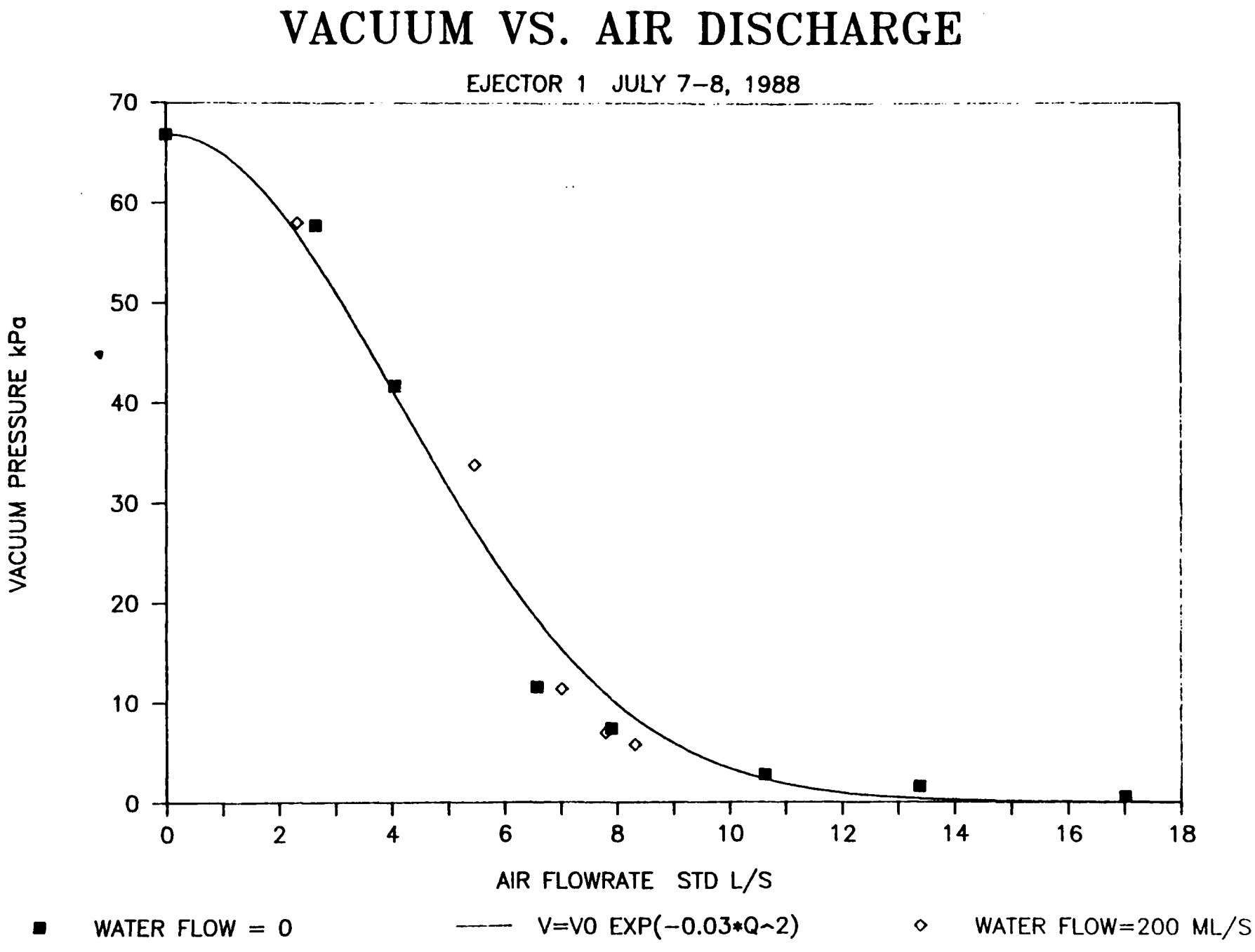

FIGURE 3. Vacuum - discharge curve for Evac ejector

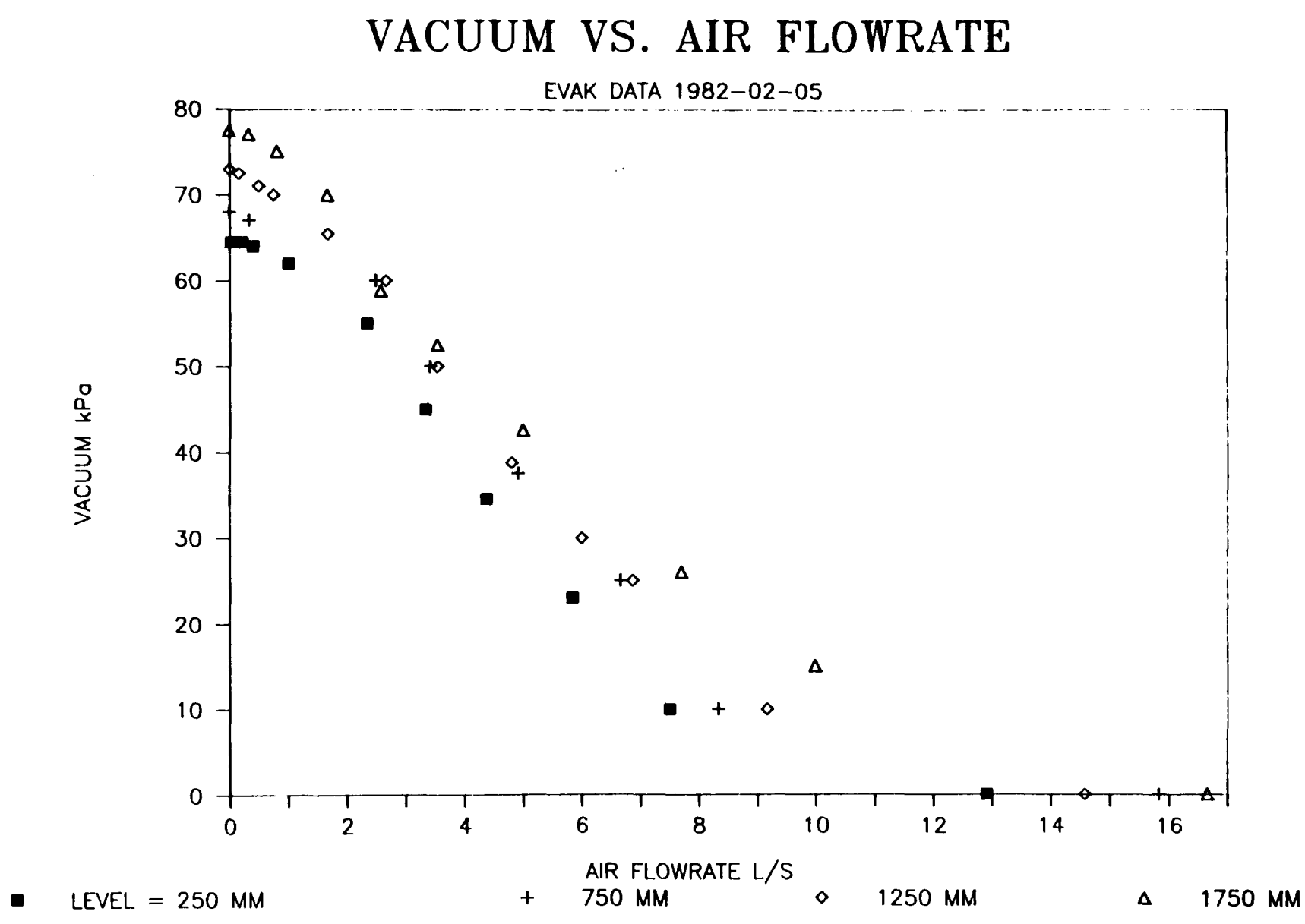

FIGURE 4. Evak test data for 184-mm impeller

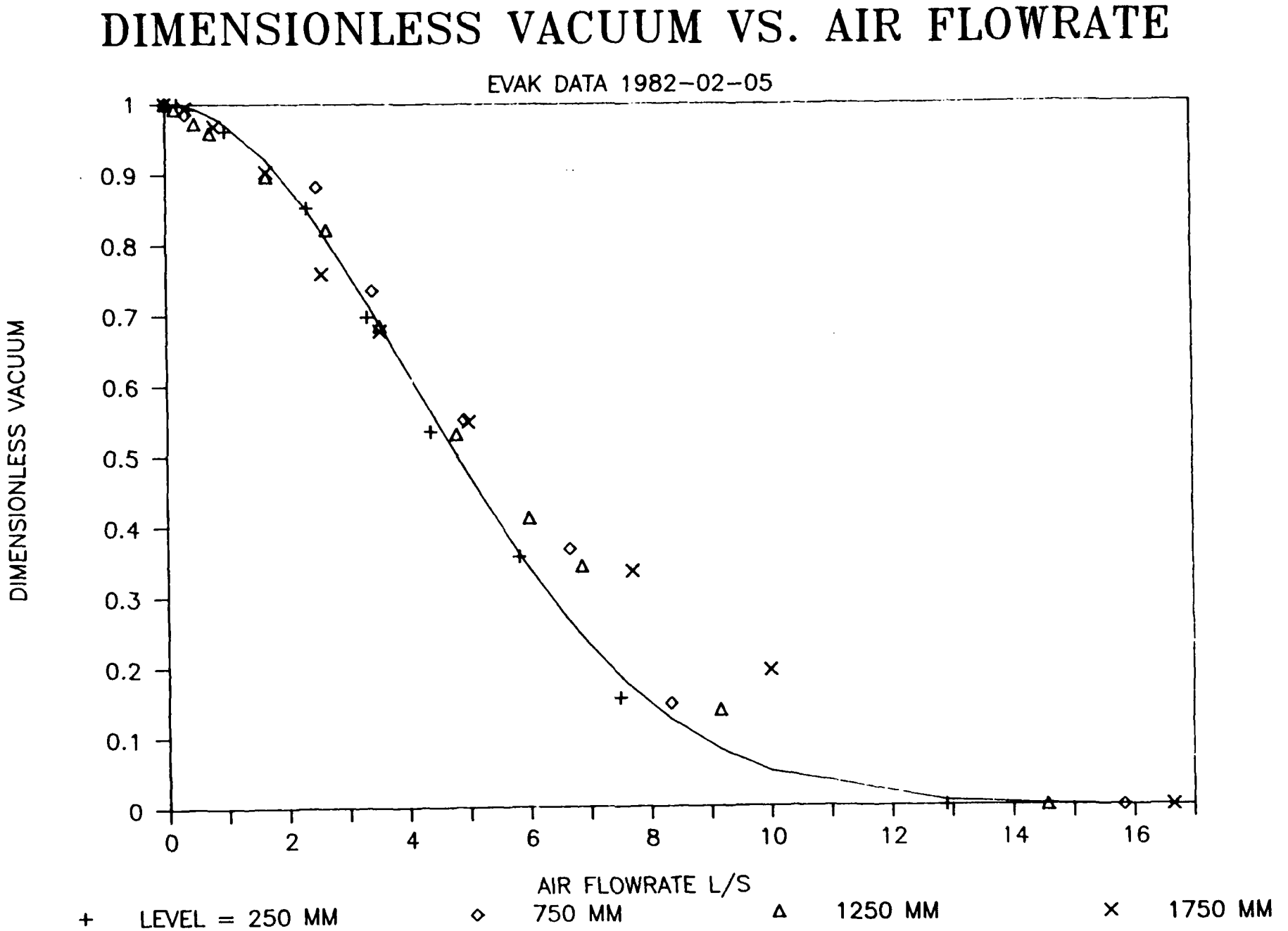

FIGURE 5. Comparison of Evak data with equation (2).

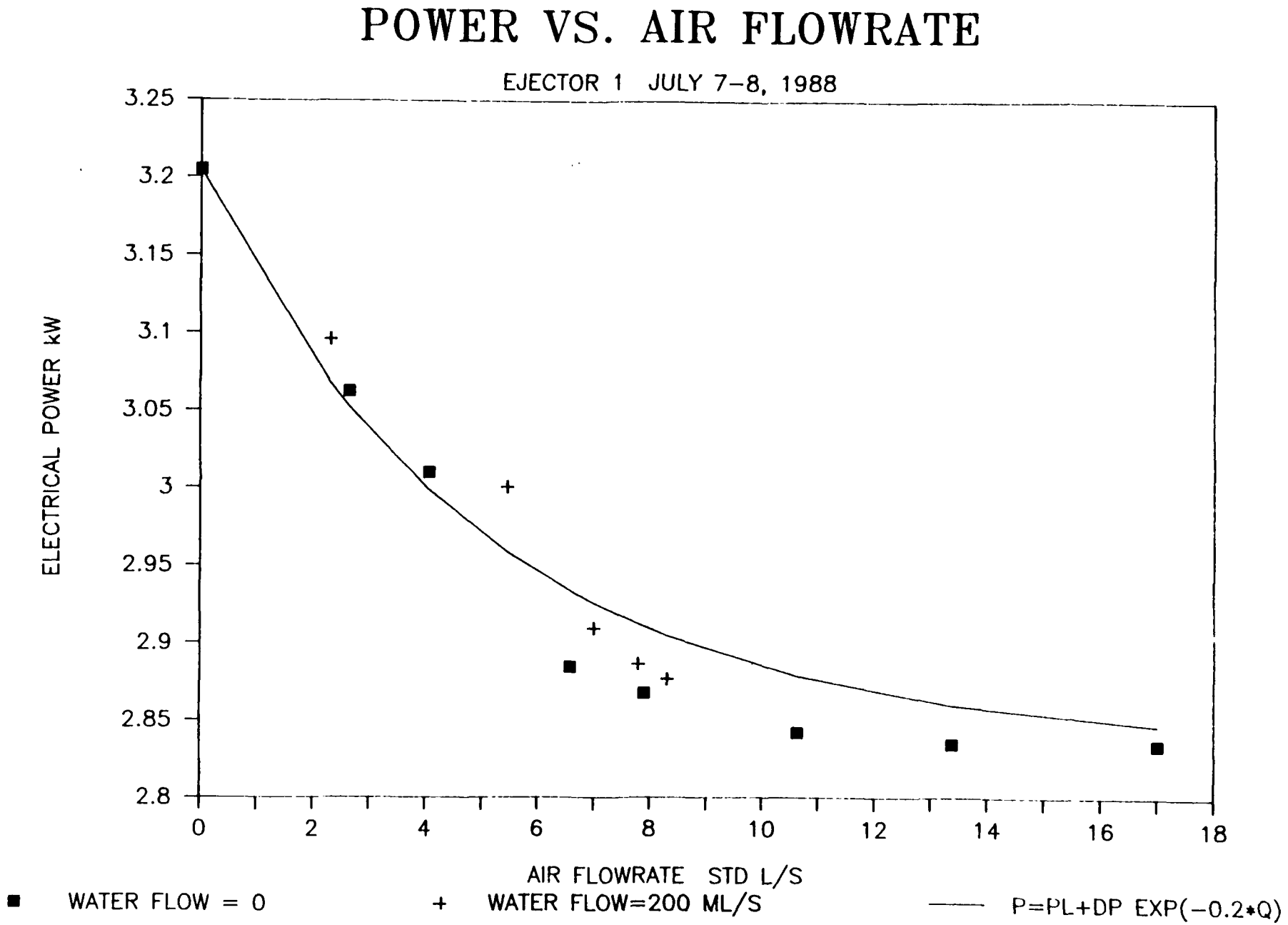

FIGURE 6. Power - discharge curve for Evac ejector.

flush period T = 5 sec

t (sec) \ V liters	0.5	1	2	3	4
1		N13 R13			
2		N15 R15			
3					

flush period T = 20 sec

t (sec) \ V liters	0.5	1	2	3	4
1					
2					
3	N20 R20	N21 R21			N22 R22

flush period T = 10 sec

t (sec) \ V liters	0.5	1	2	3	4
1			N14 R14		
2			N16 R16		
3	N17 R17	N18 R18	N19 R19		

flush period – single flush

t (sec) \ V liters	0.5	1	2	3	4
1	N25 R25	N1 R1	N2 R2	N3 R3	N4 R4
2	N24 R24	N5 R5	N6 R6	N7 R7	N8 R8
3	N23 R23	N9 R9	N10 R10	N11 R11	N12 R12
0.5	N26 R26				

FIGURE 7. Chart summary of intermittent urinal tests performed during July – August, 1988. Slope = 0, one urinal in operation, ejector set to constant run. Nominal values of V and t.

p water pres. (psig) \ T flush per. (sec)	5	10	20	single flush
22		N,R 6 N,R 7 N,R 12		N1 R1
50		N,R: 5,8, 10,13		N2 R2
74		N,R 4 N,R 9		N3 R3

FIGURE 8. Chart summary of water closet runs performed during July – August, 1988. Slope = 0, one water closet in operation. Volume added directly to bowl = 0.5 liters.

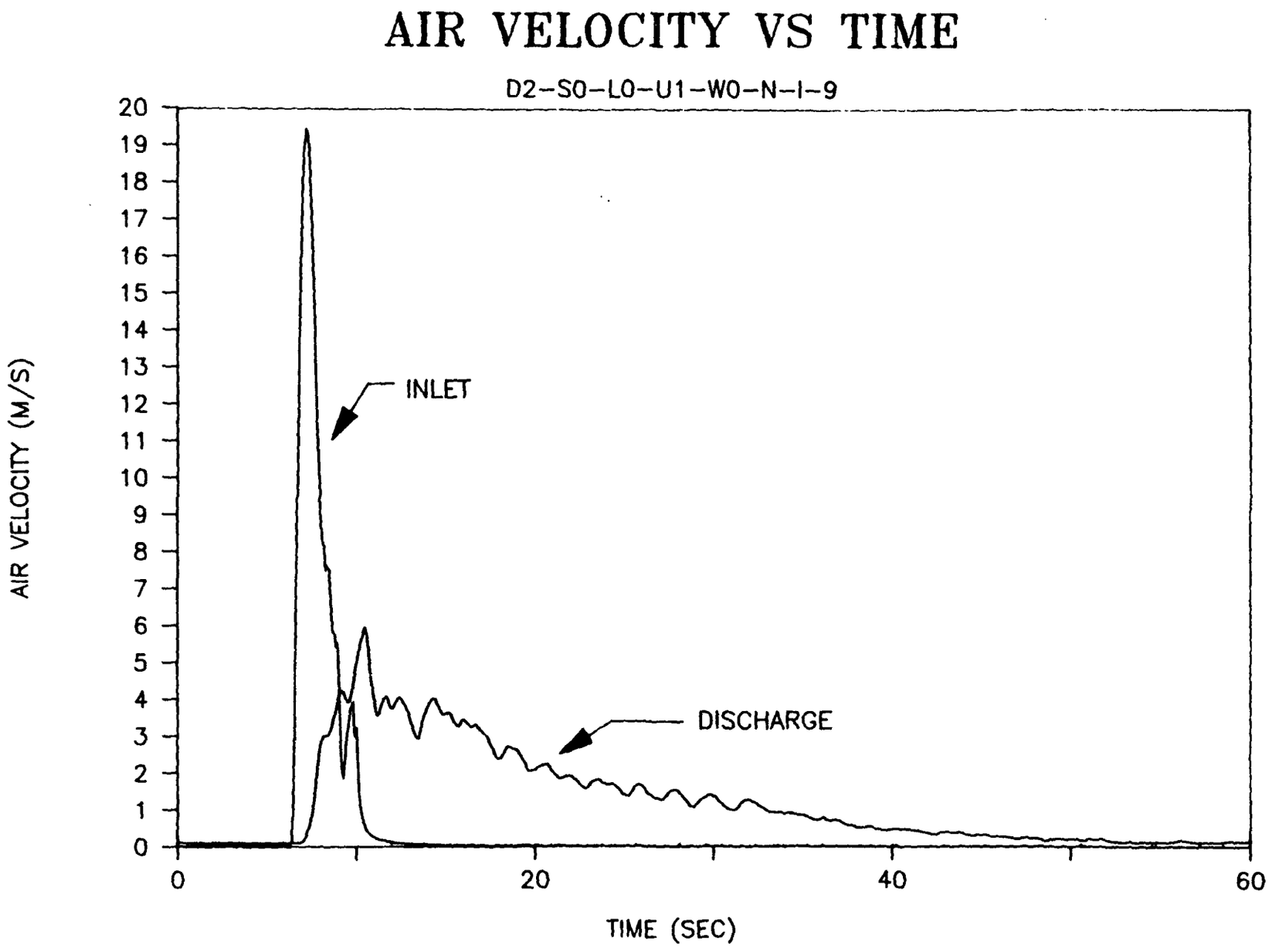

FIGURE 9. Inlet air velocity vs. time, Normal Run 9.

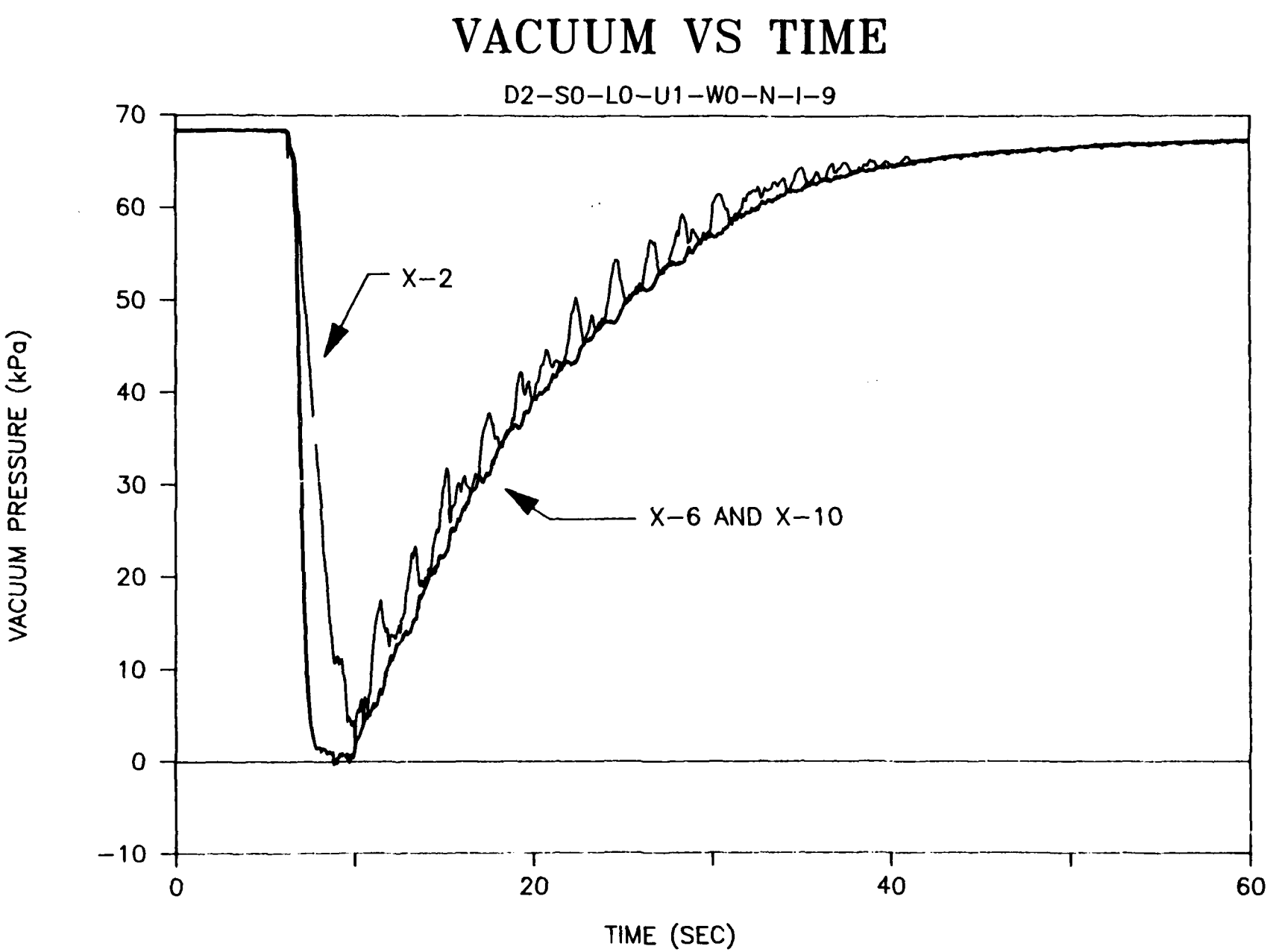

FIGURE 10. Vacuum vs. time, Normal Run 9.

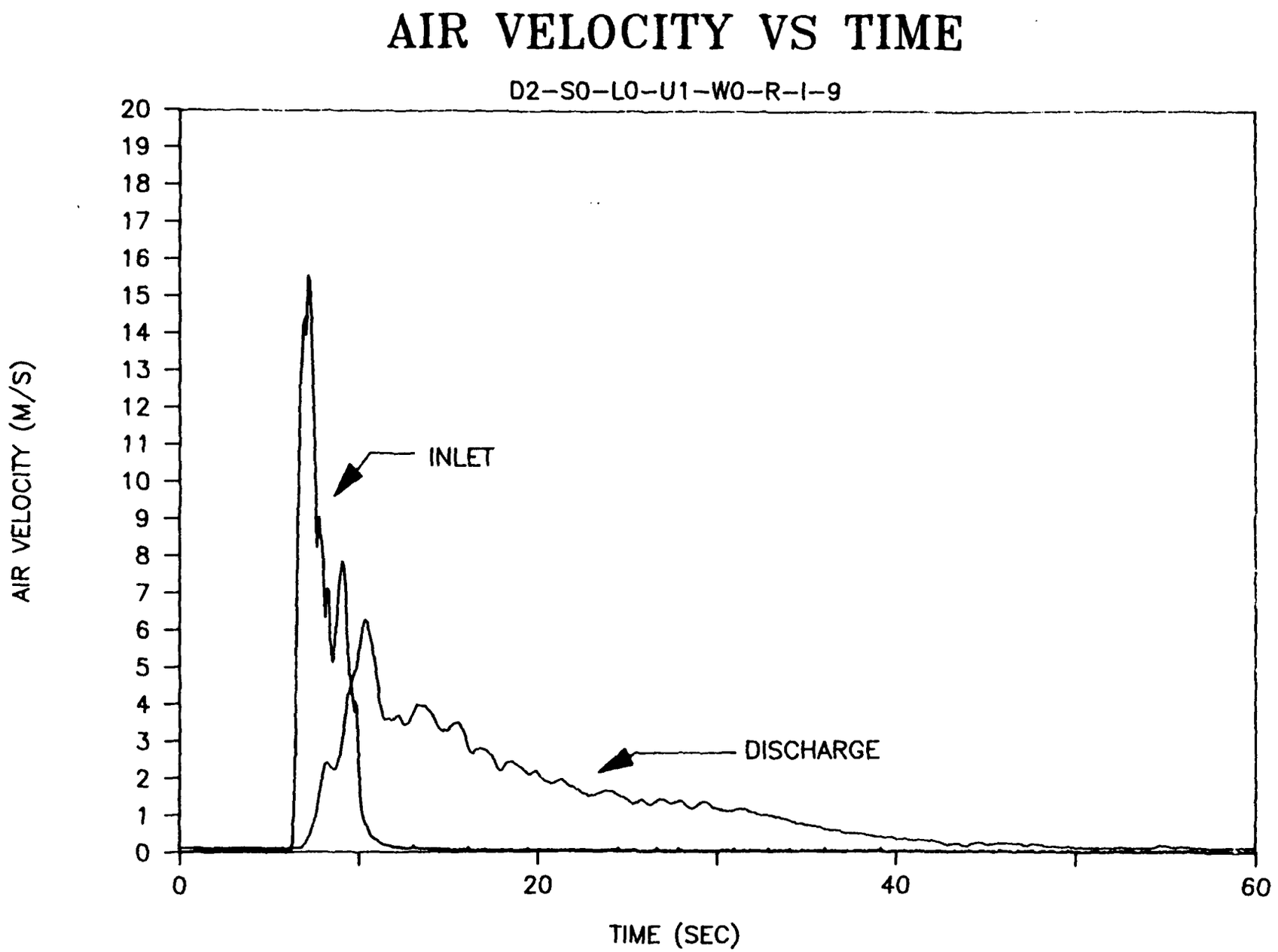

FIGURE 11. Inlet air velocity vs. time, Reverse Run 9.

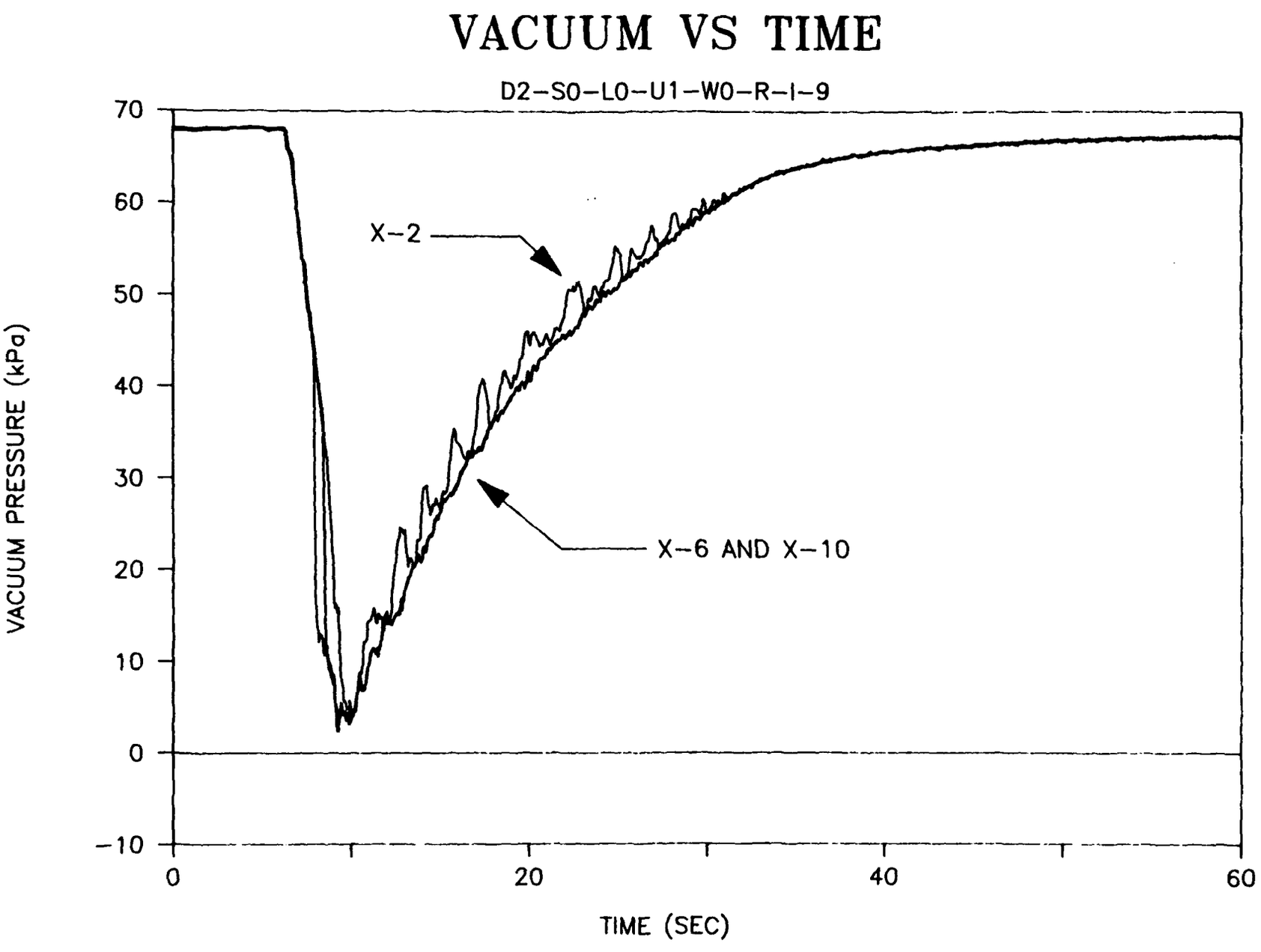

FIGURE 12. Vacuum vs. time, Reverse Run 9.

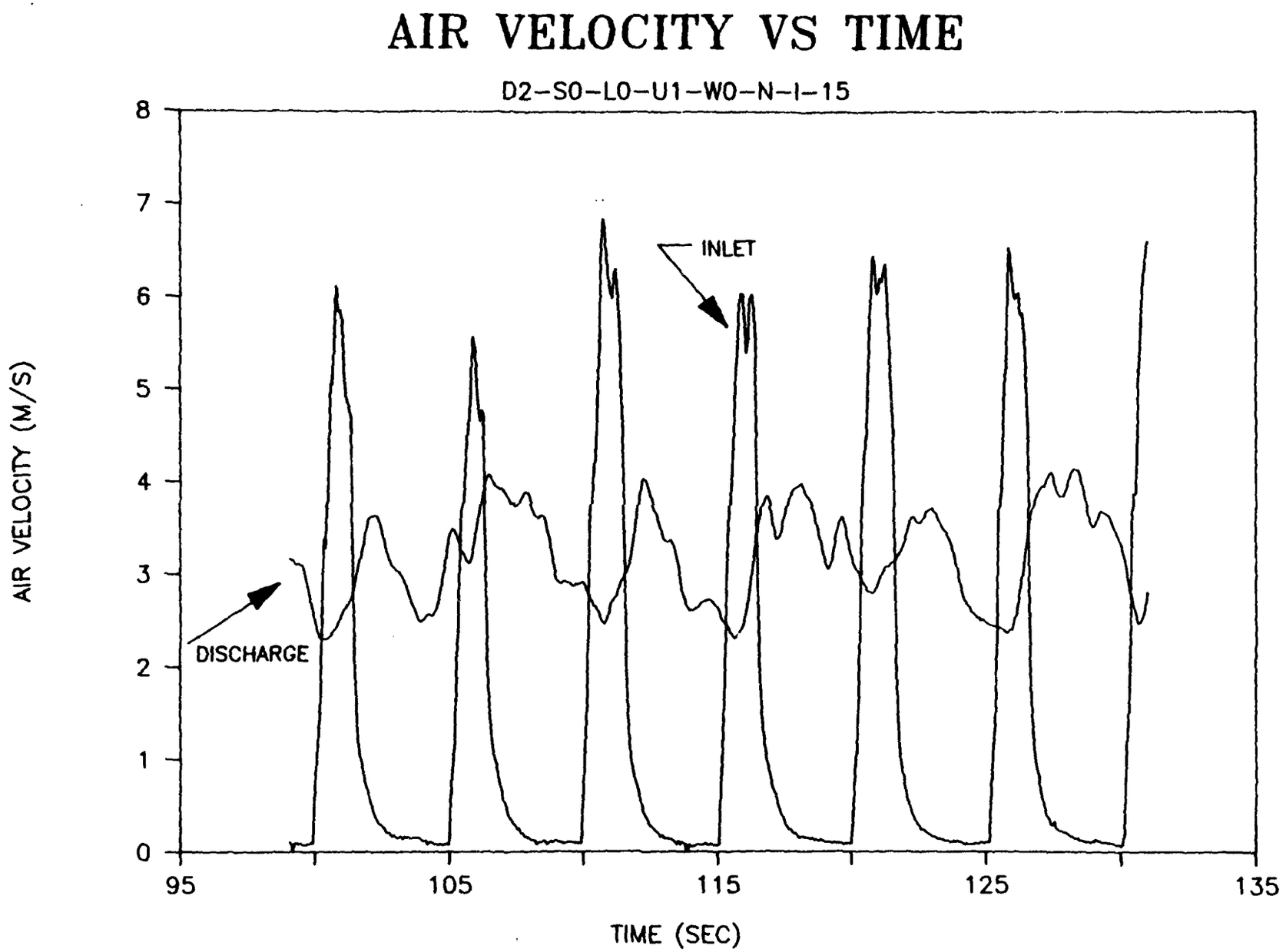

FIGURE 13. Air velocity vs. time, Normal Run 15.

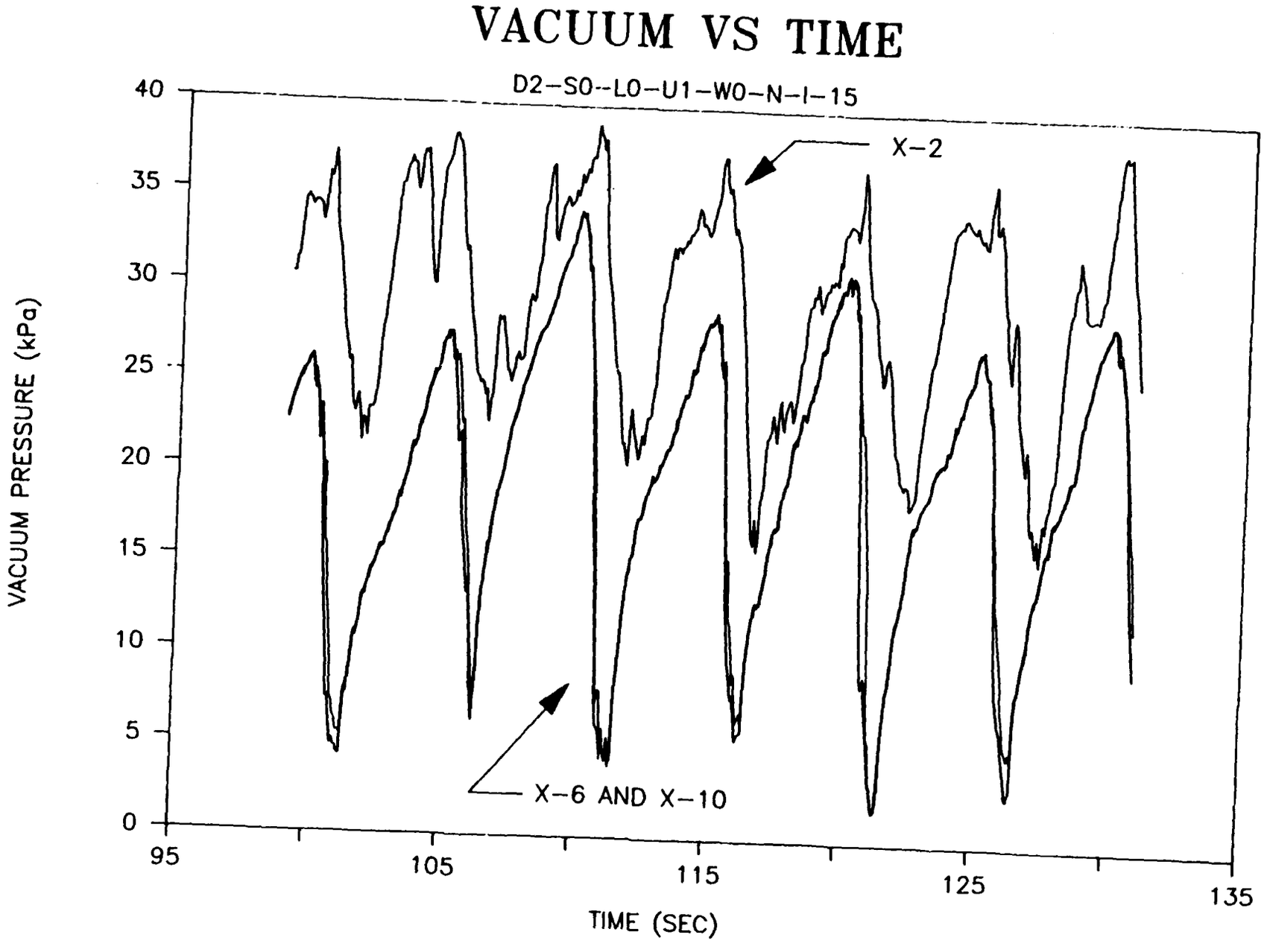

FIGURE 14. Vacuum vs. time, Normal Run 15.

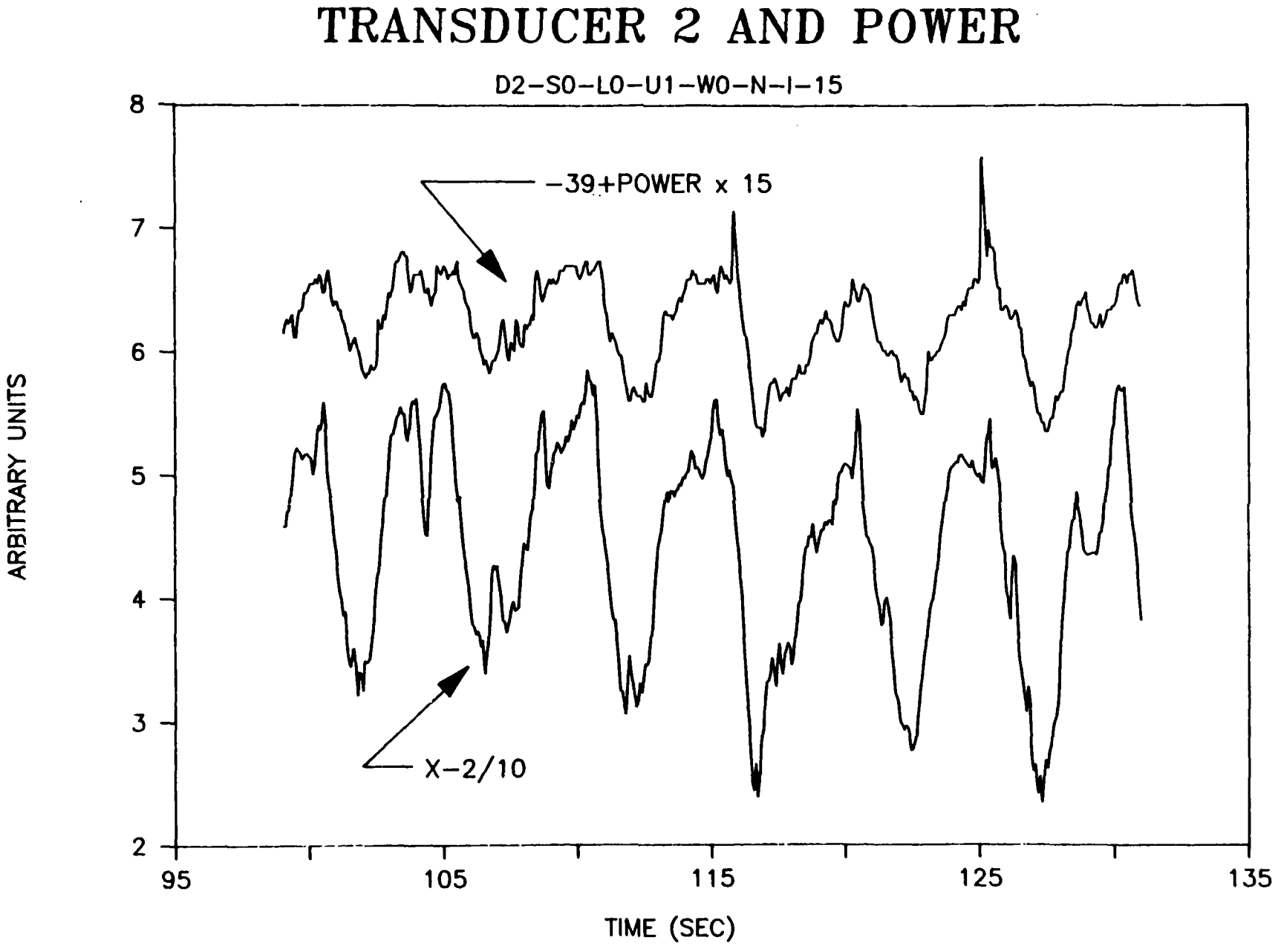

FIGURE 15. Shape similarity of manifold vacuum and power curves, Normal Run 15.

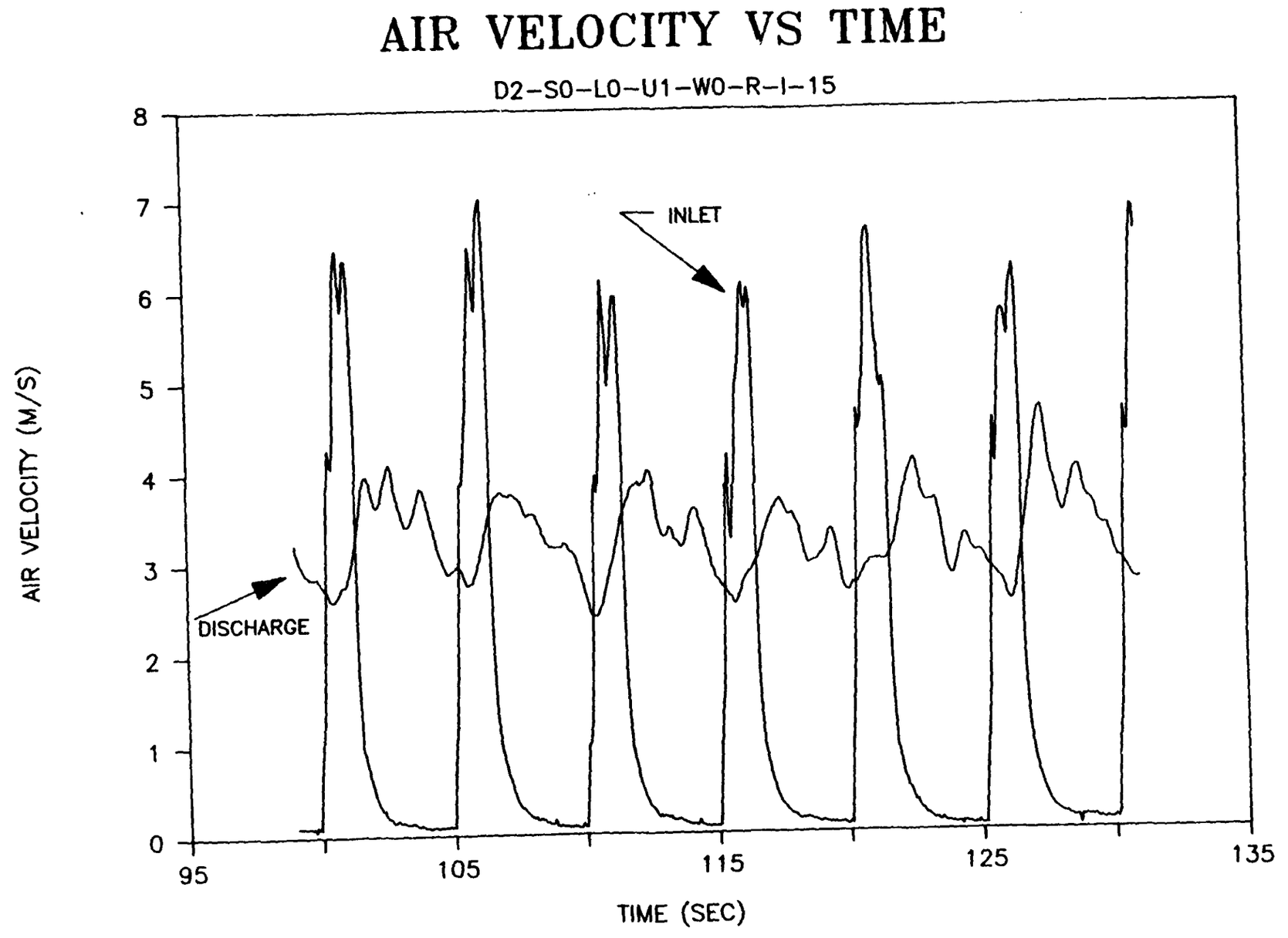

FIGURE 16. Air velocity vs. time, Reverse Run 15.

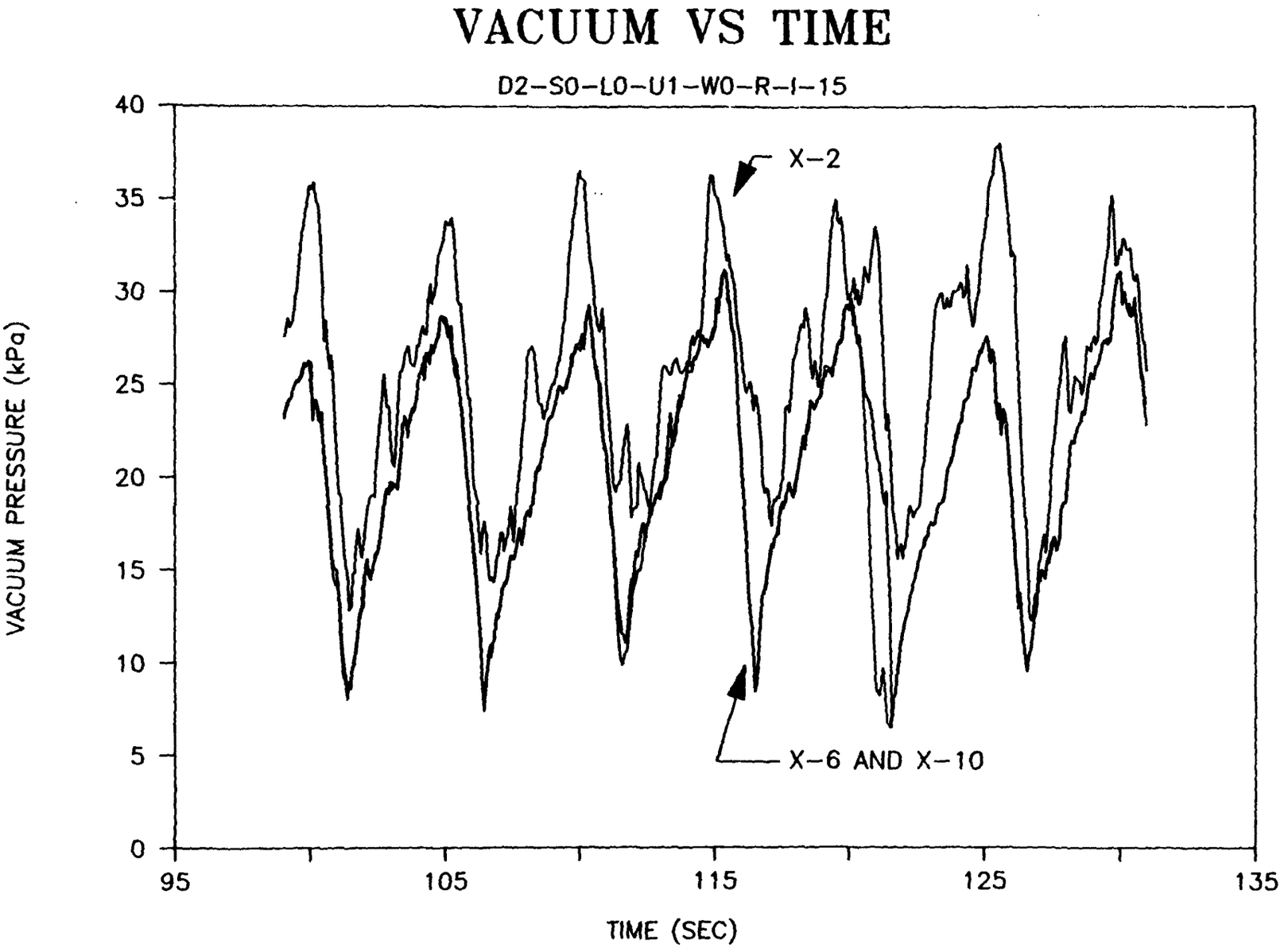

FIGURE 17. Vacuum vs. time, Reverse Run 15.

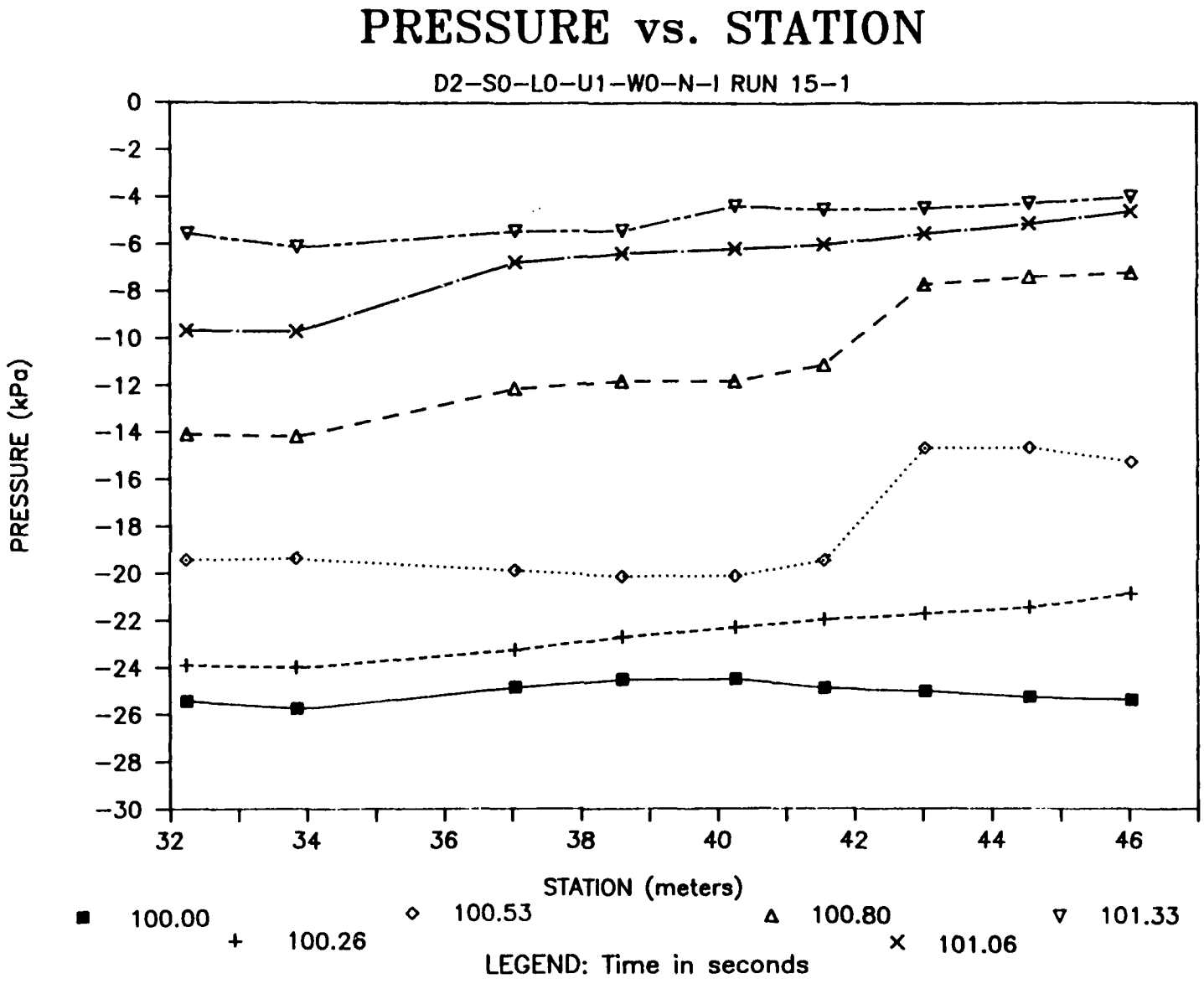

Figure 18. Instantaneous gauge pressure vs. station, Normal Run 15.
Time = 100.00 - 101.33 s.

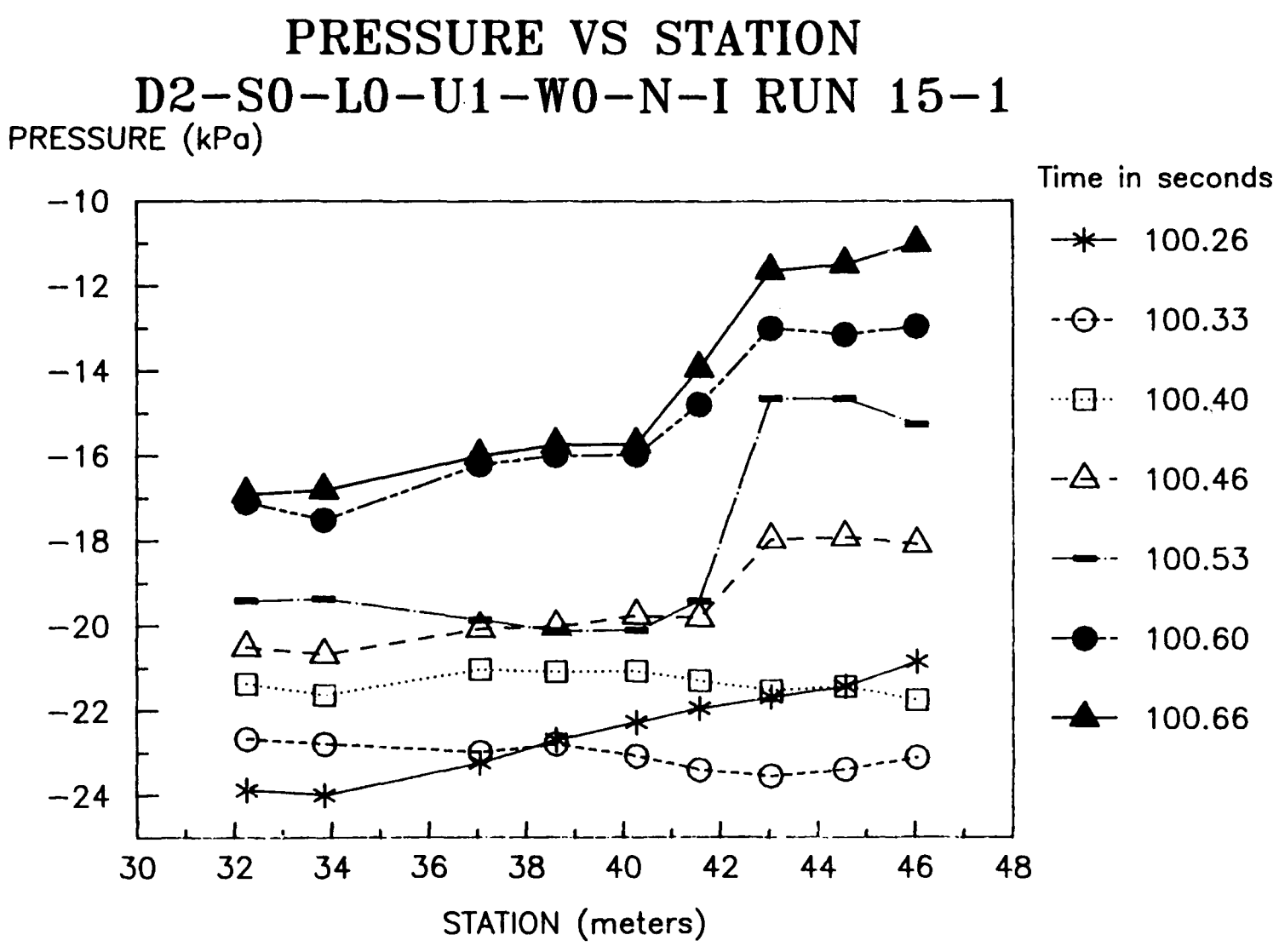

FIGURE 19. Instantaneous gauge pressure vs. station, Normal Run 15. Time = 100.26 - 100.66 s.

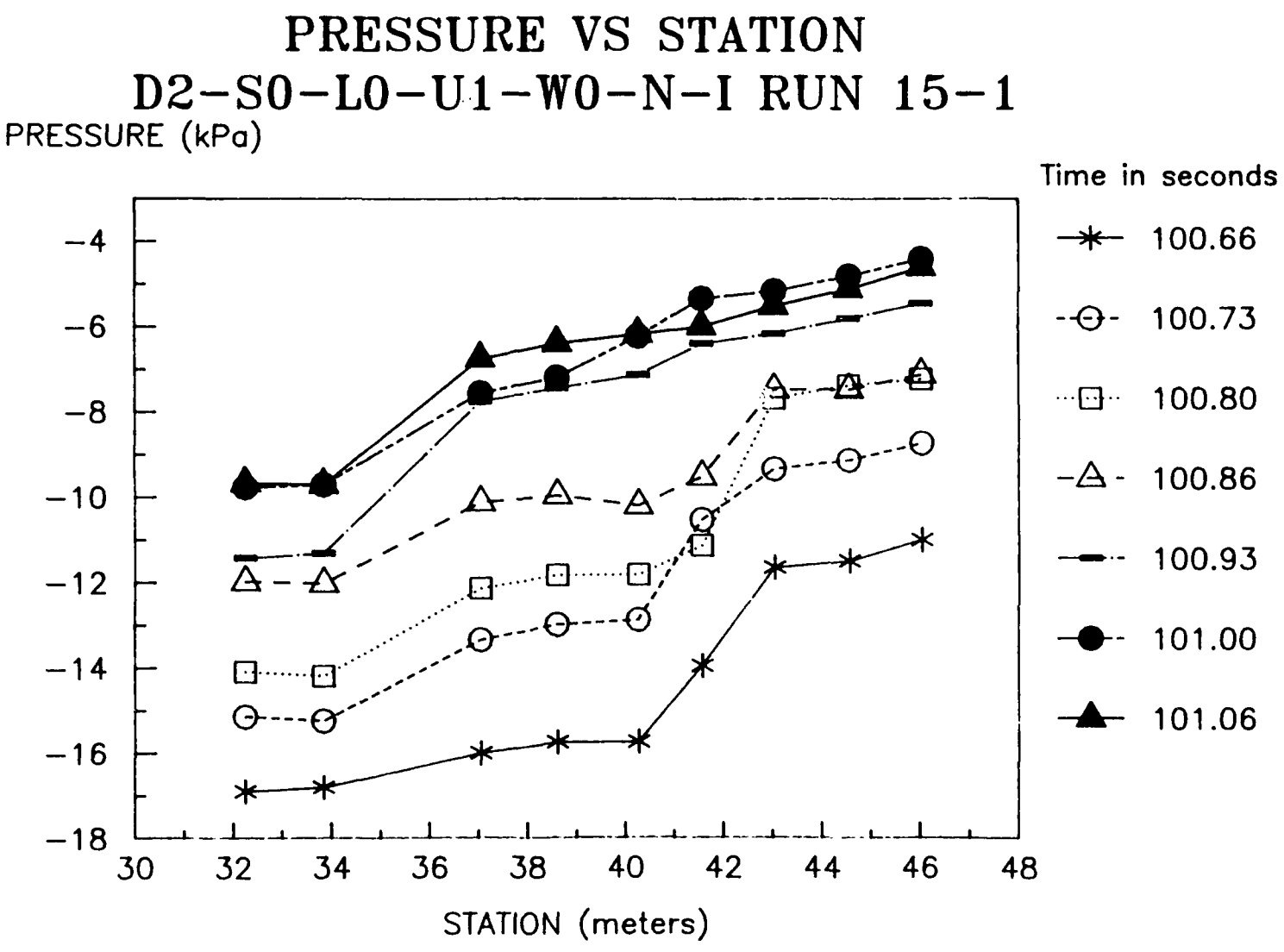

FIGURE 20. Instantaneous gauge pressure vs. station, Normal Run 15. Time = 100.66 - 101.06 s.

FIGURE 21. Example sequence of delta P vs time plots. Run N15 shown.

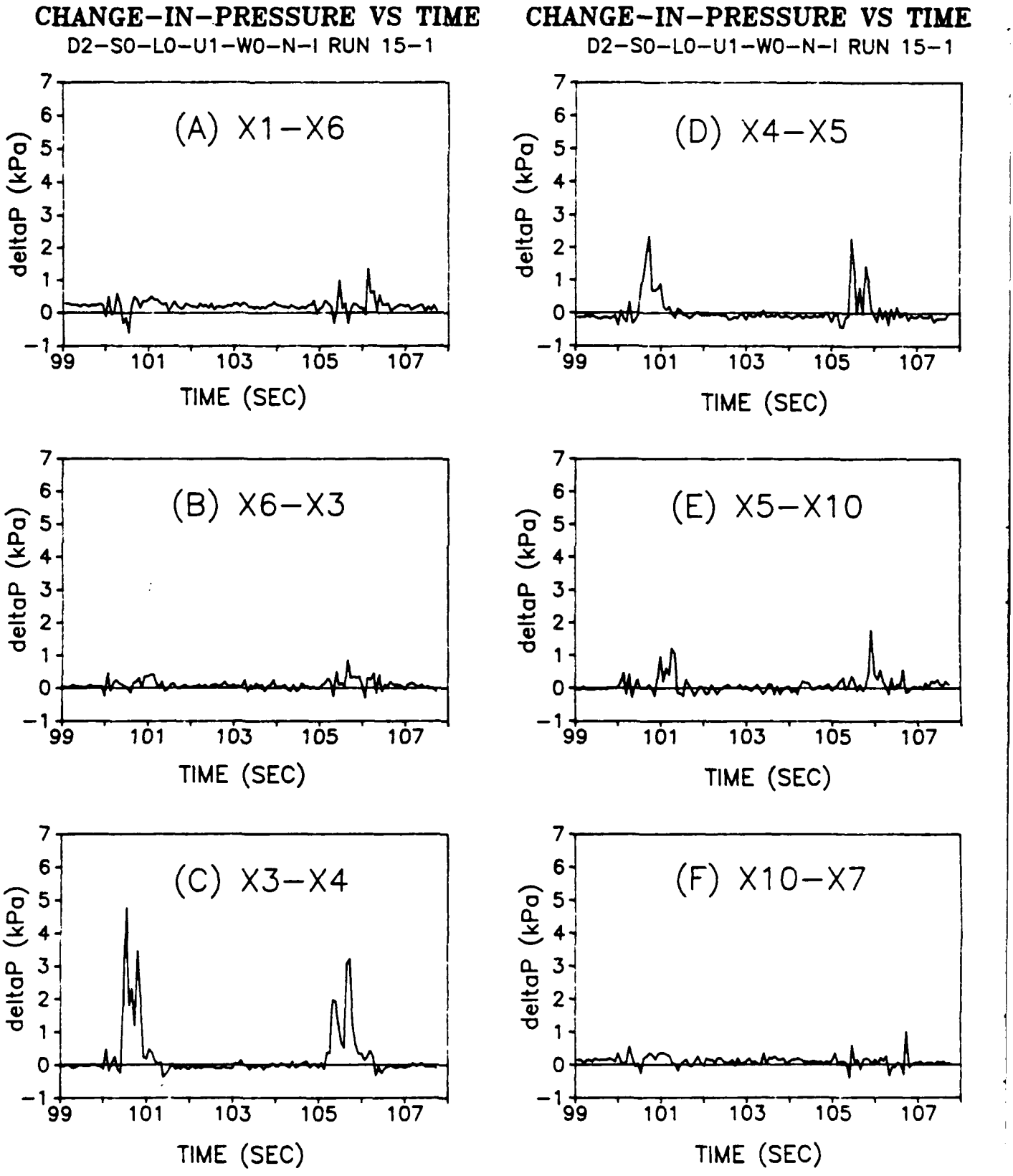

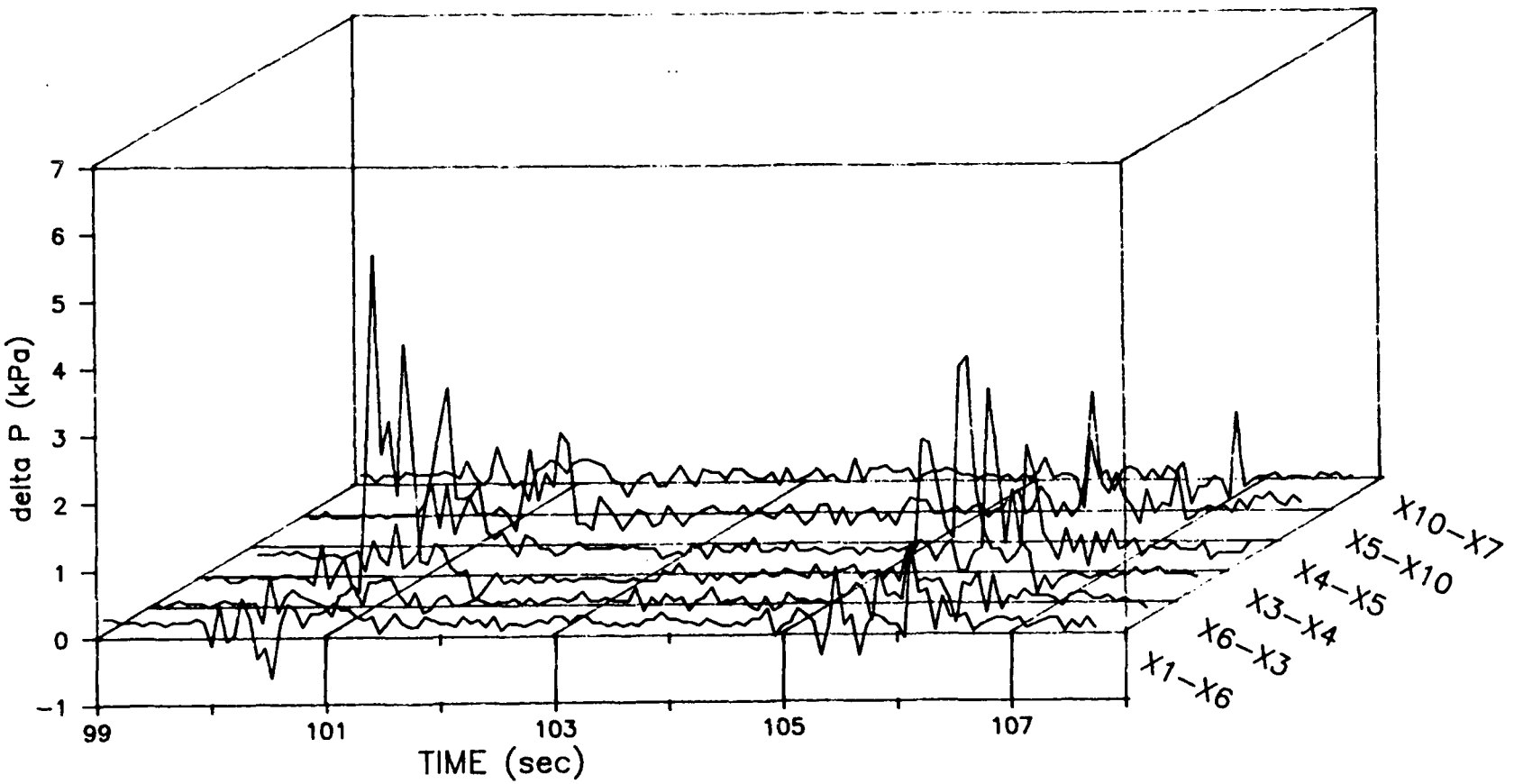

FIGURE 22. Three−dimensional plot of delta P vs. time with distance along the pipe as the third axis. Run N15 shown.

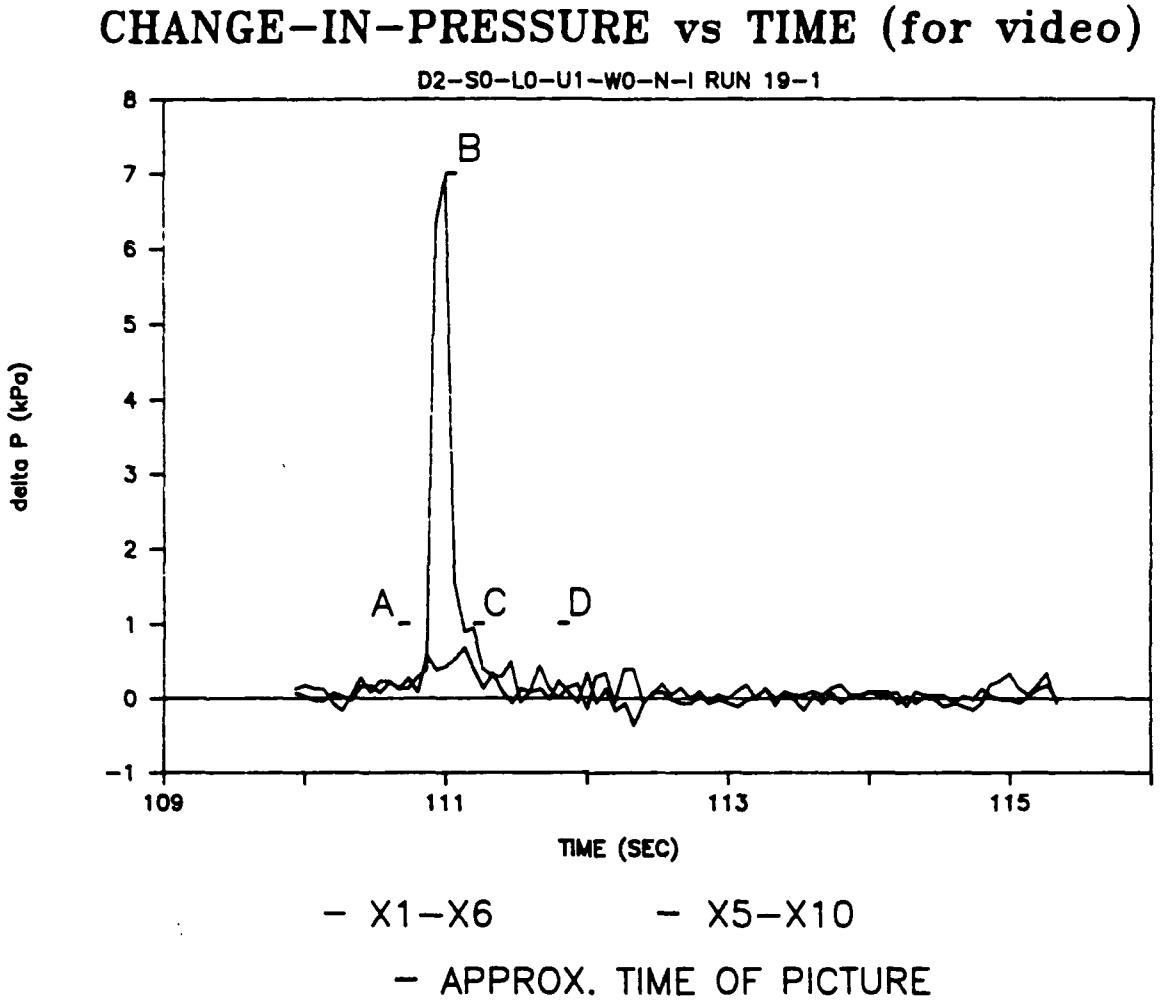

LOCATION	APPROXIMATE TIME ON PLOT	ELAPSED TIME ON VIDEO
A	110.6647 sec	12.637 sec
B	110.9980 sec	12.945 sec
C	111.1980 sec	13.009 sec
D	111.7980 sec	13.596 sec

NOTE: Approximate time on plot accurate within 0.067 sec.

FIGURE 23a. Vacuum drop vs. time, Normal Run 19.

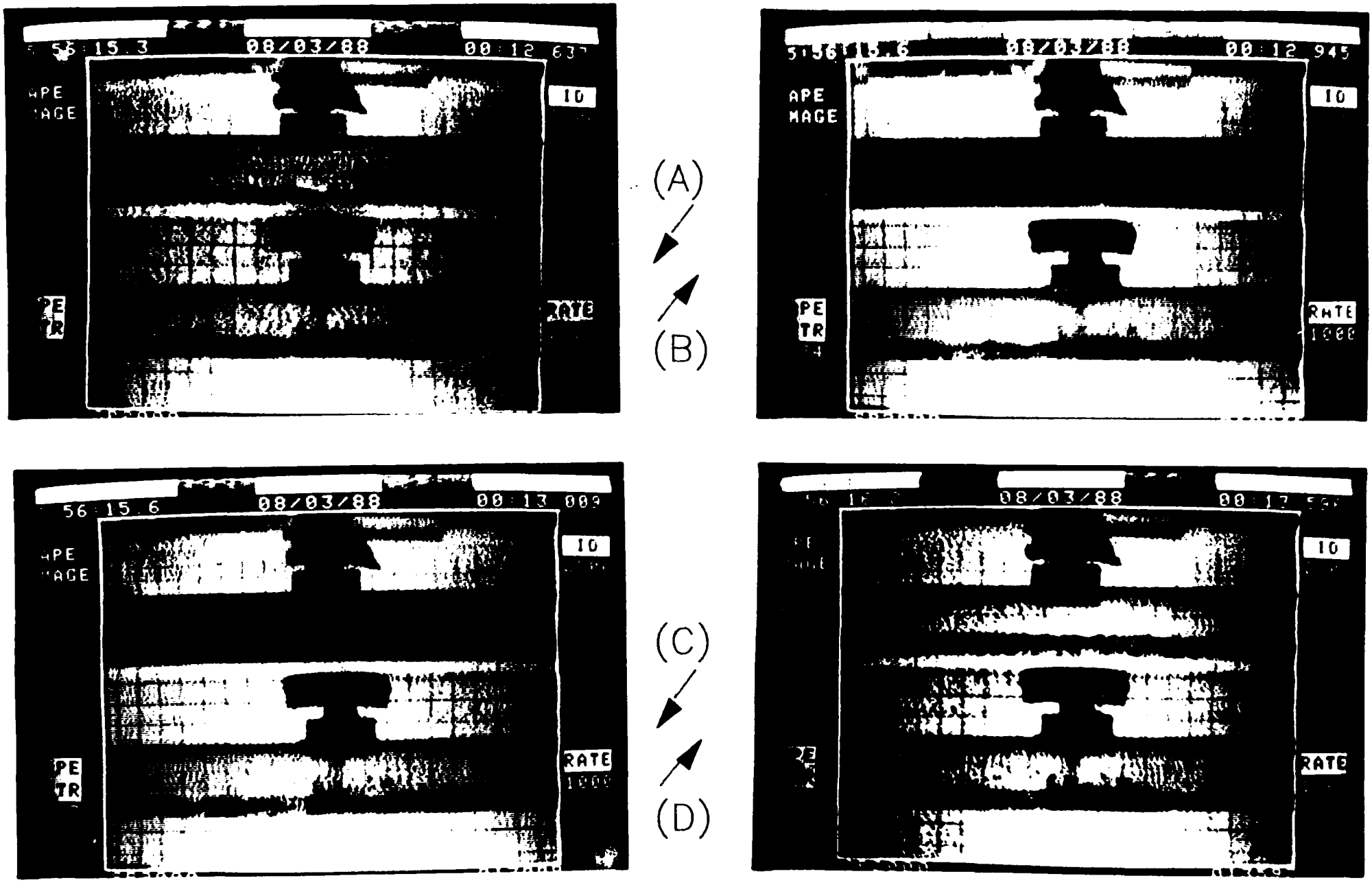

FIGURE 23b. Flow pattern at transducers 6 (top) and 10 (bottom), Normal Run 19.
Flow is from right to left at transducer 6 and left to right at 10.

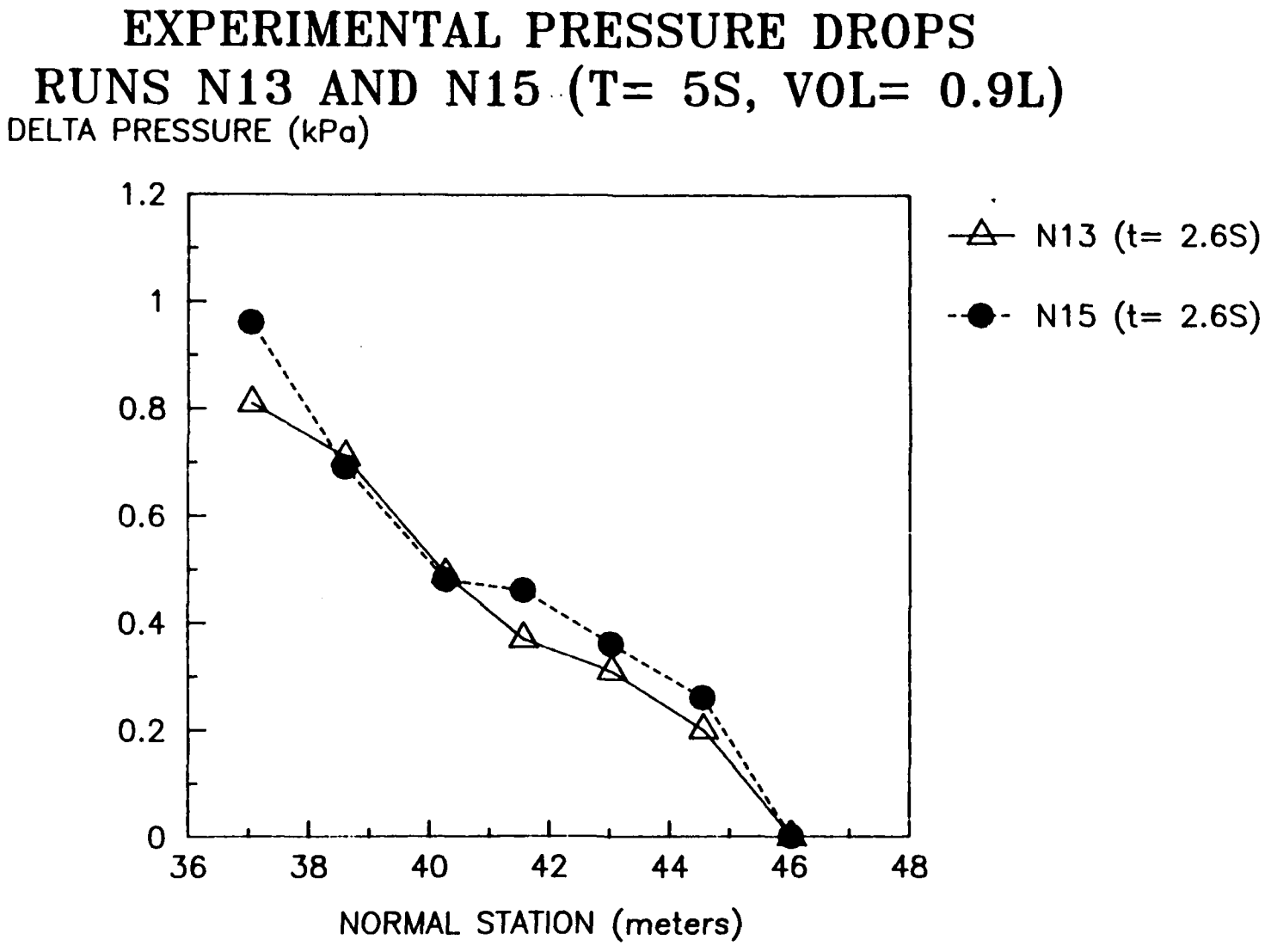

FIGURE 24. Time average vacuum drop profile, Normal Runs 13 and 15.

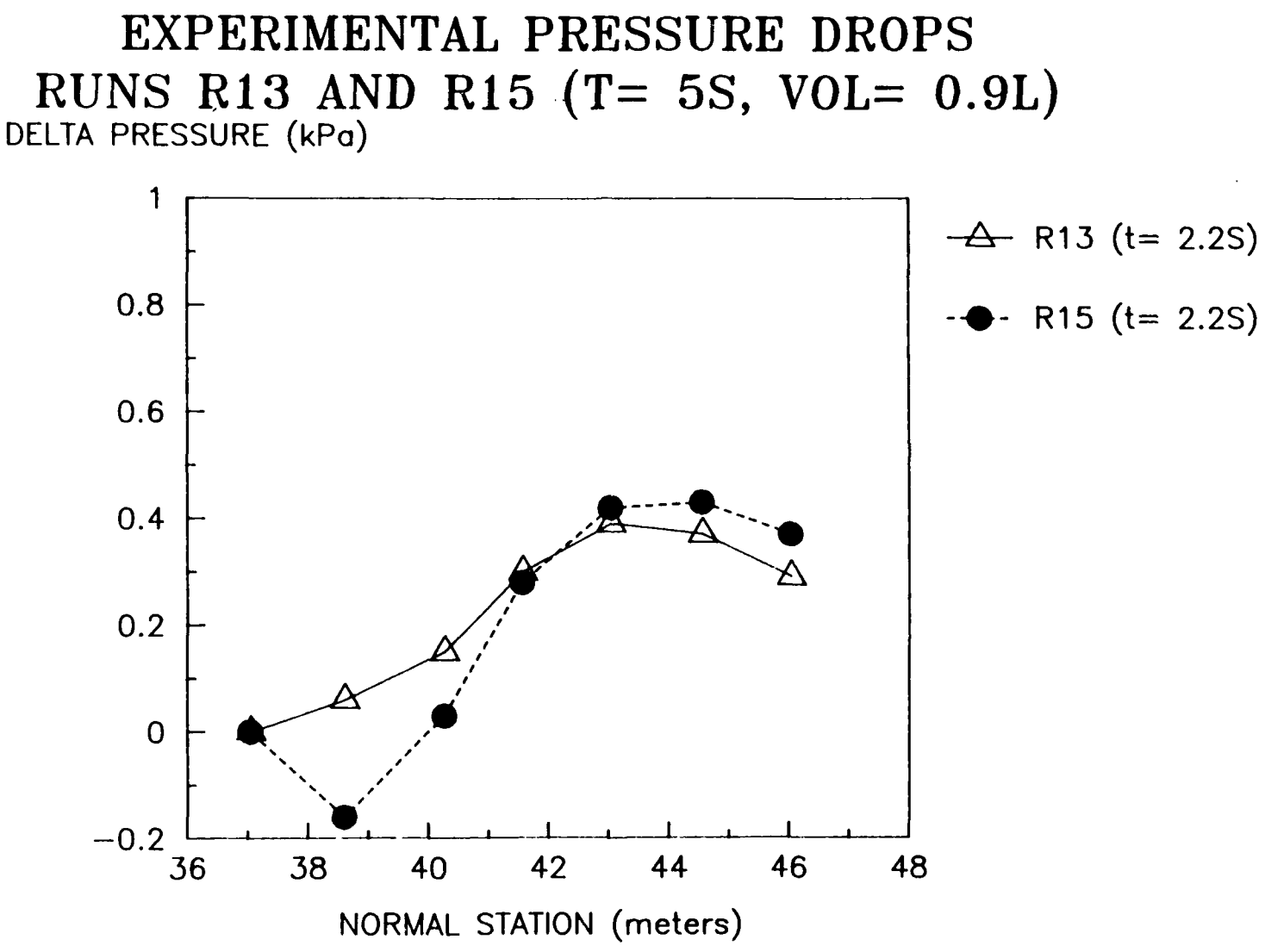

FIGURE 25. Time average vacuum drop profile, Reverse Runs 13 and 15.

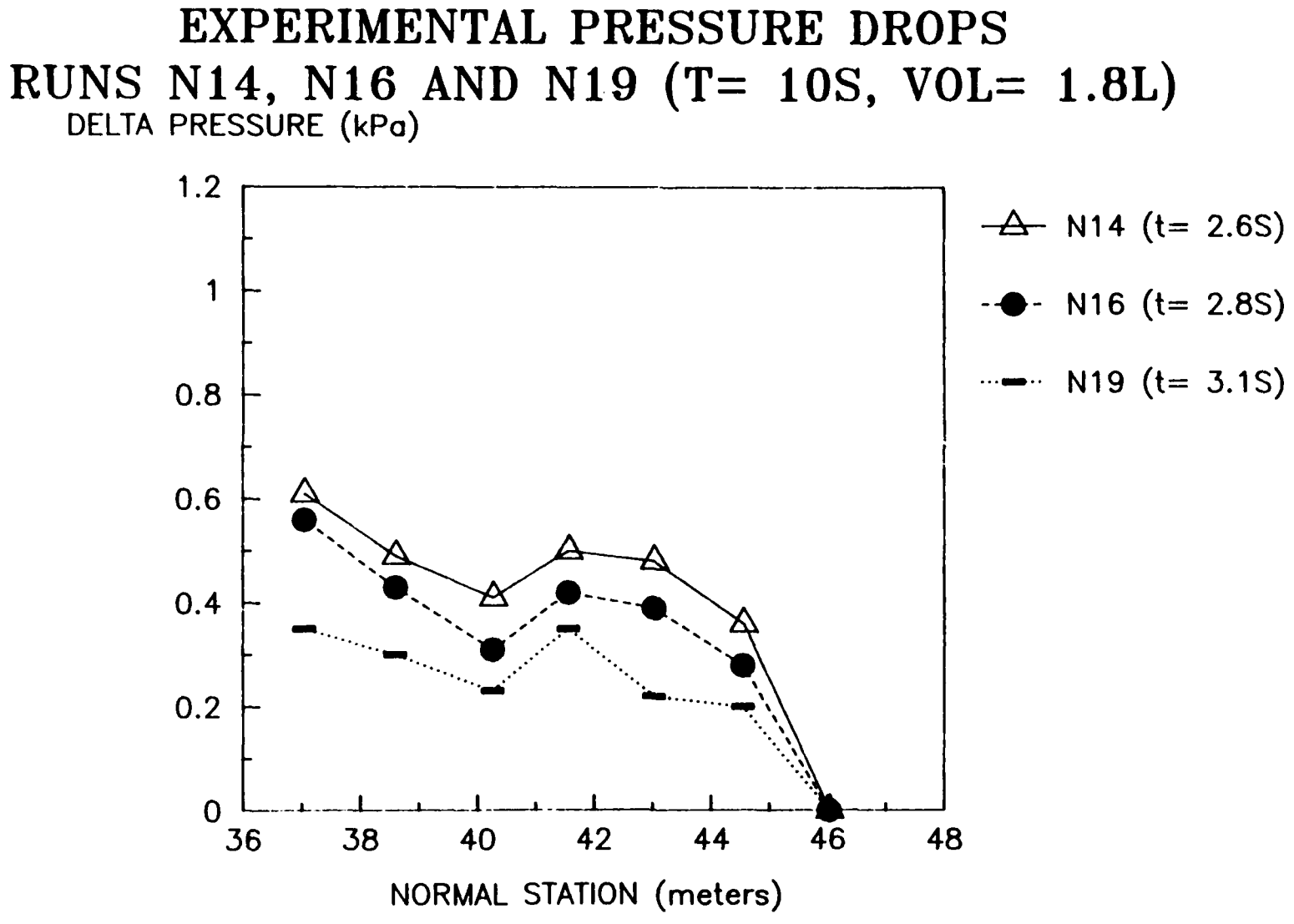

FIGURE 26. Time average vacuum drop profile, Normal Runs 14, 16, 19.

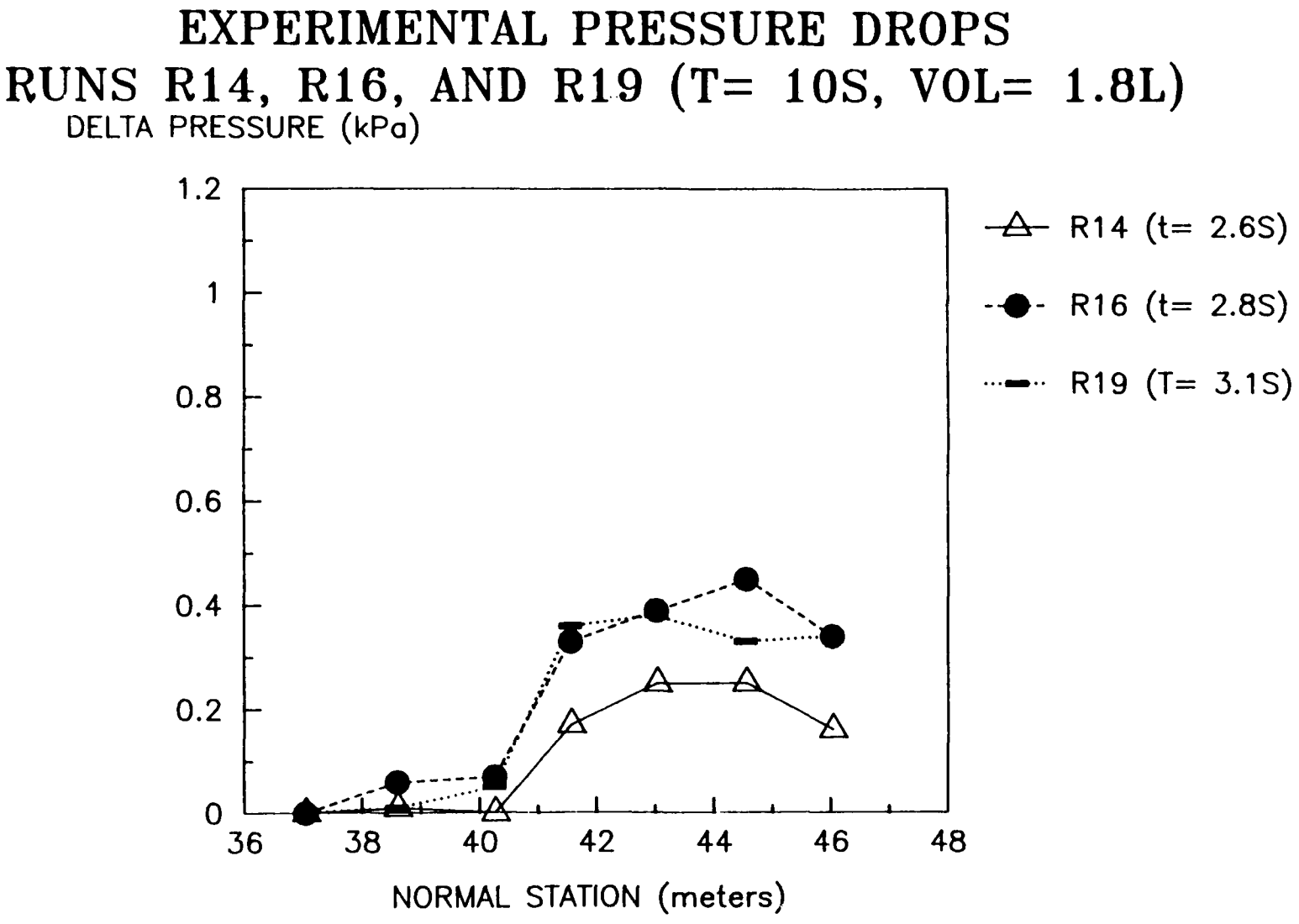

FIGURE 27. Time average vacuum drop profile, Reverse Runs 14, 16, 19.

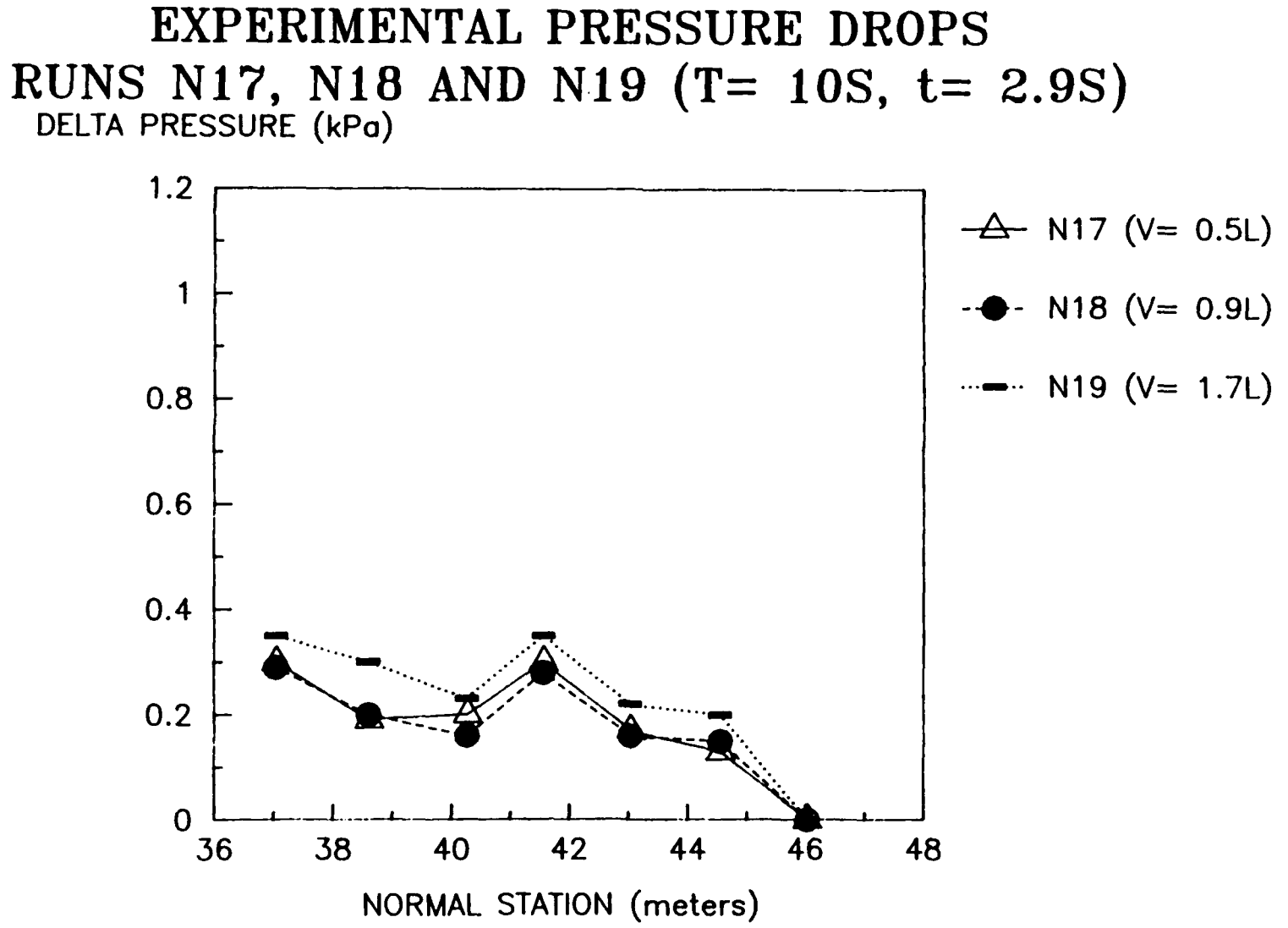

FIGURE 28. Time average vacuum drop profile, Normal Runs 17, 18, 19.

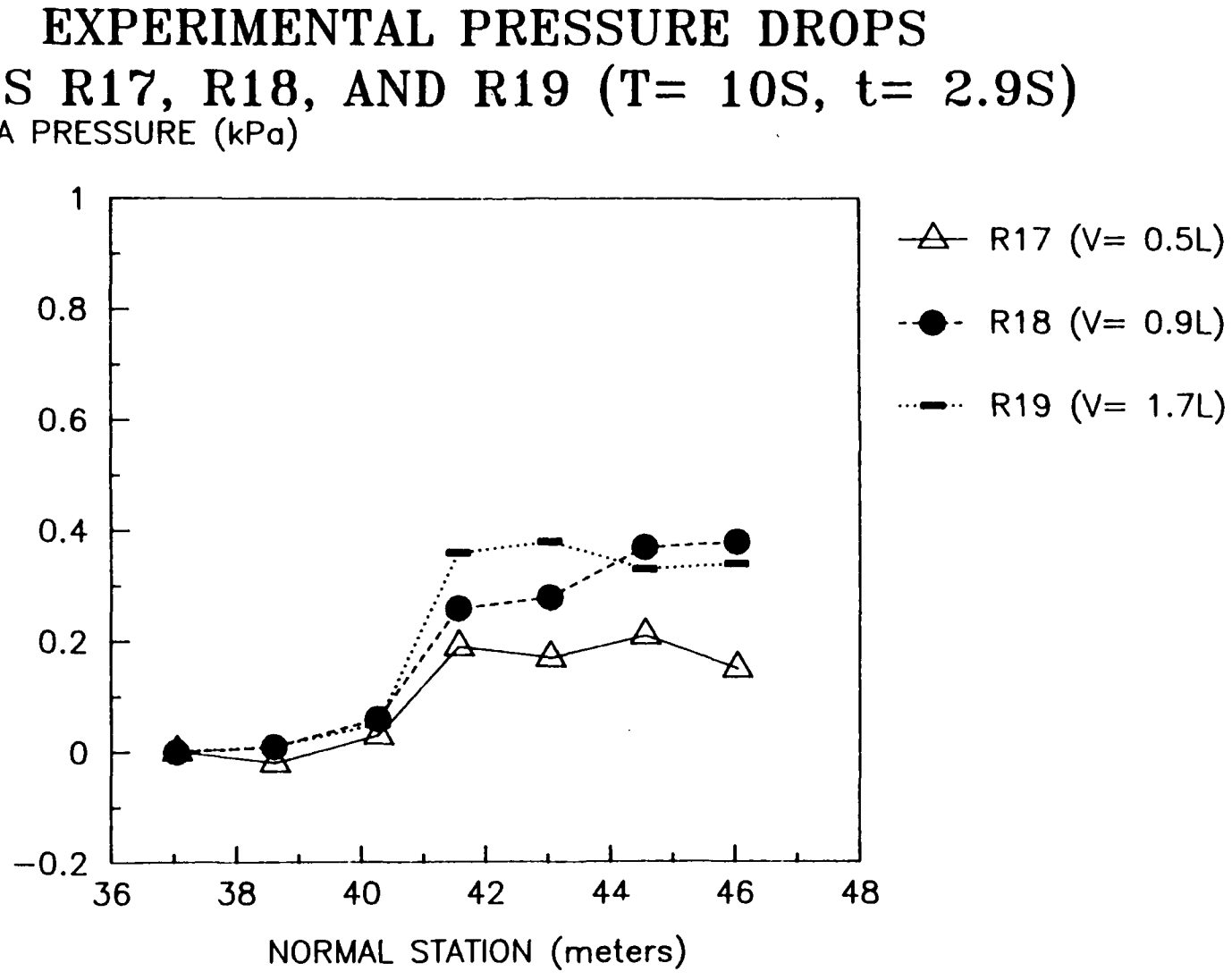

FIGURE 29. Time average vacuum drop profile, Reverse Runs 17, 18, 19.

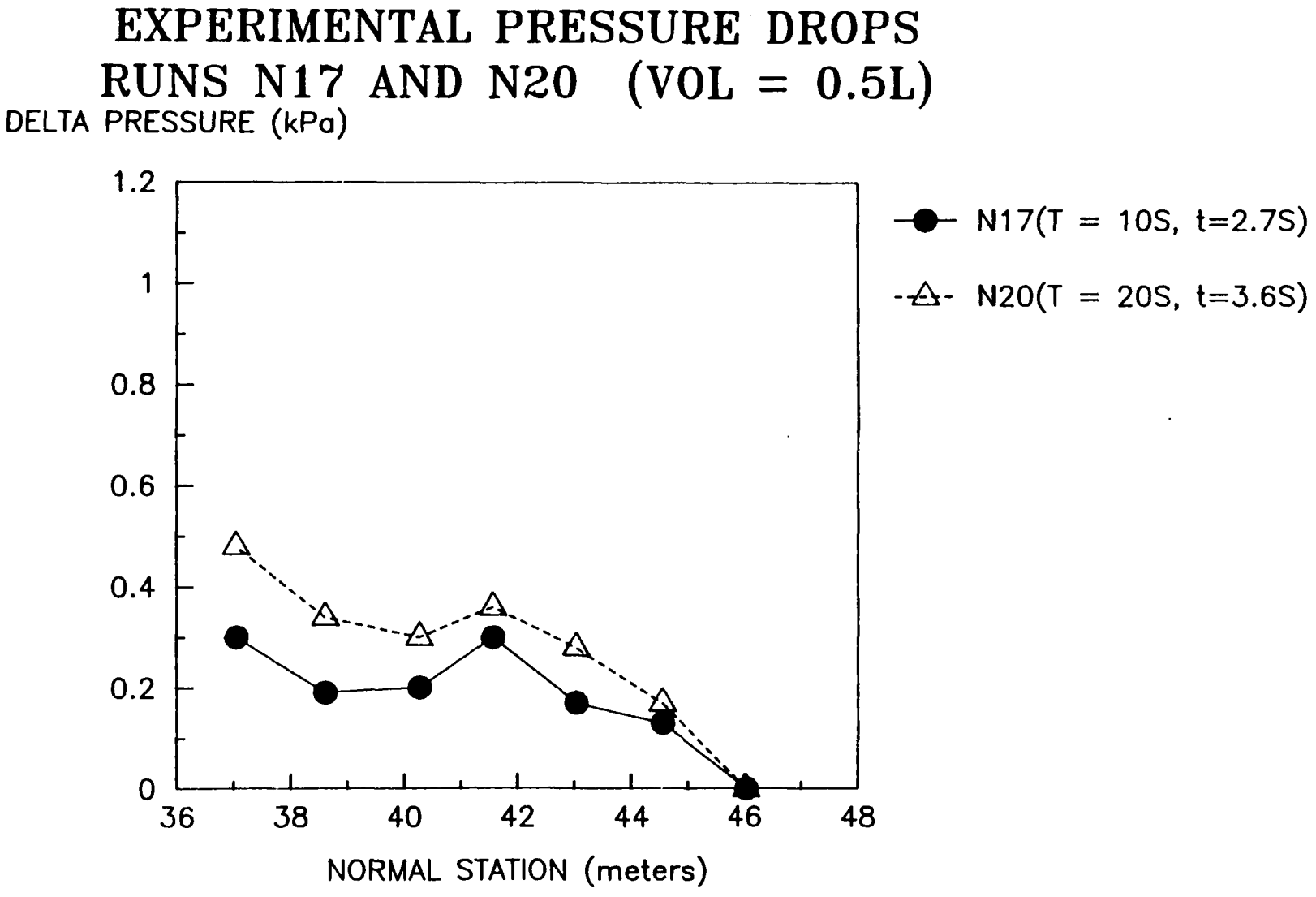

FIGURE 30. Time average vacuum drop profile, Normal Runs 17 and 20.

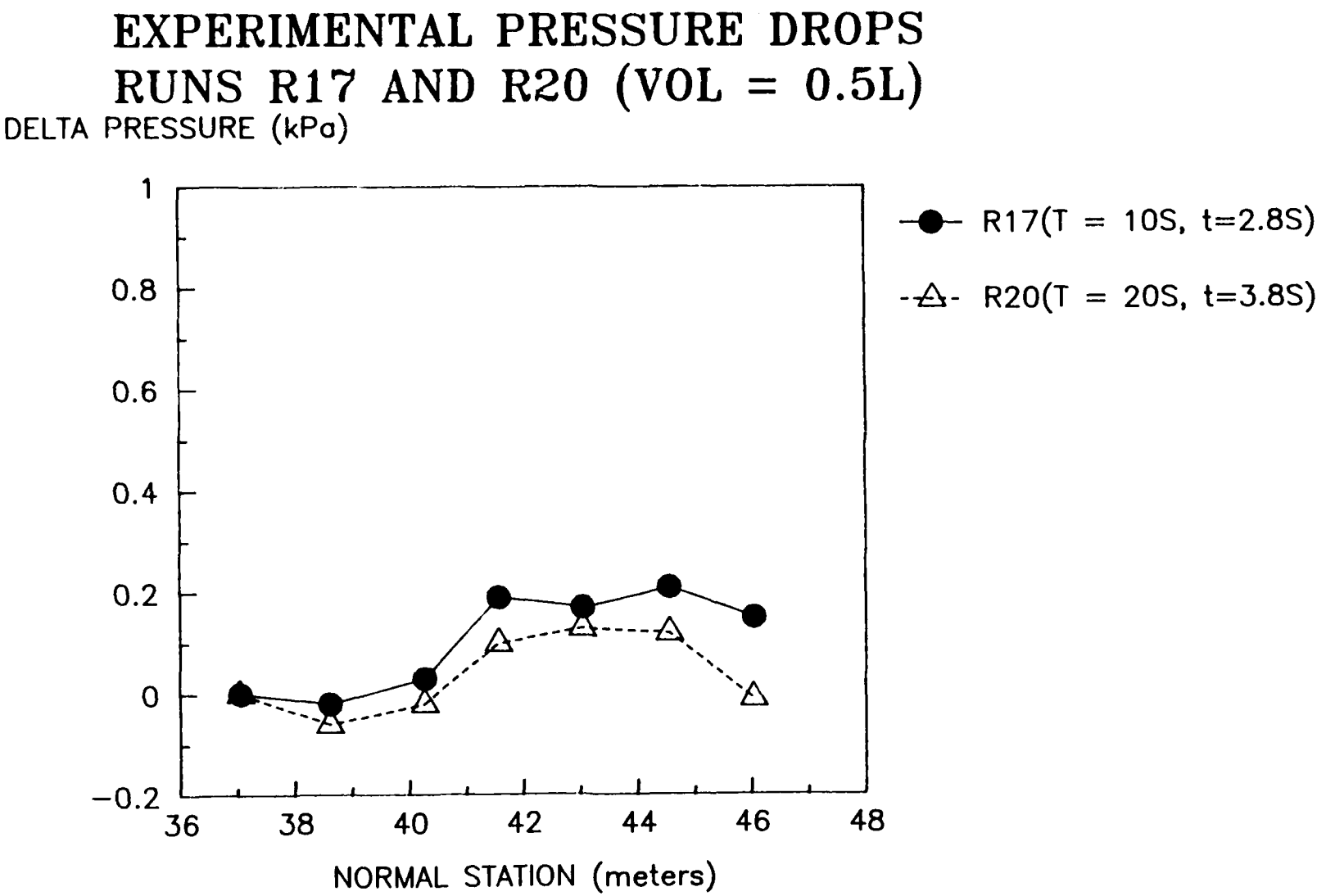

FIGURE 31. Time average vacuum drop profile, Reverse Runs 17 and 20.

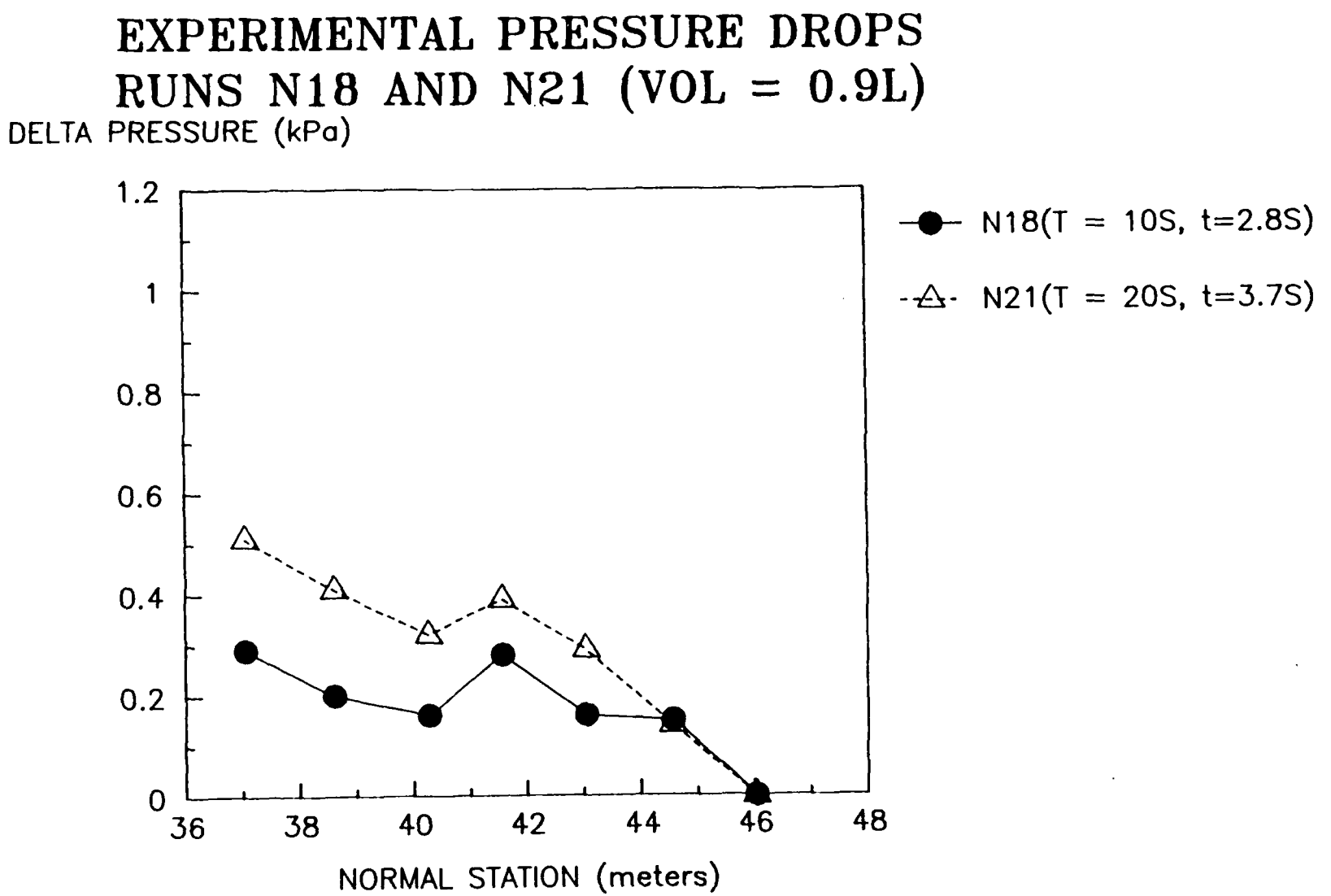

FIGURE 32. Time average vacuum drop profile, Normal Runs 18 and 21.

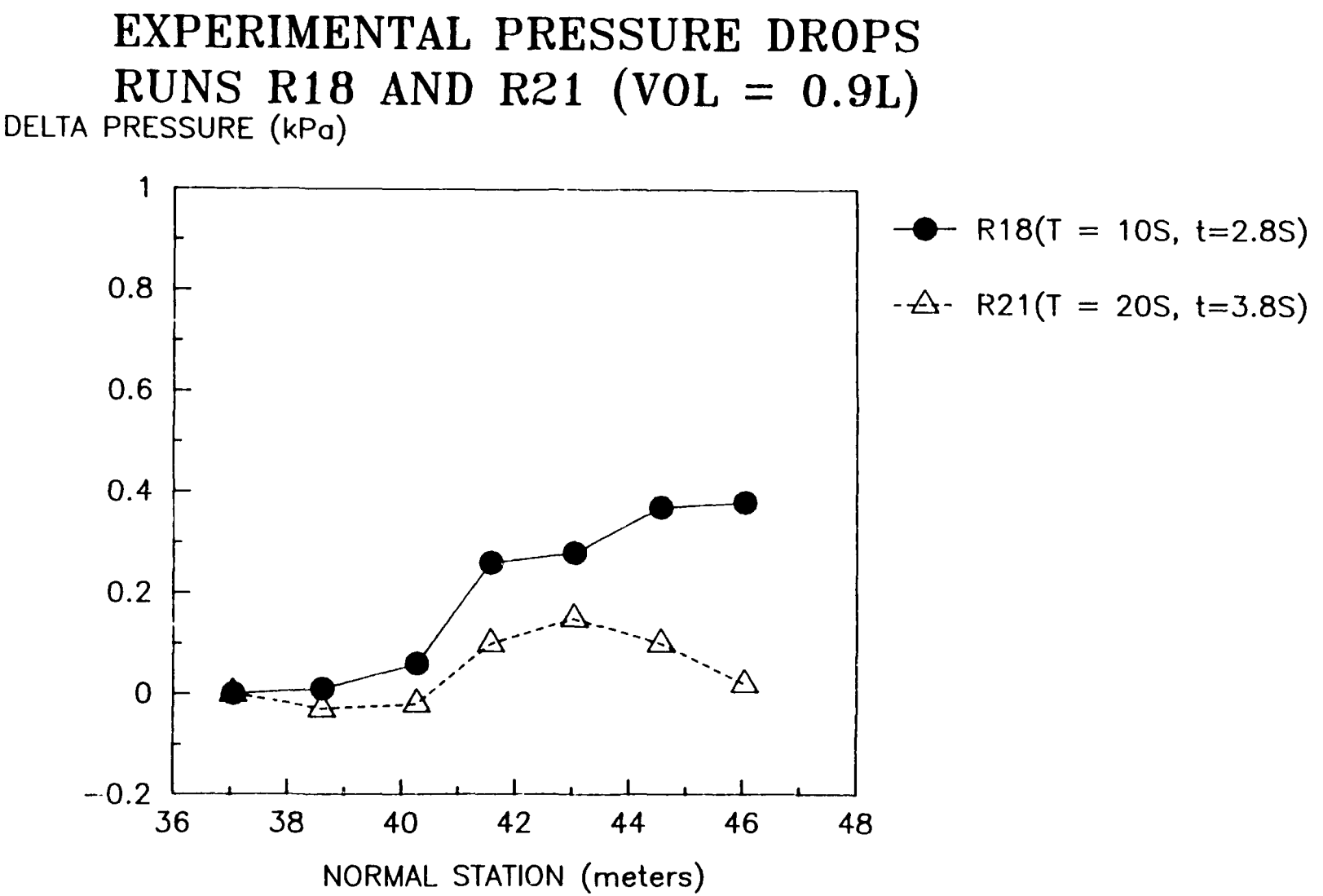

FIGURE 33. Time average vacuum drop profile, Reverse Runs 18 and 21.

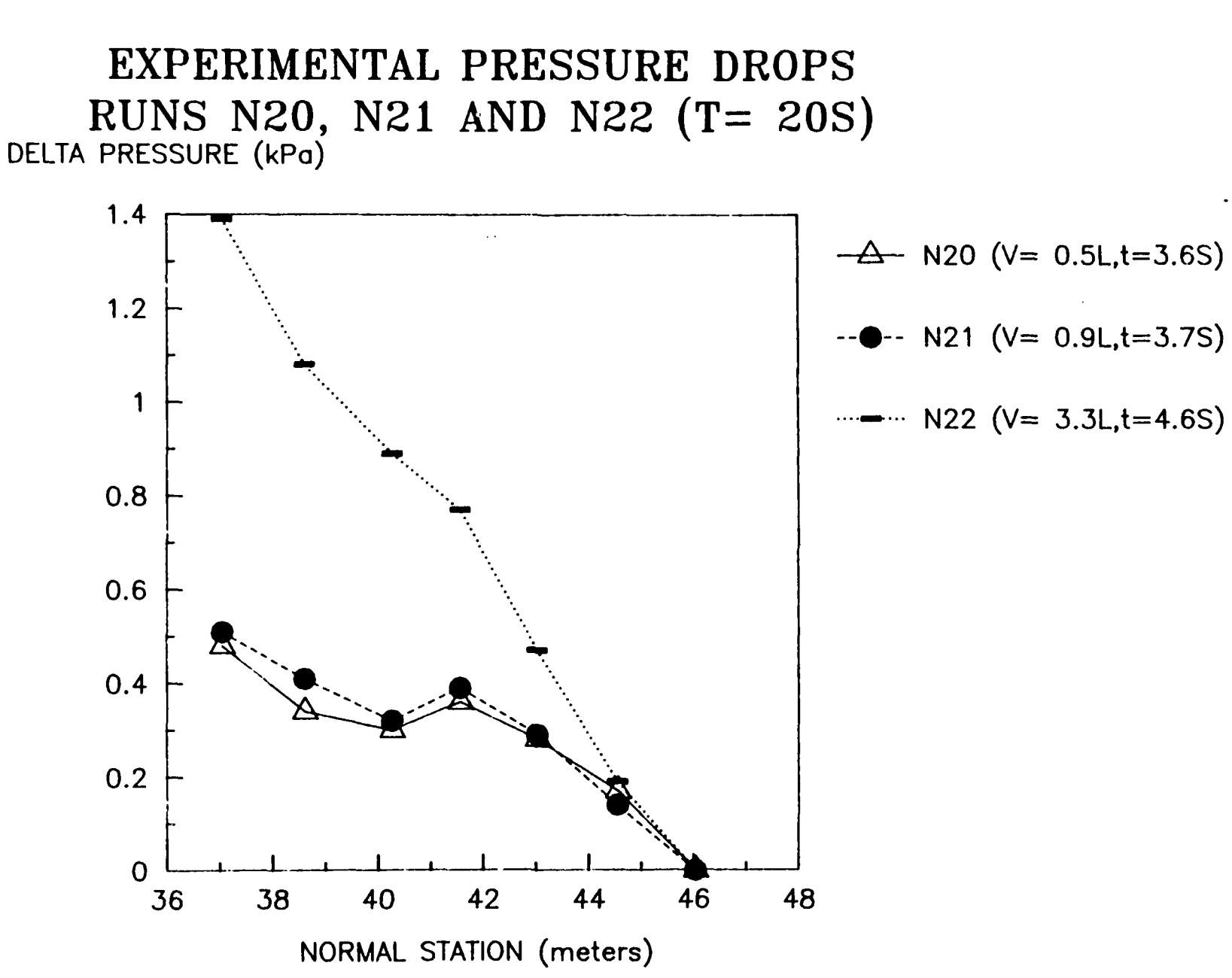

FIGURE 34. Time average vacuum drop profile, Normal Runs 20, 21, 22.

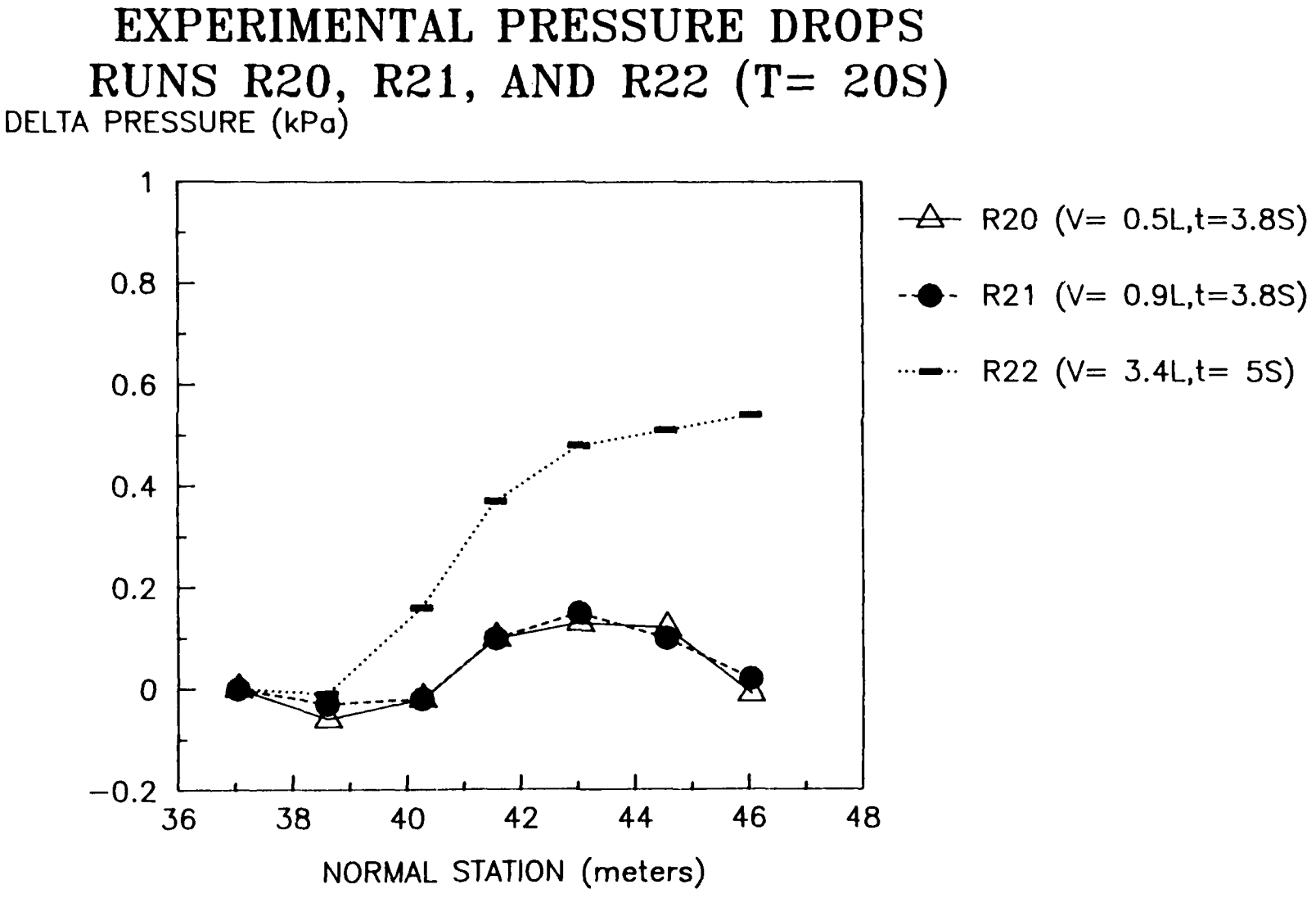

FIGURE 35. Time average vacuum drop profile, Reverse Runs 20, 21, 22.

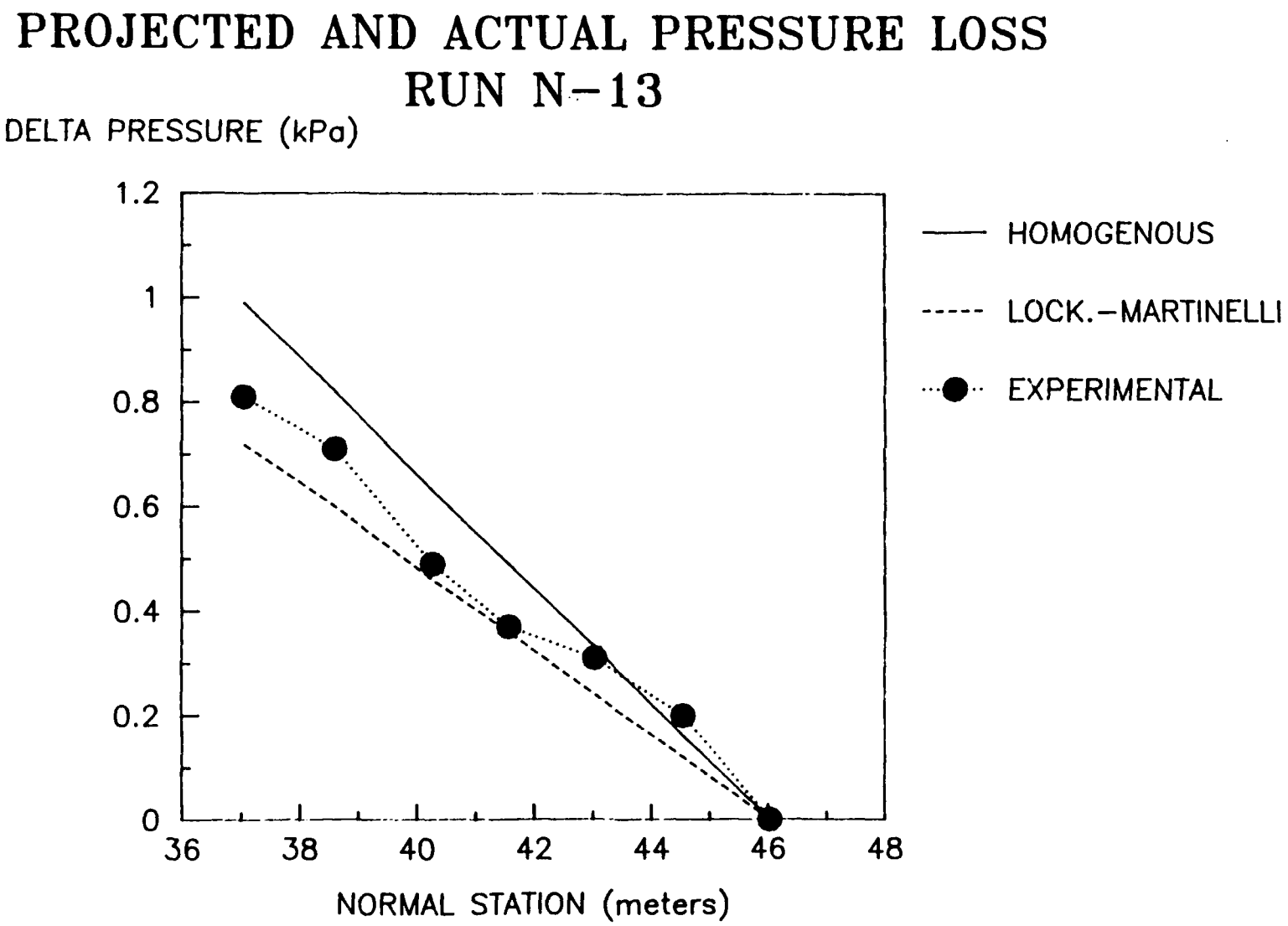

FIGURE 36. Predicted and measured time average vacuum drop profiles, Normal Run 13.

PROJECTED AND ACTUAL PRESSURE LOSS
RUN R-13

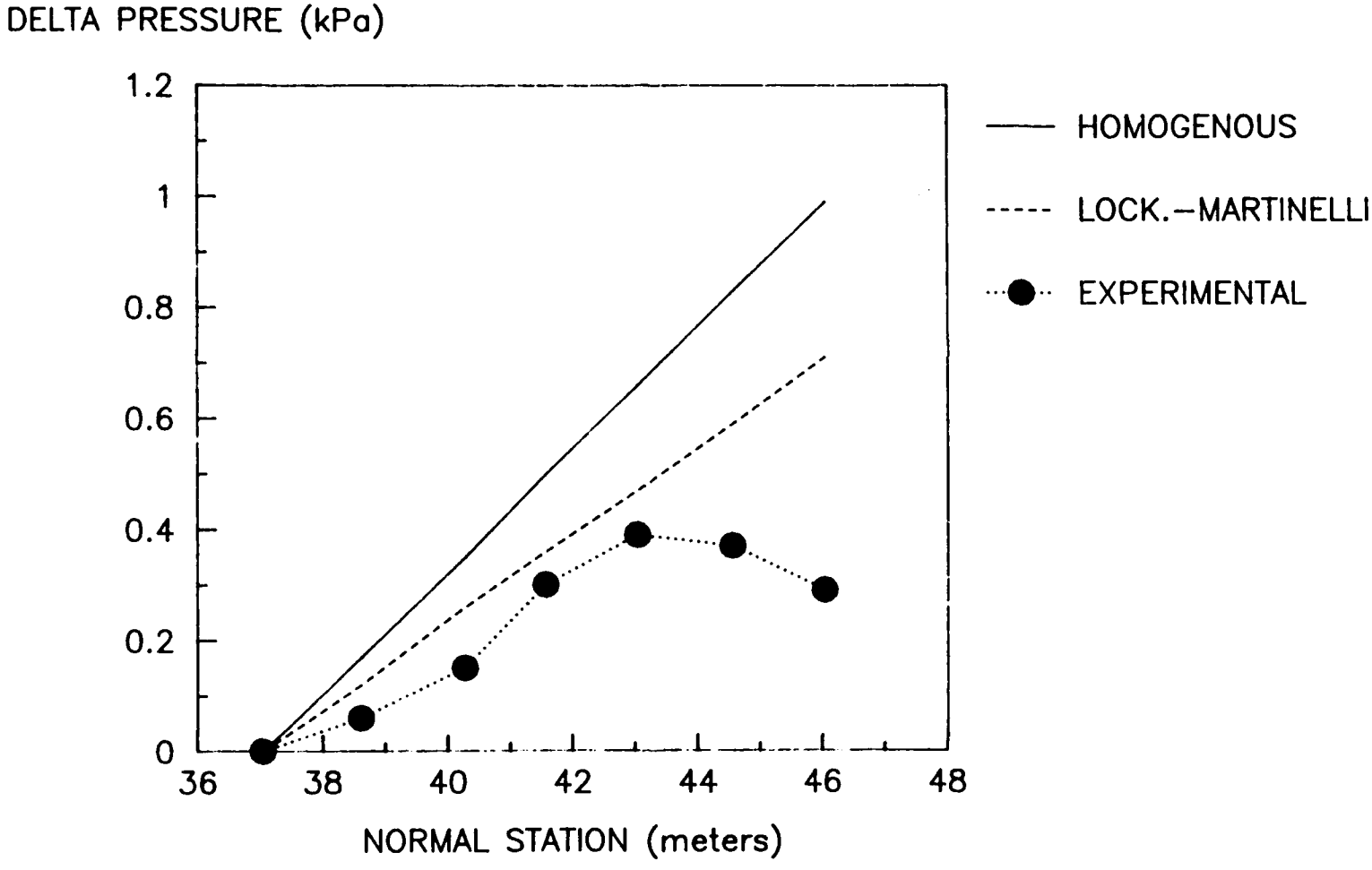

FIGURE 37. Predicted and measured time average vacuum drop profiles, Reverse Run 13.

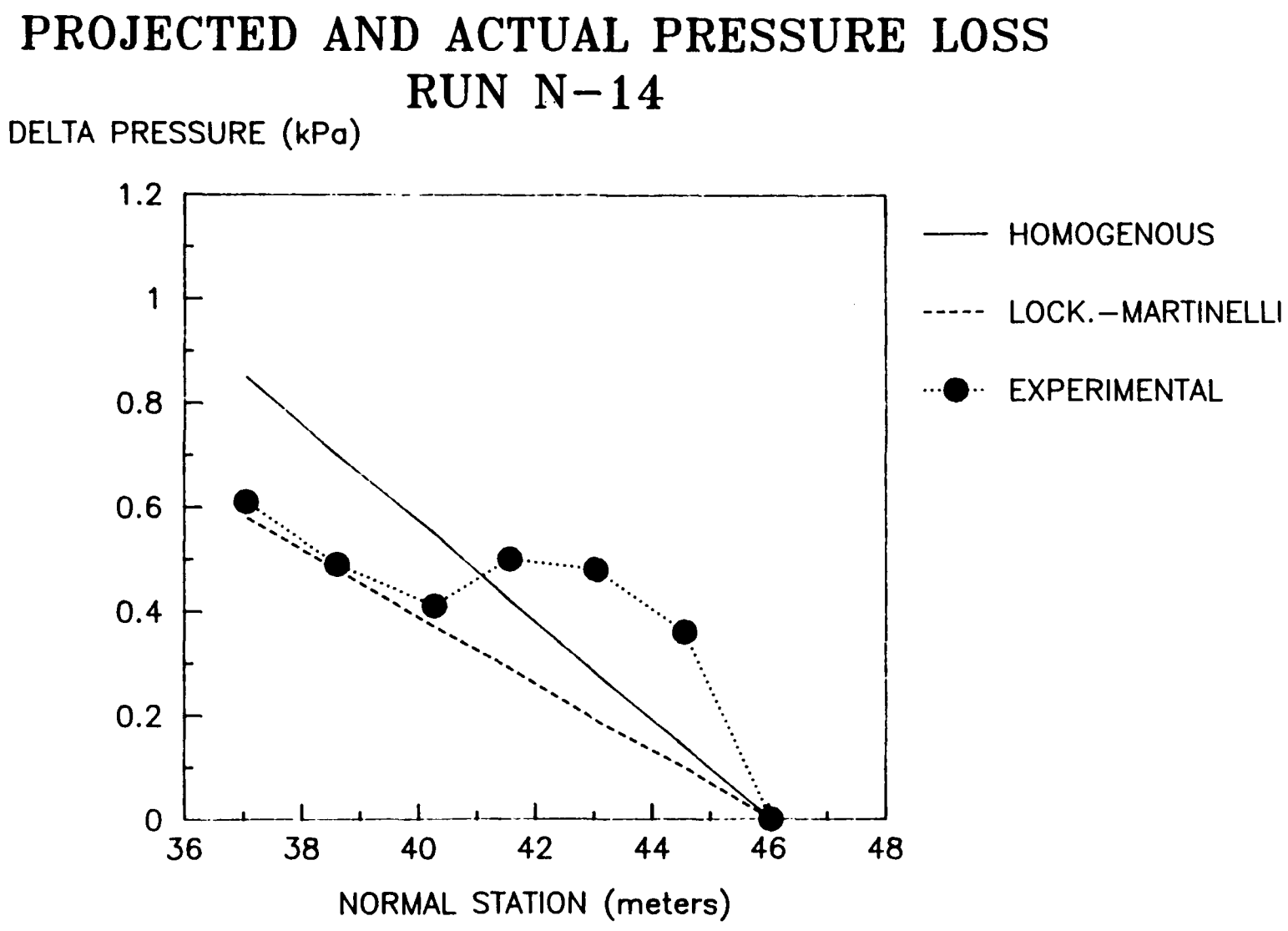

FIGURE 38. Predicted and measured time average vacuum drop profiles, Normal Run 14.

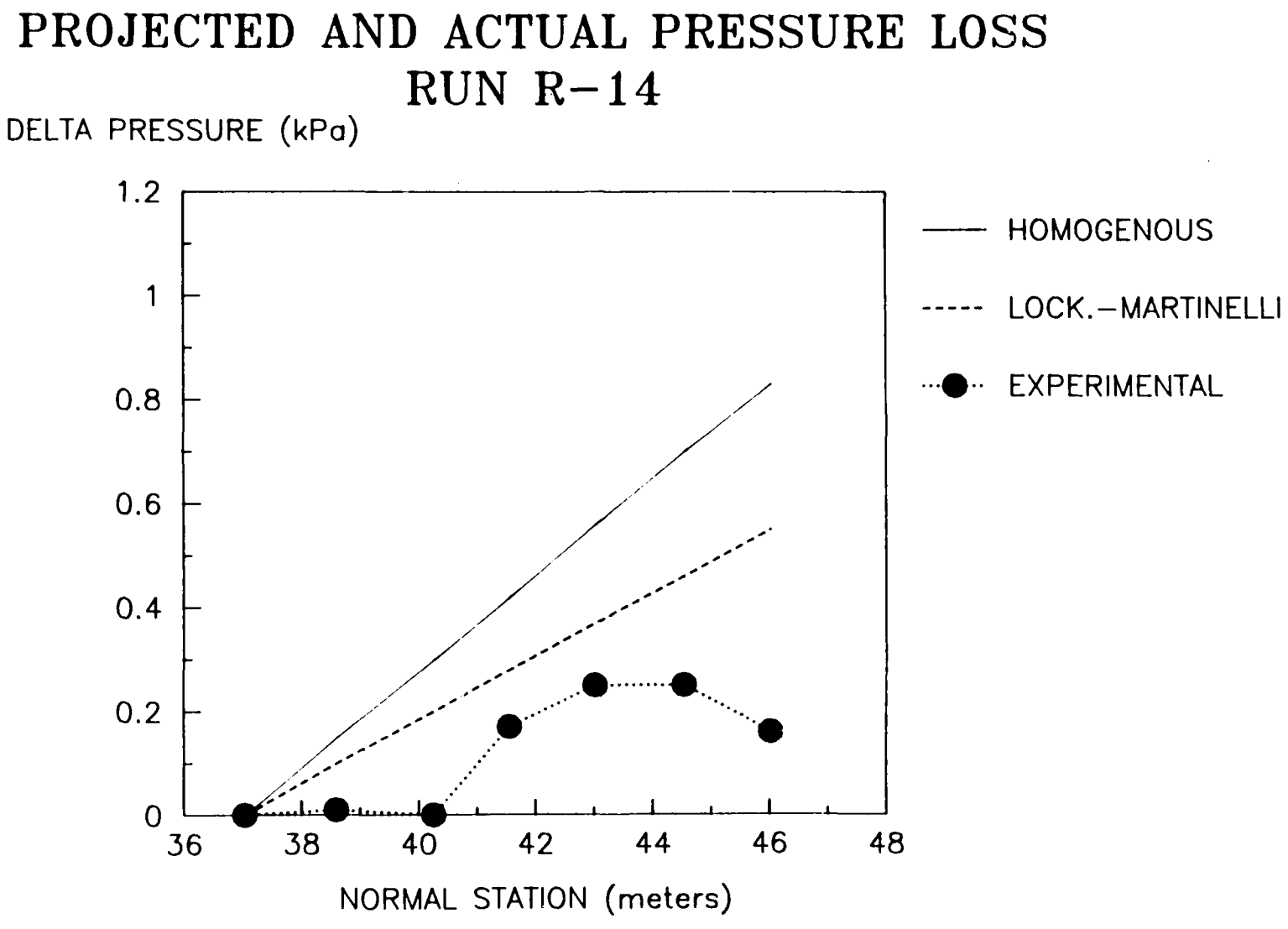

FIGURE 39. Predicted and measured time average vacuum drop profiles, Reverse Run 14.

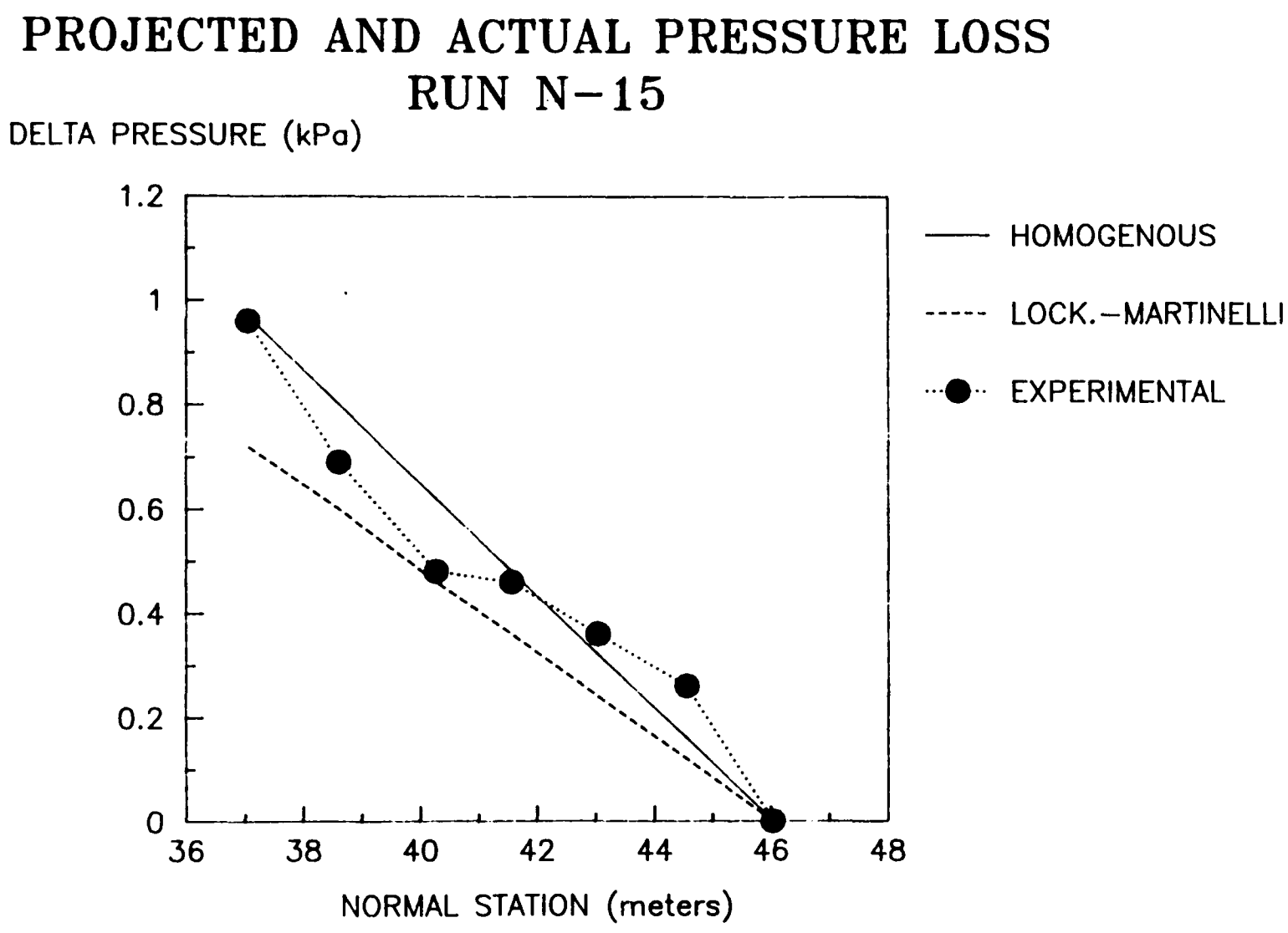

FIGURE 40. Predicted and measured time average vacuum drop profiles Normal Run 15.

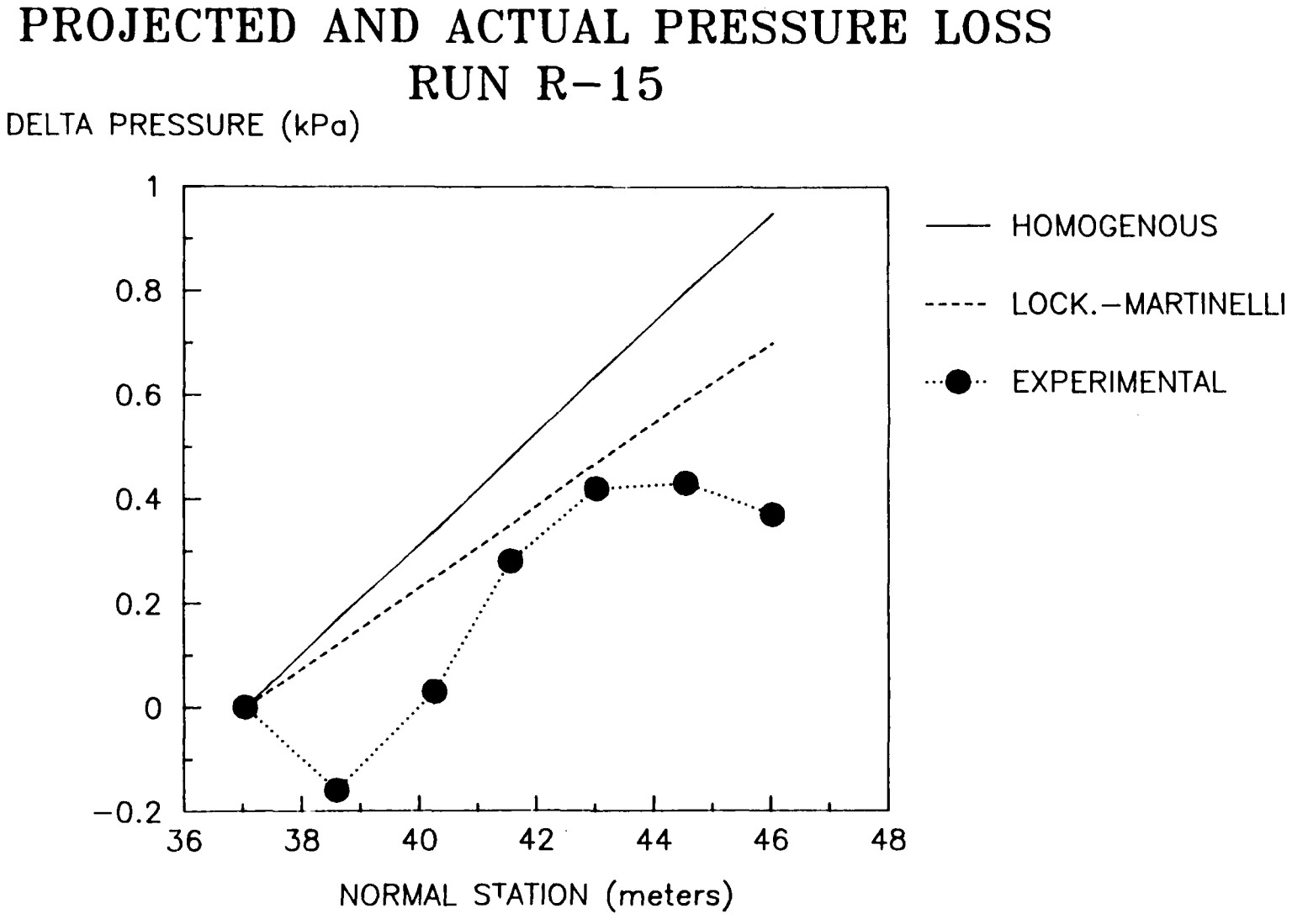

FIGURE 41. Predicted and measured time average vacuum drop profiles, Reverse Run 15.

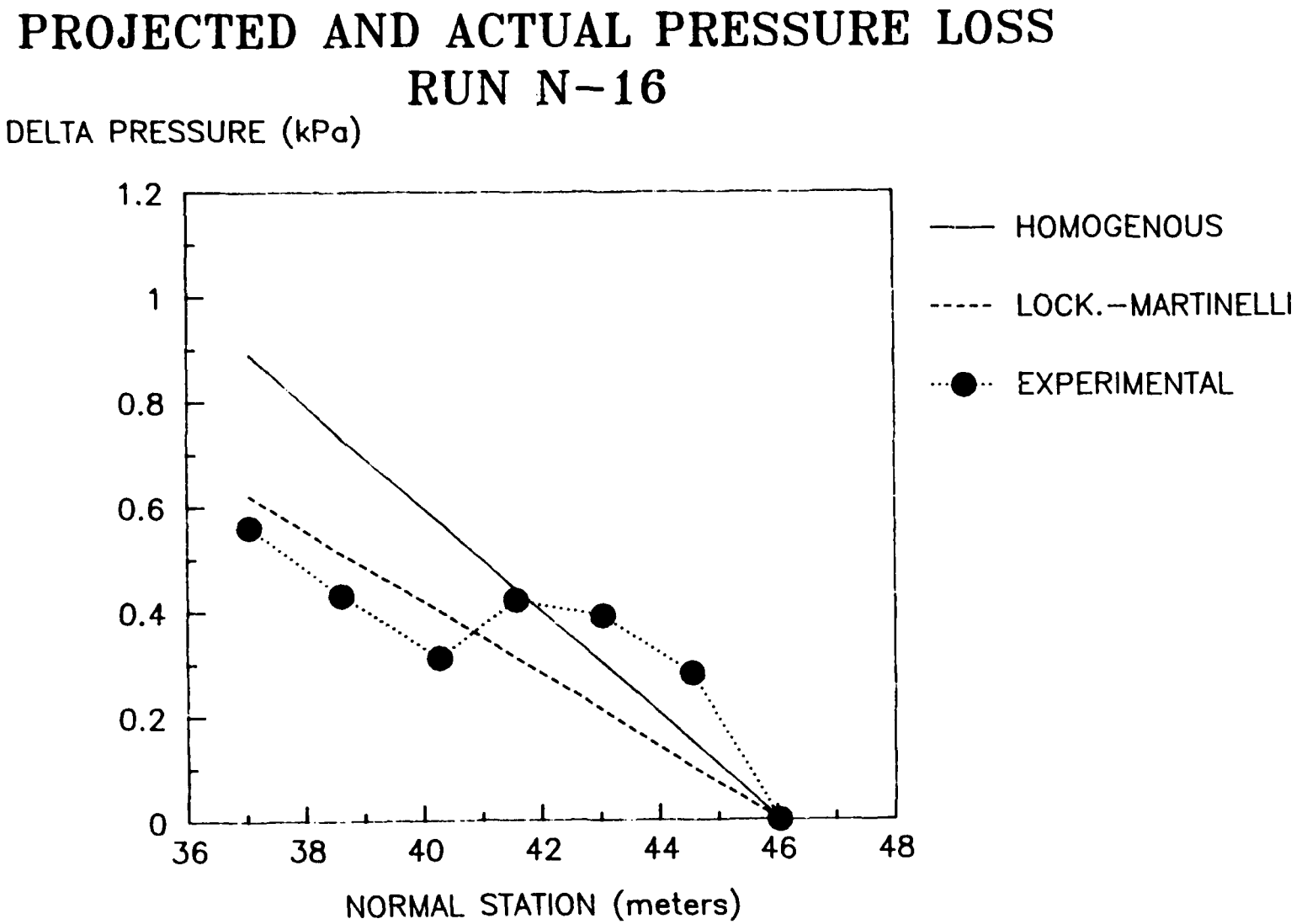

FIGURE 42. Predicted and measured time average vacuum drop profiles, Normal Run 16.

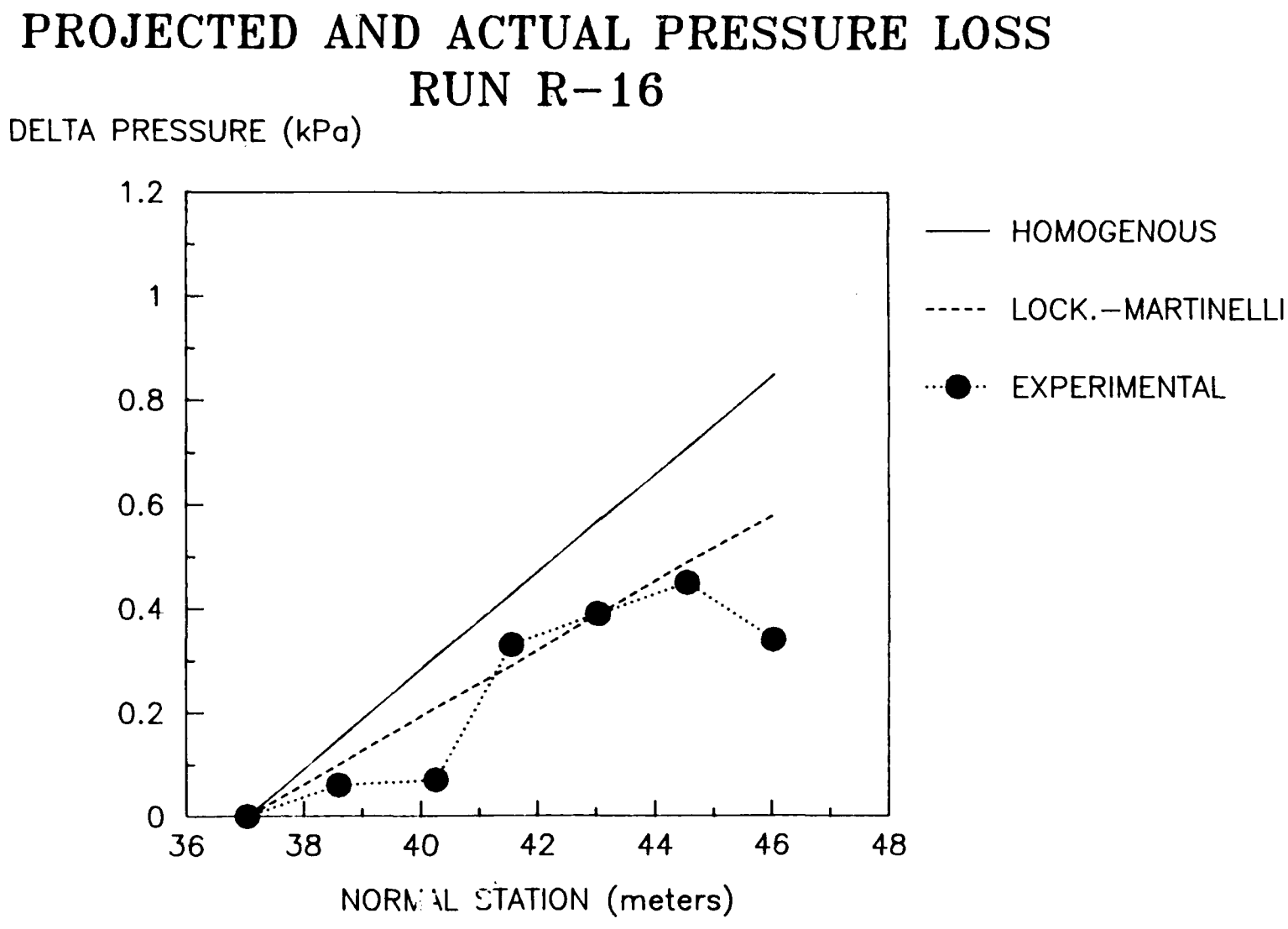

FIGURE 43. Predicted and measured time average vacuum drop profiles, Reverse Run 16.

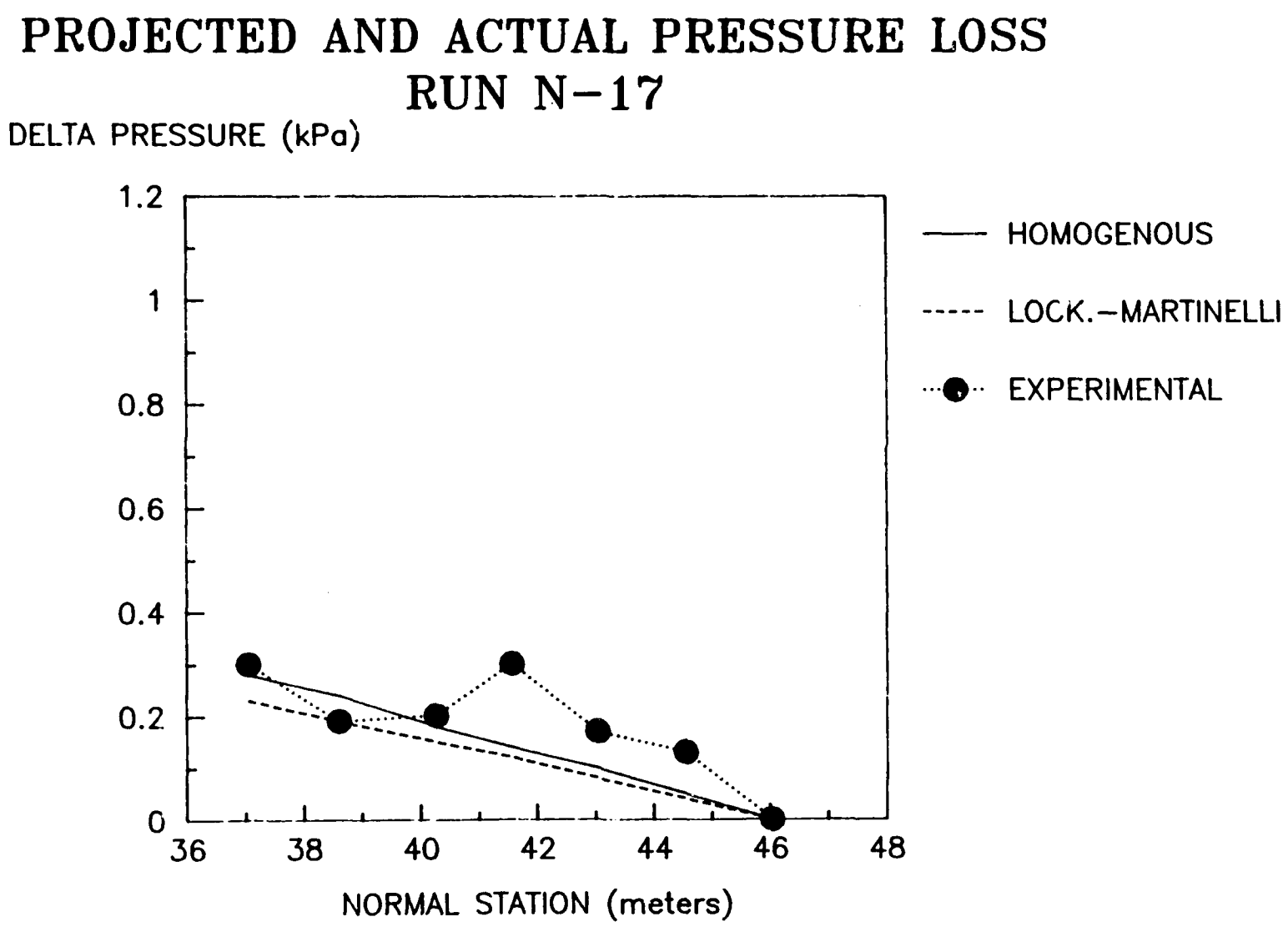

FIGURE 44. Predicted and measured time average vacuum drop profiles, Normal Run 17.

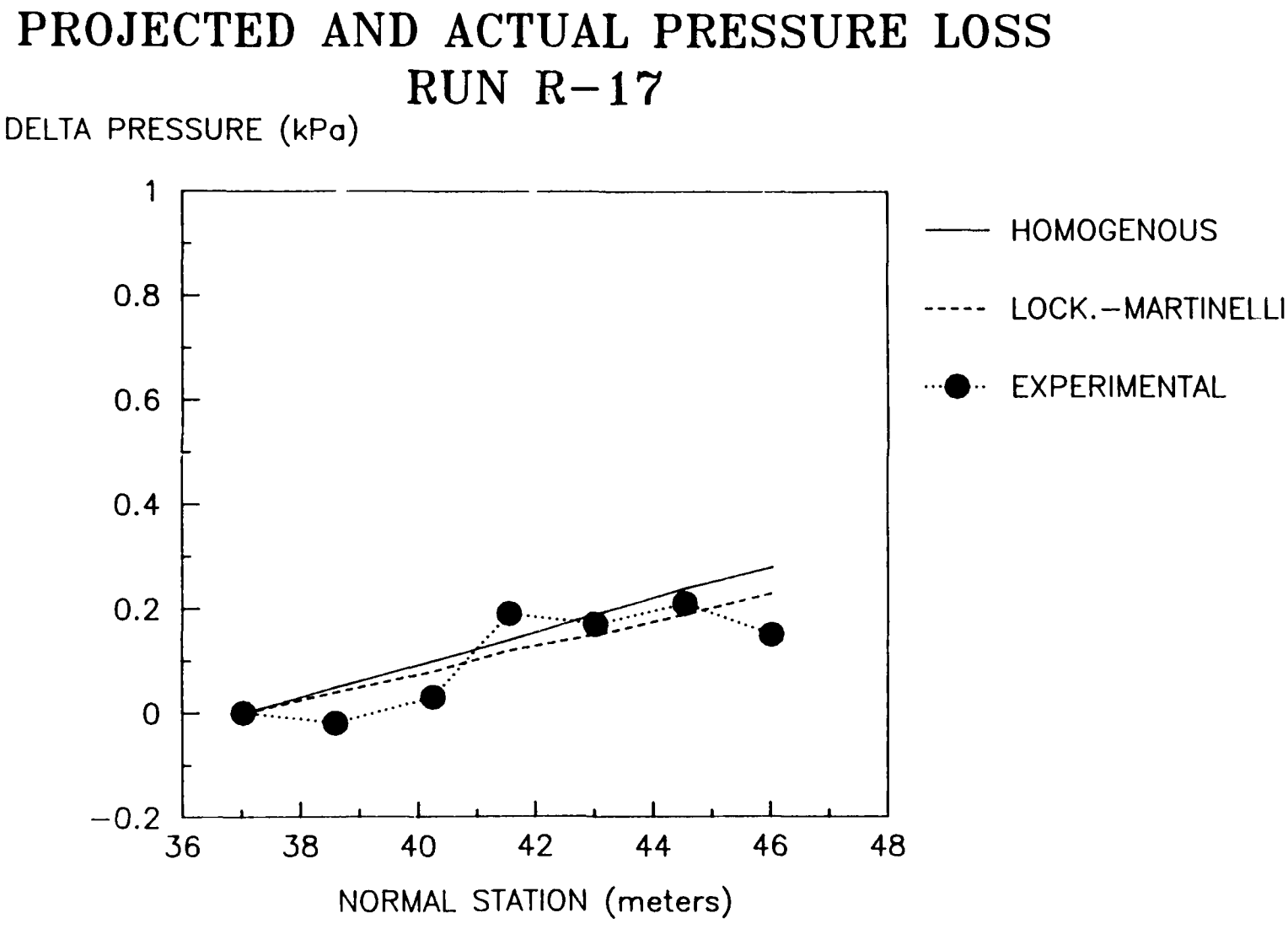

FIGURE 45. Predicted and measured time average vacuum drop profiles, Reverse Run 17.

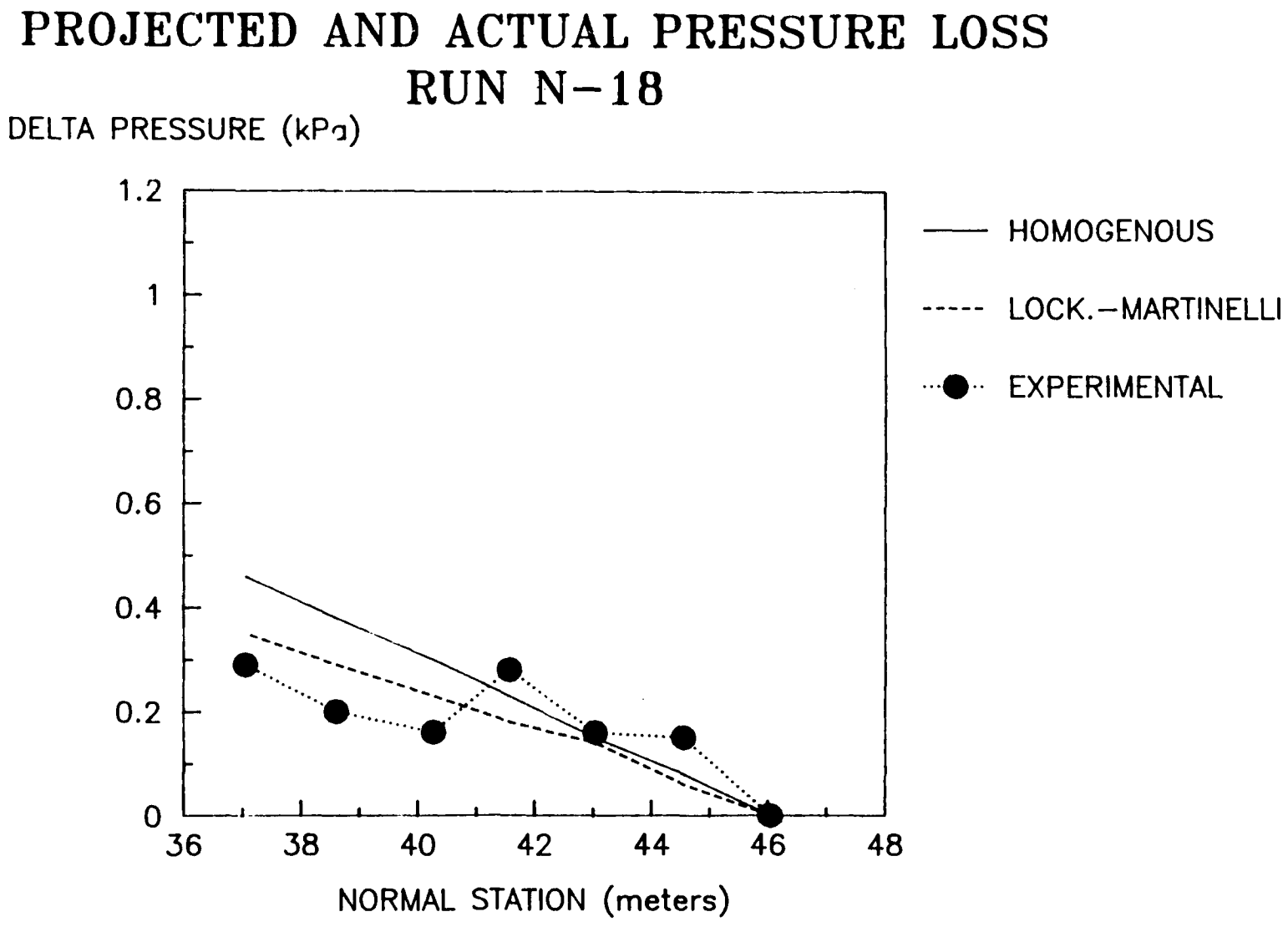

FIGURE 46. Predicted and measured time average vacuum drop profiles, Normal 18.

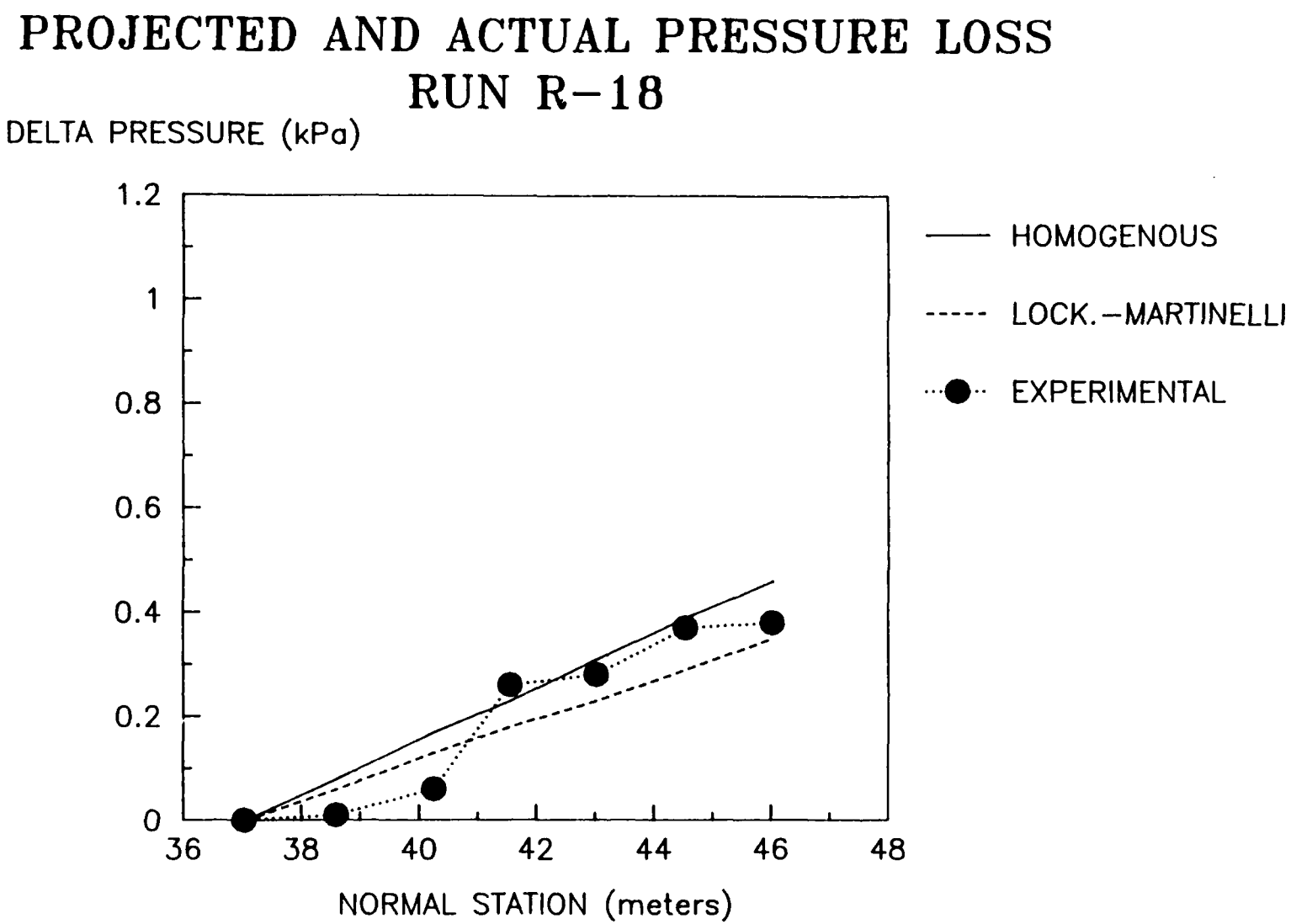

FIGURE 47. Predicted and measured time average vacuum drop profiles, Reverse Run 18.

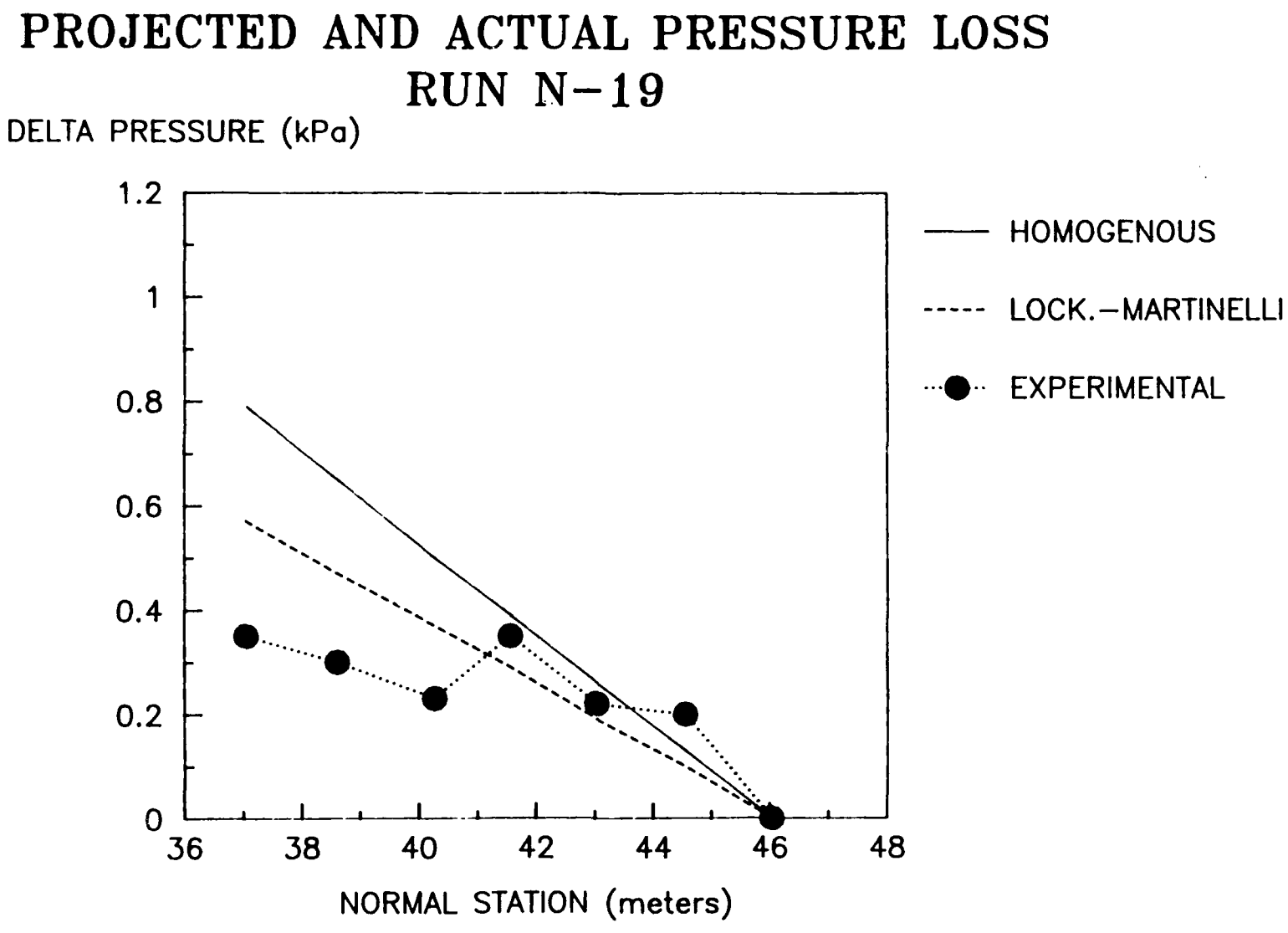

FIGURE 48. Predicted and measured time average vacuum drop profiles, Normal Run 19.

PROJECTED AND ACTUAL PRESSURE LOSS
RUN R-19

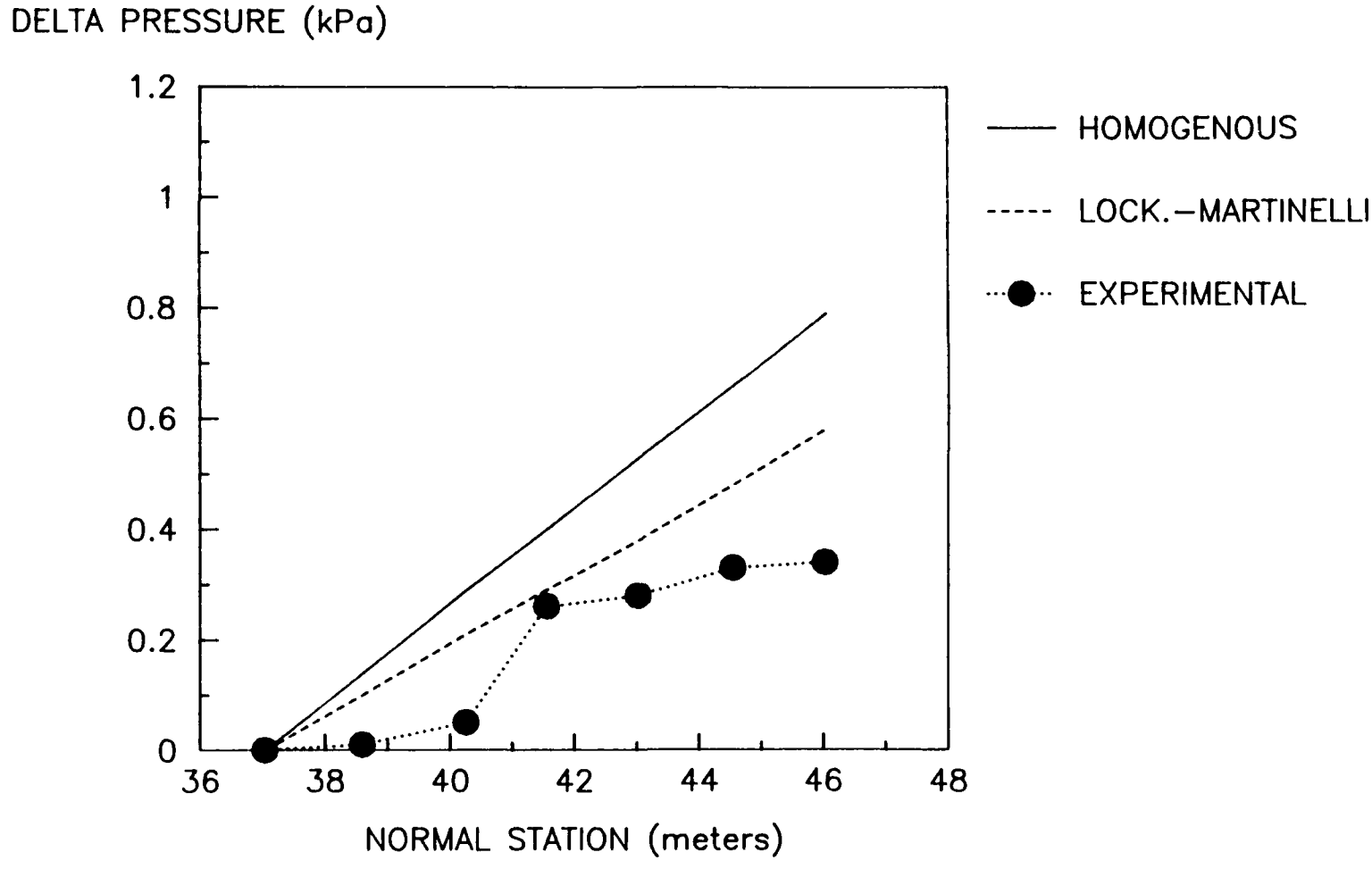

FIGURE 49. Predicted and measured time average vacuum drop profiles, Reverse Run 19.

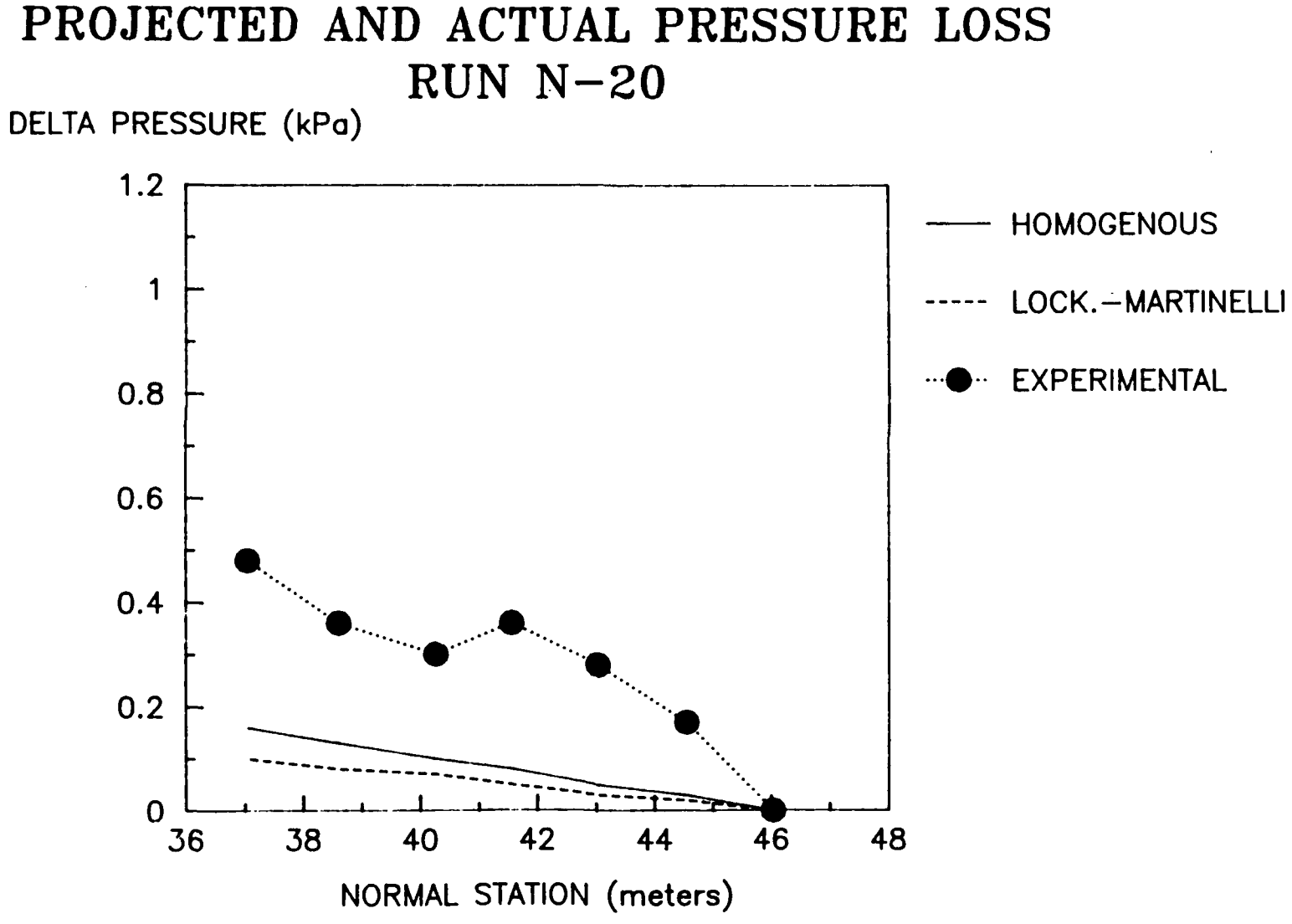

FIGURE 50. Predicted and measured time average vacuum drop profiles, Normal Run 20.

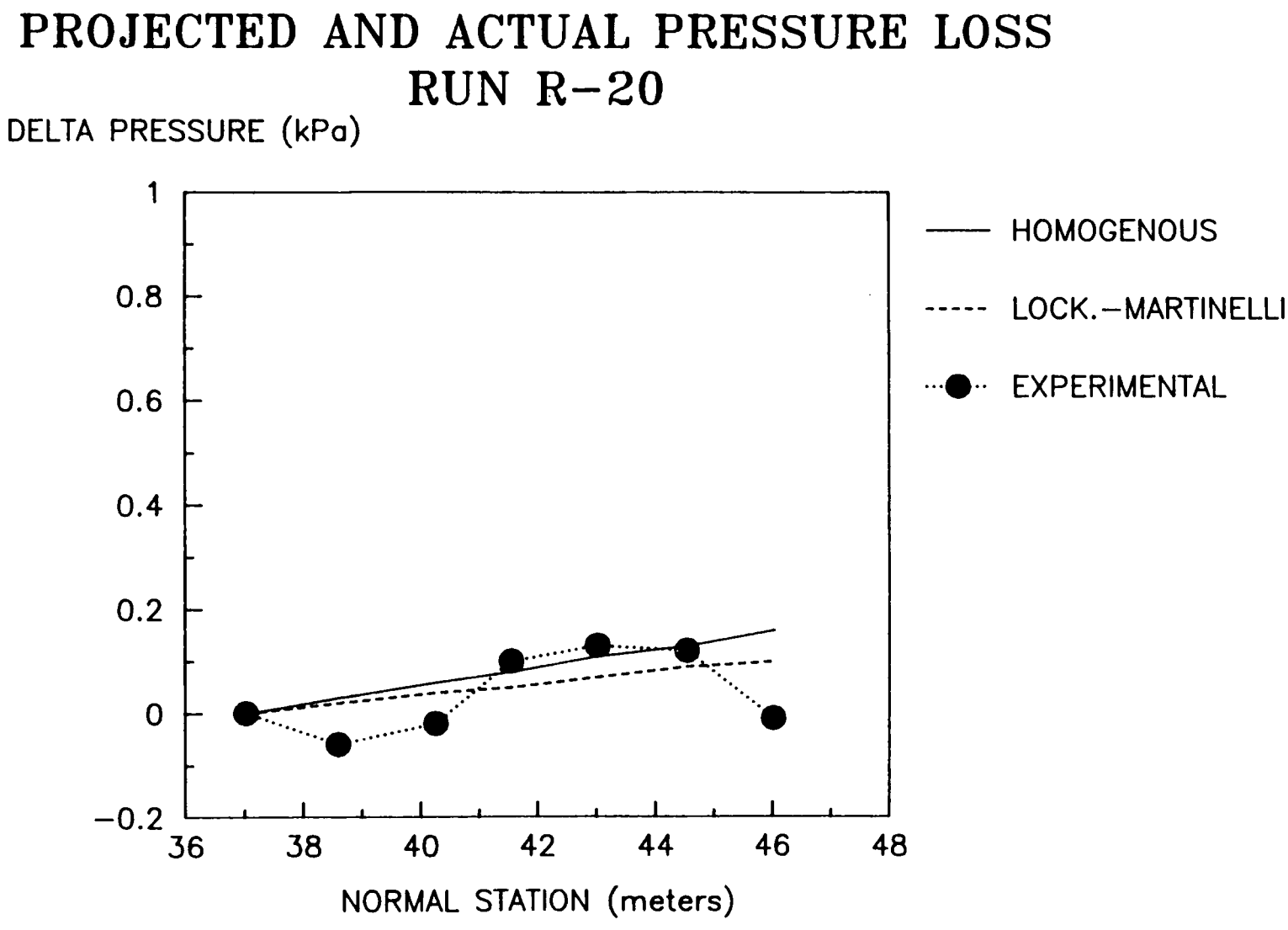

FIGURE 51. Predicted and measured time average vacuum drop profiles, Reverse Run 20.

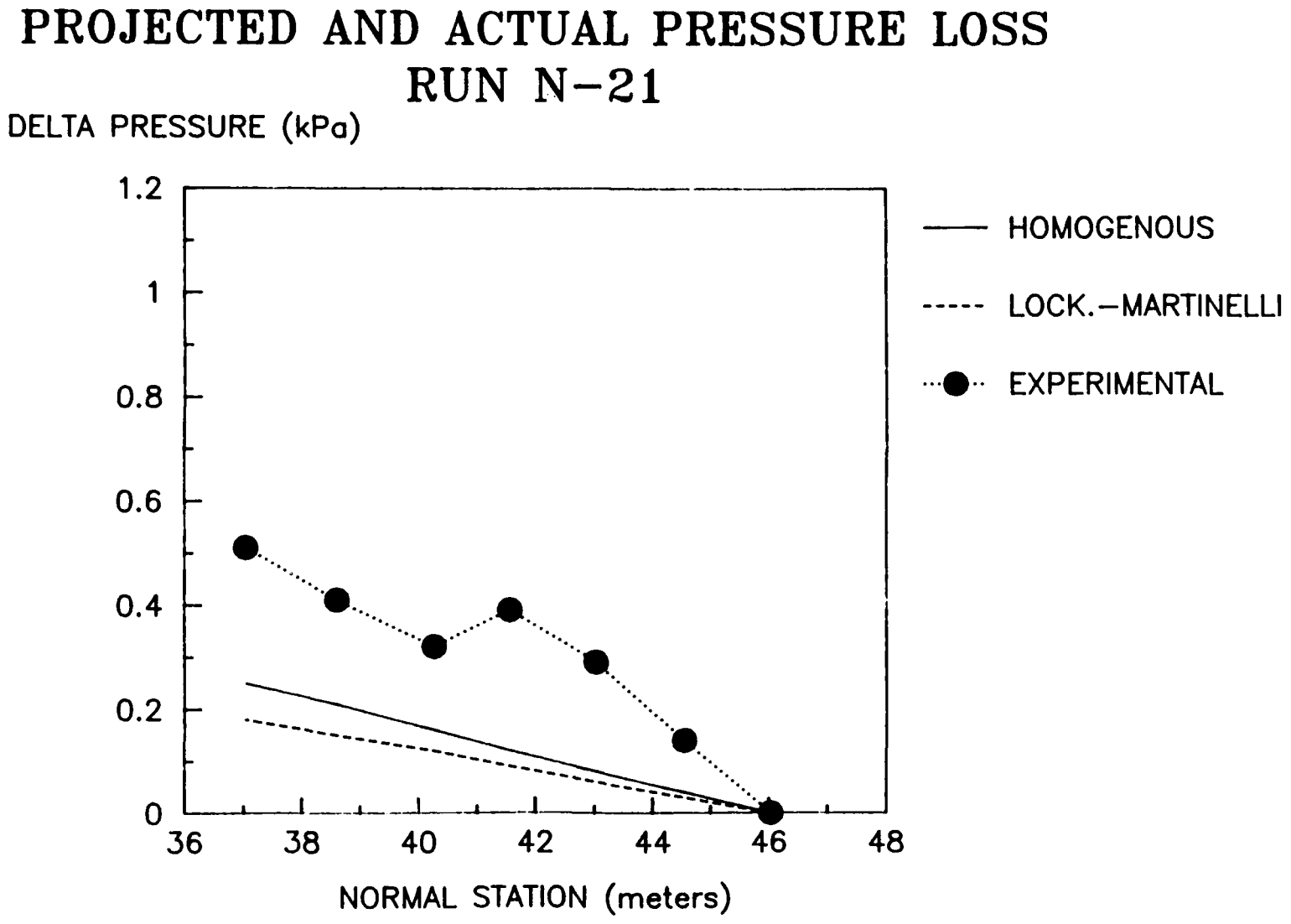

FIGURE 52. Predicted and measured time average vacuum drop profiles, Normal Run 21.

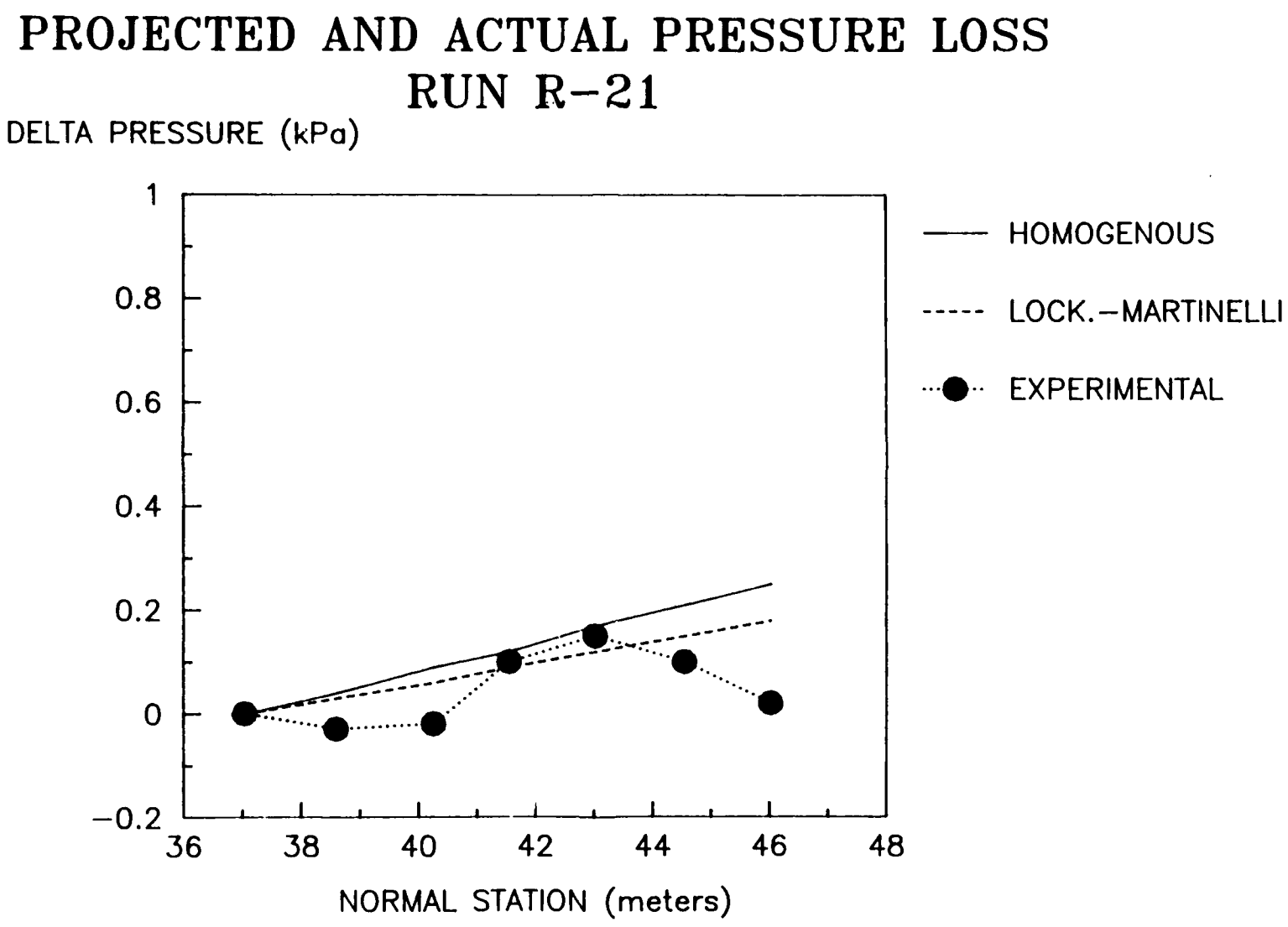

FIGURE 53. Predicted and measured time average vacuum drop profiles, Reverse Run 21.

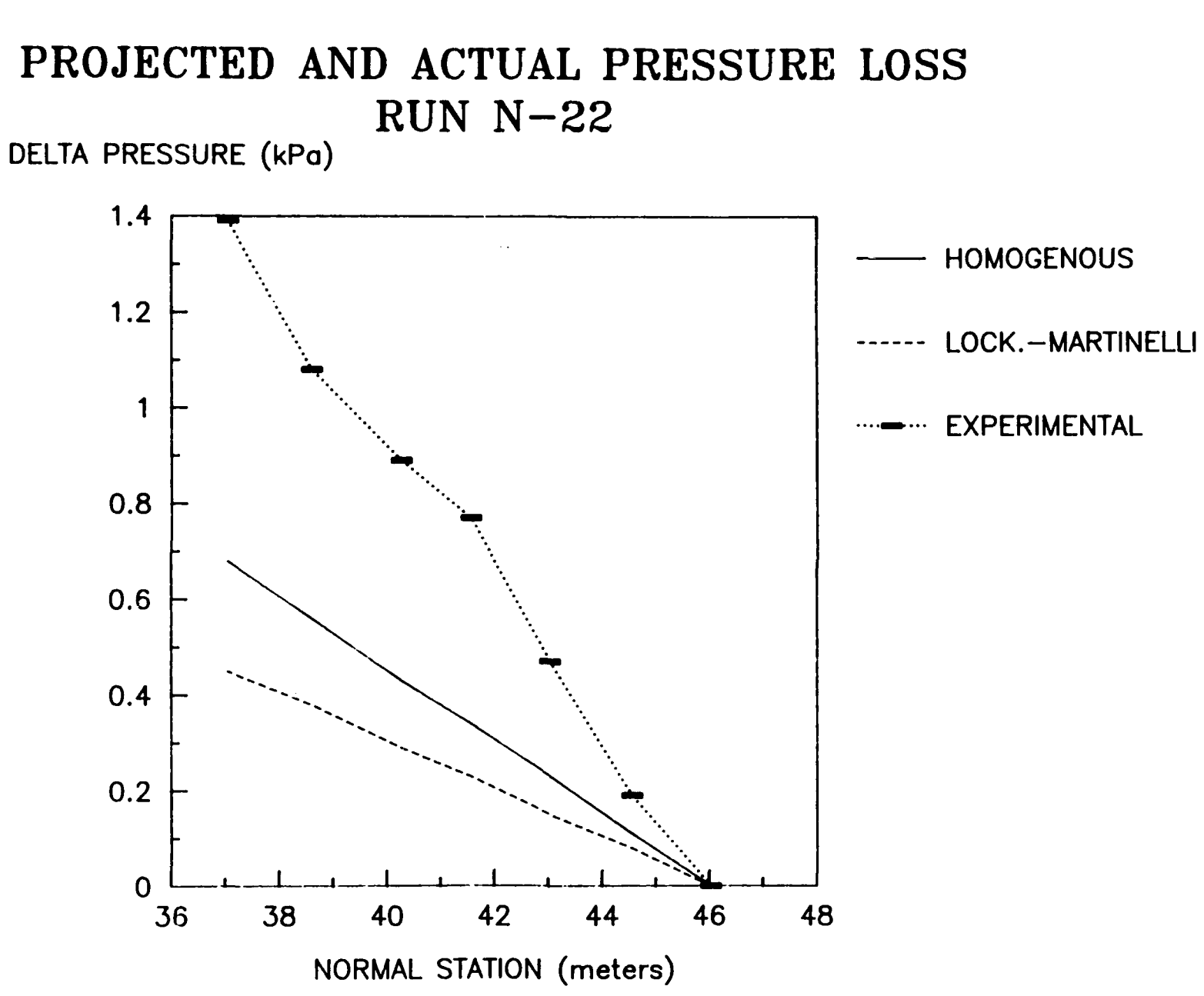

FIGURE 54. Predicted and measured time average vacuum drop profiles, Normal Run 22.

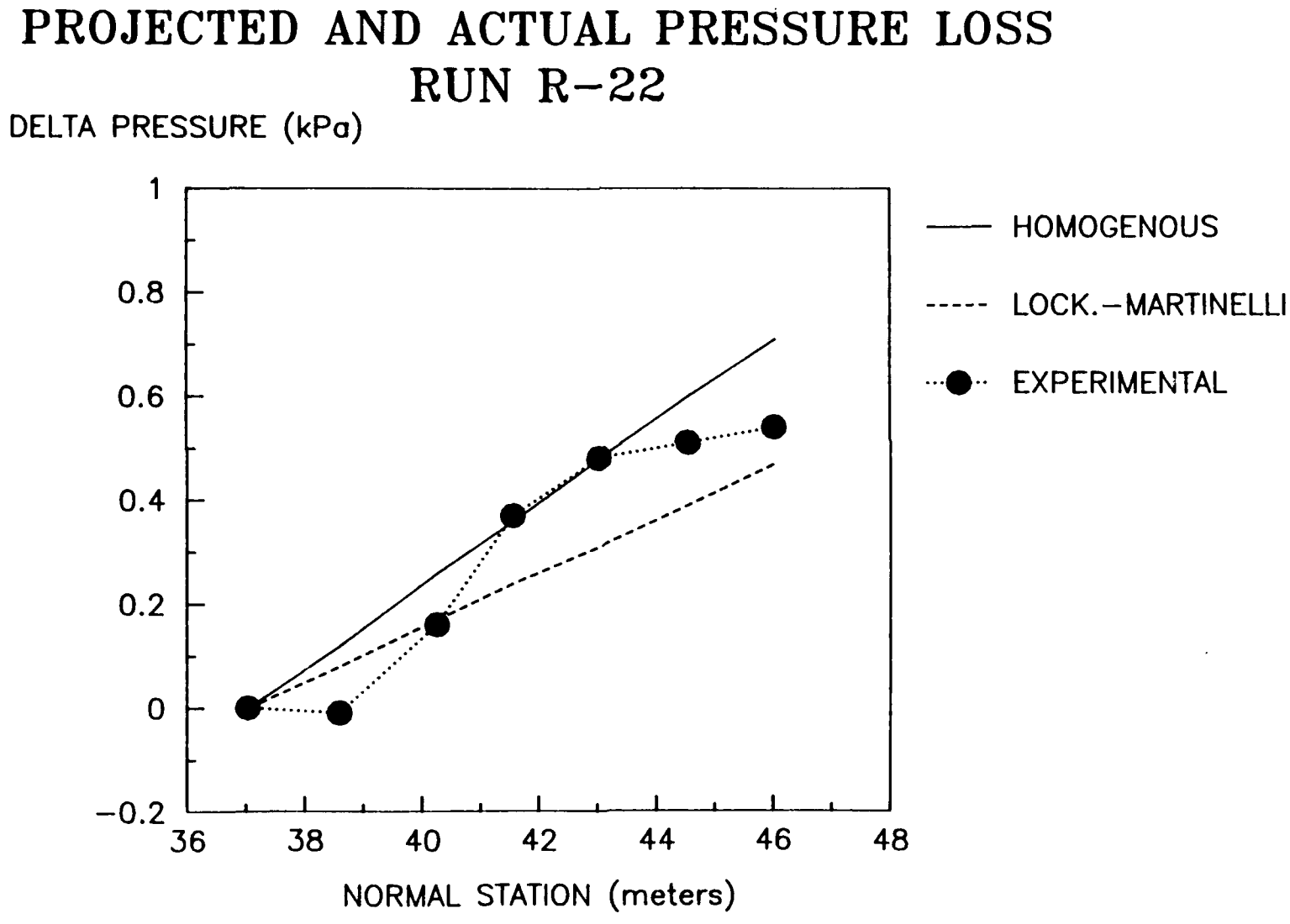

FIGURE 55. Predicted and measured time average vacuum drop profiles, Reverse Run 22.

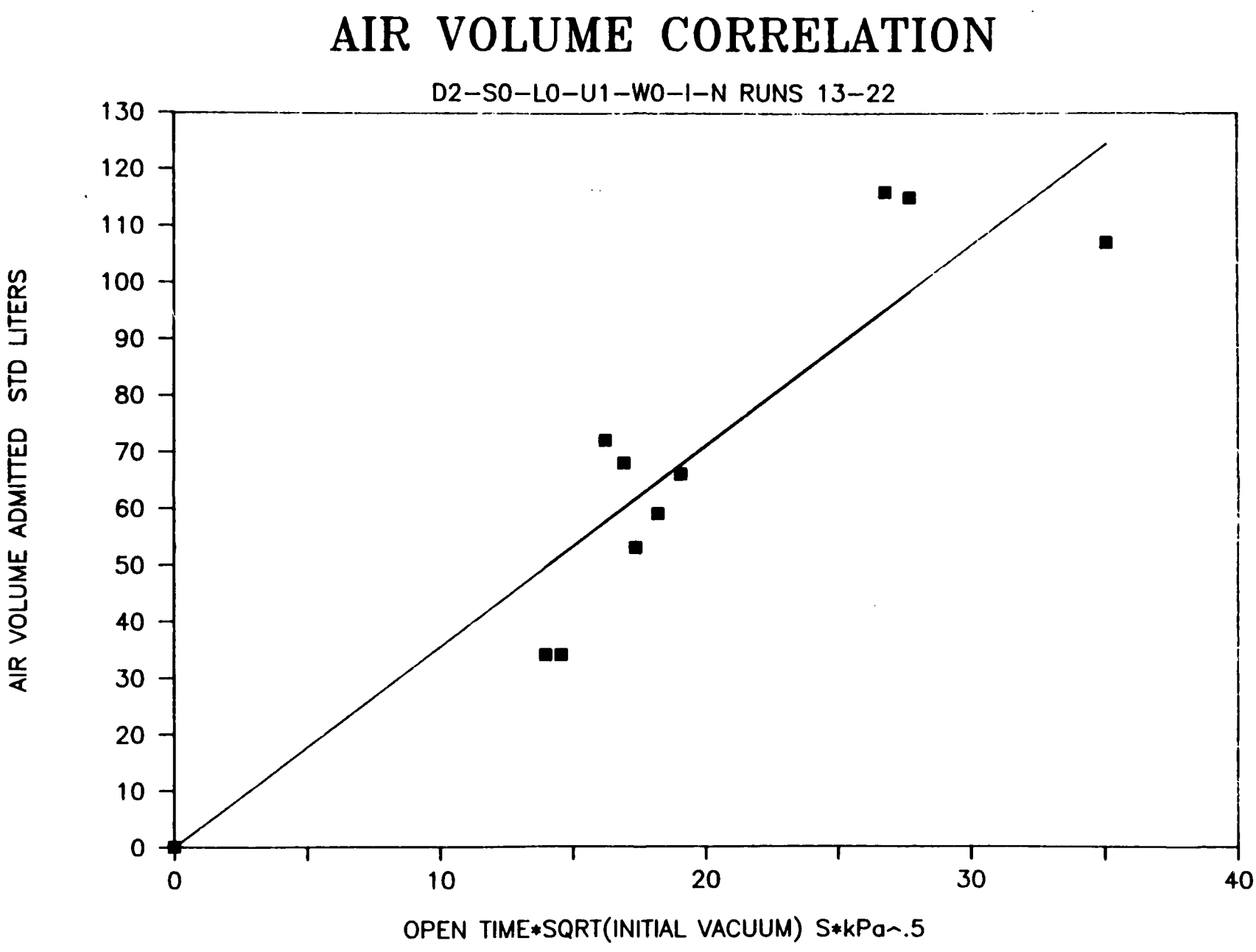

FIGURE 56. Correlation equation for air volume and data.

REFERENCES

1. R. B. Bowers and D. D. Gray, 1988. Design and Operation of a Vacuum Transport Test Facility, David Taylor Research Center Report DTRC/SME-CR-13-88, June 1988.

2. G. B. Wallis, 1969. One-Dimensional Two-Phase Flow, McGraw-Hill.

DISTRIBUTION

Copies	
6	NAVSEA
	1 SEA 05R32
	1 SEA 56Y35
	1 SEA 5032
	1 SEA 56Y32
	2 Library
1	NAVSSES (Code 034B)
2	ONT (Code 226)
1	NOSC (Code 522)
1	NCEL (Code L70)
1	NAPC (T. Klarman)
1	CNA
12	DTIC

CENTER DISTRIBUTION

Copies	Code	Name
1	28	Wacker
1	281	Gudas
3	283	Singerman
1	284	Fischer
1	2801	Crisci
1	2801	Ventriglio
1	2802	Morton
1	2803	Cavallaro
1	2809	Malec
2	2830	Schatzberg
5	2834	Alig
15	2834	Burns
1	522.1	Unclass Lib (A)
2	5231	Office Services